CRISPR-Cas9 Analysis of the HIV-Host Interaction Network

by

Kristin Davis
Department of Microbiology and Immunology
McGill University, Montréal, Canada

August 2019

A thesis submitted to McGill University in partial fulfillment
of the requirements of the degree of
Master of Science

TABLE OF CONTENTS

LIST OF FIGURES

LIST OF TABLES

LIST OF ABBREVIATIONS

AIDS: acquired immunodeficiency syndrome
ALIX: ALG2-interacting protein X
ANOVA: analysis of variance
AP-2: adaptor protein complex 2
APOBEC3G: apolipoprotein B mRNA-editing enzyme catalytic polypeptide-like 3G
Arp2: actin related protein 2
ART: antiretroviral therapy
ATP: adenosine triphosphate
AZT: azidothymidine
bnAbs: broadly neutralizing antibodies
bp: base pairs
BST2: bone marrow stromal cell antigen 2
CA: capsid
CCR5: C-C chemokine receptor type 5
CD4: cluster of differentiation 4
CD4bs: CD4-binding-site
CDC: Center for Disease Control
CHMP4B: component charged MVB protein 4B
CO_2: carbon dioxide
COP: coat protein
CRF: circulating recombinant forms
CRISPR: clustered regularly interspaced short palindromic repeats
crRNA: CRISPR RNA
CXCR4: C-X-C chemokine receptor type 4
DMEM: Dulbecco's Modified Eagle's medium
DNA: deoxyribonucleic acid
DSB: double-stranded break
ELISA: enzyme-linked immunosorbent assay
ER: endoplasmic reticulum
ERC1: ELKS/Rab6-interacting/CAST family member 1 protein
ESCRT: endosomal sorting complex required for transport
FBS: fetal bovine serum
FDA: Food and Drug Administration
FDC: fixed-dose combination
FISH: fluorescence *in situ* hybridization
GAP: GTPase activation protein
GAPDH: glyceraldehyde 3-phosphate dehydrogenase
GCPR: G-protein coupled receptor
GDI: GDP dissociated inhibitor
GDP: guanosine triphosphate
GeCKO: genome-scale CRISPR knockout
GEF: guanine nucleotide exchange factor
GFP: green fluorescent protein
GO: gene ontology
gRNA: guide RNA
GTP: guanosine diphosphate
HDF: host dependency factor
HDR: homology-directed repair
HIV: human immunodeficiency virus
HTLV: human T-lymphotrophic virus
IF: immunofluorescence
IFITM: interferon-induced transmembrane protein
IFN: interferon
IL-2: interleukin 2

IN: integrase
INSTI: integrase strand-transfer inhibitor
kb: kilobase pairs
kDa: kilodalton
KO: knockout
LAMP1: lysosome-associated membrane glycoprotein 1
LAV: lymphadenopathy-associated virus
LC3: microtubule-associated protein light chain 3
LE/Lys: late endosome/lysosome
LEDGF: lens epithelium-derived growth factor
LRA: latency-reversing agent
LTR: long terminal repeat
MA: matrix
MAP: microtubule-associated protein
MAPK8IP2: mitogen-activated protein kinase 8 interacting protein 2
MOI: multiplicity of infection
mRNA: messenger RNA
MSM: men who have sex with men
MTOC: microtubule-organizing center
mTOR: mechanistic target of rapamycin
MxB: myxovirus resistance protein B
NAAT: nucleic acid amplification test
NC: nucleocapsid
NGS: next-generation sequencing
NHEJ: nonhomologous end-joining
NIH: National Institute of Health
NLS: nuclear localization signal
NNRTI: non-nucleoside reverse transcriptase inhibitor
NPC: nuclear pore complex
NRTI: Nucleoside Reverse Transcriptase Inhibitor
NTP: nucleoside triphosphate
NUC: nuclease lobe
Nup: nucleoporin
PACSIN3: protein kinase C and casein kinase substrate in neurons 3
PAM: protospacer adjacent motif
PANTHER: Protein Analysis Through Evolutionary Relationships
PBS: phosphate-buffered saline
PBS: primer binding side
PEI: polyethylenimine
PFA: paraformaldehyde
PHAC: Public Health Agency of Canada
PI: PAM-interacting
PI: protease inhibitor
PIC: pre-integration complex
PICALM: phosphatidylinositol-binding clathrin assembly protein
PIP_2: phosphatidylinositol 4,5-bisphosphate
PR: protease
PrEP: pre-exposure prophylaxis
REC: recognition lobe
RILP: Rab-interacting lysosomal protein
RLU: relative light unit
RNA: ribonucleic acid
RNAi: RNA interference
RNP: ribonucleoprotein
RPMI: Roswell Park Memorial Institute medium
RRE: Rev response element
RT: reverse transcriptase

RTC: reverse transcriptase-RNA/DNA complex
SAMHD1: SAM domain and HD domain-containing protein 1
SDS-PAGE: sodium dodecyl sulfate–polyacrylamide gel electrophoresis
SERINC5: serine incorporator 5
sgRNA: synthetic guide RNA
shRNA: short-hairpin RNA
siRNA: small interfering RNA
SIV: simian immunodeficiency virus
SP: spacer peptide
SQSTM1: sequestosome 1
STD: sexually transmitted disease
STRING: Search Tool for the Retrieval of Interacting Genes
TALEN: transcription activator-like effector nuclease
TAR: *trans*-activation response element
Tat: *trans*-activator of transcription
TBST: Tris-buffered saline with 0.1% Tween 20
TGN: *trans*-Golgi network
TNPO3: transportin 3
tracrRNA: *trans*-activating CRISPR RNA
TRIM5α: tripartite-motif-containing 5α
TSG101: tumor susceptibility factor 101
UNAIDS: United Nations program on HIV/AIDS
V3: variable 3 domain
VAMP-2: vesicle-associated membrane protein 2
VAPB: vesicle-associated membrane protein-associated protein B
Vps: vacuolar protein-sorting-associated protein
VPS4: vacuolar protein sorting-associated protein 4
vRNA: viral RNA
VSV-G: *Indiana vesiculovirus* G protein
WHO: World Health Organization
WT: wild type
ZFN: zinc-finger nuclease

ABSTRACT

As an obligate intracellular pathogen, the human immunodeficiency virus type 1 (HIV-1) relies on host cellular components for replication. The virus has developed an arsenal of methods to productively reproduce within cells while evading host defenses, such as hijacking the cellular membrane trafficking pathway. This pathway facilitates the transport and delivery of molecular cargo within intracellular membrane-bound vesicles and is exploited by HIV-1 for its own intracellular trafficking purposes; however, the cellular players involved in this process remain to be elucidated. To investigate the interactions between HIV-1 and members of the intracellular trafficking circuits, we employed a sophisticated CRISPR-Cas9 arrayed genetic screen causing loss-of-function in 140 genes of the membrane trafficking family. The screen was performed in the HIV-1 reporter cell line, TZM-bl, which was modified to stably express the Cas9 endonuclease. Our screen focused on host factors that significantly alter HIV-1 infectivity, measured by Tat-dependent LTR-driven luciferase activity, and virion production, quantified by p24 capsid protein present in the cell-free supernatant. Of the 140 queried genes, we have uncovered 10 candidate genes that significantly inhibited HIV-1 replication compared to the non-targeting control (selected threshold ≥ 2-fold decrease in viral infectivity or virus production) and proved to be viable knockouts. Protein interaction studies indicate that many of our hits are enriched in endocytosis. To further our inquiry into these candidate hits, we are generating stable CRISPR-knockout cell lines in a T-cell model, SUP-T1, and using protein expression studies and microscopic visualization techniques to investigate the underlying molecular mechanisms exacerbating these phenotypes. Deciphering the relationships between HIV-1 and the membrane trafficking pathway using a revolutionary CRISPR-based genetic screening approach will not only improve our current understanding of viral pathogenesis, but may also translate into novel antiviral targets towards an HIV-1 cure.

RÉSUMÉ

En tant que pathogène intracellulaire obligatoire, le virus de l'immunodéficience humaine de type 1 (VIH-1) dépend des facteurs cellulaires de l'hôte pour sa reproduction. Le virus a développé un arsenal de méthodes pour se reproduire de manière productive dans les cellules tout en en évitant les défenses. Une de ces méthodes consiste en la réquisition du trafic membranaire. Cette voie qui, en temps normal, facilite le transport et la livraison de molécules cargo, est exploitée par le VIH-1 à ses propres fins de trafic intracellulaire. Cependant, les acteurs cellulaires impliqués dans ce processus sont encore inconnus. Pour étudier les interactions entre le VIH-1 et les acteurs du trafic membranaire, nous avons utilisé la technologie génétique sophistiquée CRISPR-Cas9 pour provoquer une perte de fonction de 140 gènes de la famille du trafic membranaire. Cette analyse a été réalisée dans les cellules TZM-bl que nous avons modifiées pour qu'elles expriment de manière stable l'endonucléase Cas9. Nous nous sommes intéressés aux facteurs cellulaires qui modifient de manière significative l'infectivité du VIH-1 mesurée par l'activité de la luciférase induite par Tat et la production de virus quantifiée par la protéine p24, composante de la capside virale, présente dans le surnageant. Sur les 140 gènes explorés, nous avons découvert 10 gènes candidats qui inhibaient significativement la reproduction du VIH-1 par rapport au contrôle non ciblant (seuil sélectionné ≥ 2 fois la diminution de l'infectivité virale ou de la production virale) et qui se sont révélés viables. Les études sur les interactions protéiques indiquent que la majorité de nos gènes candidats sont enrichis durant l'endocytose. Pour approfondir notre enquête sur ces candidats potentiels, nous générons des lignées cellulaires knock-out CRISPR stables dans un modèle de lymphocytes T, SUP-T1, et nous utilisons des études d'expression des protéines et des techniques de visualisation microscopique pour étudier les mécanismes moléculaires sous-jacents exacerbant ces phénotypes. L'exploration des relations entre le VIH-1 et les voie de trafic intracellulaires en utilisant une approche de dépistage génétique basée sur le système CRISPR-Cas9 améliorera non seulement notre compréhension actuelle de la pathogenèse virale, mais pourrait également se traduire par la découverte de nouvelles cibles antivirales menant au traitement du VIH-1.

ACKNOWLEDGMENTS

My graduate school experience has been a far cry from a regular one. I first met Dr. Mark Wainberg in November 2016 and instantly knew I belonged in his lab. His inexhaustible passion and dedication towards HIV/AIDS research was breathtaking. Although I never got to start my graduate degree in Dr. Wainberg's lab, his brief presence in my life has ignited my own passion for research. I will always remember his kindness and those of his lab members who have continued to support me every day since I started at the Lady Davis Institute. Nevertheless, this gave me the opportunity to work with two incredible researchers whose mentorship has extended beyond my expectations of graduate school. Dr. Chen Liang and Dr. Andrew J. Mouland have provided me with the space to grow and learn all the while being accessible and supportive. Co-supervision is a challenge that we undertook fearlessly and we turned out to make a great team.

I will always remember Dr. Liang for his generosity and his counsel. He also gave me the opportunity to be a teaching assistant for the course *Viral Pathogenesis*, which proved to be a tremendously rewarding experience and for which I will always be grateful. It will be hard to forget Dr. Mouland. Our stimulating intellectual discussions have been instrumental to my development as a scientist. Looking back, I think Dr. Mouland knew what I was capable of before I did. He constantly pushed me to make sure I attained my full potential; I know that the drive and tenacity he encouraged in me will continue to serve me in my future endeavors.

I got to work with so many talented people, all of which would be impossible to list here. I would like to especially acknowledge Dr. Shringar Rao and soon-to-be Dr. Saina Beitari who have not only answered millions of my questions without any reservations, but who have been, and continue to be, my ultimate role-models as powerful women in science.

My degree would not have been possible without the generous financial support of the Microbiology and Immunology Department during the first year of my degree. Likewise, I extend my gratitude to the TD Bank Group for their generous LDI/TD studentship and to Dr. Wilfred Yaphe for the endowment award in his name. This research is funded by two operating grants from the Canadian Institutes of Health Research (CIHR): MOP-56974 (Mouland) and MOP-133479 (Liang).

WITH THANKS

To my advisory committee members Dr. Anne Gatignol and Dr. Jerry Pelletier for their accessibility, guidance, and constructive feedback;

To all past and present Dr. Mouland and Dr. Liang lab members for their technical support in the lab, particularly Bin Xu for the creation of CRISPR-knockout cell lines as well as Meijuan Niu, Anne Monette, Maya Nijnoff Asser, and Lois Chen, for their contributions to the Rab7a project;

To Christian Young for his patience and guidance in my flow cytometry experiments;

To Maureen Oliveira and Ilinca Ibanescu for their tremendous help in the luciferase and p24 experiments;

To Cesar Collazos and Maureen Oliveira for letting me share office space;

To Craig McCullogh for his constant encouragement and close reading of this thesis;

To my sister Charlotte for making Montreal "home";

Lastly, to my parents for their endless support and for providing me with all the means to successfully reach my goals, including this one.

Sincerely,

Kristin Davis

PREFACE

The candidate has adhered to thesis requirements in accordance with the McGill University Graduate Program Studies guidelines. The candidate has chosen to organize her thesis in the traditional format, beginning with a comprehensive literature review and introduction, establishing a project rationale, hypothesis, and research aims, followed by the materials and methods, results, discussion, and conclusion sections, ending with a formatted bibliography and appendix.

AUTHOR CONTRIBUTIONS

The candidate and co-supervisors Dr. Andrew J. Mouland and Dr. Chen Liang conceived and designed the experiments. The candidate performed the data collection, analyses, and preparation of the figures.

CHAPTER 1: LITTERATURE REVIEW AND INTRODUCTION

1. HIV

1.0 HIV: A Brief Historical Perspective

In the early 1980s, doctors in San Francisco and New York City noted an increasing number of patients with rare forms of pneumonia, cancer, and opportunistic infections brought on by a profound state of immune suppression[1,2]. Of note was the fact that these mysterious illnesses were exhibited preferentially in men who have sex with men (MSM)[1,2]. These were the first documented cases of what is now known as the acquired immunodeficiency syndrome (AIDS)[3]. The early manifestation of AIDS-related illnesses suggested causation by an infectious agent due to a specific decrease in the number of T-lymphocytes that express the cluster of differentiation 4 (CD4) antigen on their surface, also known as the $CD4^+$ T-cells[3]. In accordance to their fundamental role in regulating the immune system, a loss in these cells provided an explanation for the onset of opportunistic infections in AIDS-afflicted patients.

Identifying the agent responsible for AIDS represented a unique challenge. In 1982, the Center for Disease Control (CDC) reported an incidence of AIDS in hemophiliacs receiving blood transfusion, hinting at the fact the AIDS-causing agent could be no greater than a virus[4]. In 1983, Dr. Barré-Sinoussi and Dr. Montagnier at the Pasteur Institute in Paris obtained a clear viral isolate from a lymph node of an AIDS patient, identifying it as a retrovirus that kills $CD4^+$ T-cells and named it the lymphadenopathy-associated virus (LAV)[5]. Further characterization of the virus proved difficult due to challenging propagation and sustained *in vivo* tissue culture[6]. In 1984, Dr. Gallo at the University of Maryland achieved laboratory culture of the virus. He noted similar clinical presentations of the AIDS virus with that of the human T-lymphotrophic virus (HTLV), prompting a renaming to HTLV-III[6]. In 1986, the AIDS-causing retrovirus officially adopted the name of the human immunodeficiency virus (HIV) by the International Committee on Taxonomy of Viruses[7]. In 1987, the Food and Drug Administration (FDA) approved the first drug developed to treat HIV, azidothymidine (AZT), for clinical use, saving millions of lives worldwide[8]. In 2008, Dr. Barré-Sinoussi and Dr. Montagnier were awarded the Nobel Prize in Physiology or Medicine for their discovery of HIV, the causative agent of AIDS[9].

Since its beginnings, HIV has claimed the lives of more than 35 million people and continues to affect more than 37 million people worldwide (WHO, 2017). Due to the collective effort of research scientists, pharmacologists, philanthropists, physicians, and patients, there now exists a myriad of antiretroviral drugs to treat HIV to a level of sustained viral suppression. Despite this remarkable achievement, the quality of life of individuals living with HIV is subpar, fueling the need to tackle the long-standing problem of finding a cure for HIV.

1.1 HIV: Classification and Evolution

The human immunodeficiency virus (HIV) is classified to the genus *Lentivirus*, within the subfamily *Orthoretrovirinae* of the *Retroviridae* family[7]. The taxonomic classification of HIV uncovers many of its characteristics; *lenti*, meaning slow, refers to the chronic nature of the viral infection and *retro* symbolizes the reverse flow of genetic information from RNA to DNA catalyzed by the unique retroviral enzyme reverse transcriptase (RT)[7]. The two types of HIV: HIV type 1 (HIV-1) and HIV type 2 (HIV-2) are denoted based on their inferred ancestral origins[7,10]. Extensive genetic analyses suggests that these two types are the products of separate cross-species transmissions of a related lentivirus, the simian immunodeficiency virus (SIV), from chimpanzees (HIV-1) and sooty mangabeys (HIV-2), early in the 20th century[10]. Numerous zoonotic transmission events of SIV to humans may have contributed to the evolution and genetic diversity between HIV strains[10]. Due to this genetic diversity, HIV-1 viruses are further divided into a major group (group M) and three minor groups (groups N, O, and P) based on sequence similarity[10]. Group M is the most common circulating HIV-1 type and is responsible for the HIV/AIDS epidemic[11]. Group M is further categorized into 12 subtypes (A to K) based on their inferred geographical and genetic relatedness[12]. Recombination between subtypes is known to occur; these are classified epidemiologically as circulating recombinant forms (CRFs) of the virus[12].

1.2 HIV: Epidemiology and Routes of Transmission

In 2017, an estimated 36.9 million people worldwide were living with HIV, of which 1.8 million represented new infections that year (WHO, 2017). HIV-1 is the most prevalent HIV infection worldwide, whereas infection with HIV-2 is exclusive to Western Africa and presents lower levels of infectivity and virulence[10]. In Canada, the estimated number of people living with HIV-1 infection is 63,110 based on public health data gathered in 2016 (PHAC, 2016). The Joint United Nations program on HIV/AIDS (UNAIDS) spearheads a project called 90-90-90 to achieve

cessation of the global HIV epidemic by 2020 (UNAIDS, 2014). The target of the project is for 90% of all people living with HIV to recognize their status, and 90% of these to receive sustained antiretroviral therapy (ART), of which 90% will have achieved viral suppression by 2020 (UNAIDS, 2014). The progress made towards the 90-90-90 UNAIDS target for Canada is advancing greatly, with estimated numbers of 86-81-91 (PHAC, 2016).

HIV spreads through populations by contact with contaminated bodily fluids, including blood, semen, pre-seminal fluids, rectal fluids, vaginal fluids and breast milk[13,14]. Transmission occurs by virus exposure at the genital, anal, and oral mucosa, or by entering the blood stream by percutaneous injection or damaged tissue[14,15]. Modes of transmission include unprotected sexual intercourse with an infected partner and the sharing of contaminated drug injection equipment[15,16]. Hence, key populations with an increased vulnerability to HIV infection are MSM, intravenous drug users, prison inmates and other persons living in unhygienic close quarters, sex workers and their clients, as well as persons identifying as transgender[15-17]. Strategies to prevent HIV transmission in at-risk populations include the use of condoms during sex, the use of sterilized needles for drug injection and taking the HIV-specific preventative medicine called pre-exposure prophylaxis (PrEP)[15,18]. Educating individuals about HIV/AIDS, especially youth, has been shown to reduce HIV incidence rates and promote better sexual health[19]. Less frequently, HIV can also be spread vertically from infected mother-to-child *in utero*, intrapartum, or postnatally during breastfeeding[13,20]. Mother-to-child transmission is preventable with a strict antiretroviral regimen, resulting in undetectable viral loads in pregnant women for the duration of the pregnancy and breastfeeding period[21]. Blood transfusion related transmissions are now extremely rare due to current-day disease screening of donated blood[22].

Snapshots of the communities mostly affected by HIV nowadays reveal the underlying social determinants and health inequalities driving their increased risk for infection and exposes the consequences of stigmatization and difficulty in accessing healthcare services. These problems need to be addressed concurrently with new treatment options in the continued mission to eradicate HIV.

1.3 HIV: Clinical Presentation, Diagnosis and Treatment

The classical clinical manifestations of prolonged HIV infection are the onset of aggressive opportunistic infections and malignancies. These infections may be protozoal in origin including

pneumocystis carinii pneumonia, or fungal such as oral candidiasis and to a lesser extent bacterial and viral[1,2]. Certain malignancies have marked HIV/AIDS such as Kaposi's sarcoma, an otherwise uncommon cancer with a typical presentation of purple-coloured skin lesions[2]. These diseases often declare the occurrence of AIDS in HIV infected individuals. Presently, testing for sexually transmitted diseases (STDs) including HIV is essential routine healthcare for the sexually active in most developed countries and is now more appreciated in developing countries[23,24]. Early diagnosis of HIV is optimal as treatment can be started right away, therefore halting further virus propagation and preventing the development of AIDS [24,25].

Diagnosis is confirmed by blood test, either by detection of anti-HIV antibodies produced by the body, called a rapid test, or by measuring HIV protein or viral (v)RNA, termed p24 antigen test and nucleic acid amplification test (NAAT), respectively[23]. These laboratory tests are limited by early "window periods" in which concentrations of anti-HIV antibodies and the virus are below the detectable threshold of laboratory tests[26]. Thus, this window period is conducive to false negative results[26]. NAATs have the shortest window period, detecting vRNA as early as 7 days post-infection; thus, they are considered the gold standard confirmatory diagnostic for HIV screening in Canada[27]. The increasing availability of HIV self-testing kits has helped at-risk populations determine their status, promptly linking them to available healthcare services[28].

Presently, there are numerous FDA-approved antiretroviral agents to treat HIV infection and even more promising drug candidates currently undergoing clinical investigation. These drugs are classified in five categories based on their stage of intervention within the HIV replication cycle. Examples of each class of HIV-1 inhibitors are presented in table 1.

Table 1: Current antiretroviral drugs to treat HIV infection.

Drug Class	Mechanism of Action	Examples of FDA-Approved Drugs (Generic Names)	Refs.
Nucleoside Reverse Transcriptase Inhibitors (NRTIs)	Abolish the enzymatic activity of HIV RT by mimicking its natural substrate - DNA	Azidothymidine (AZT) Tenofovir Disoproxil Fumarate (TDF) Lamivudine (3TC)	8,29,30
Non-Nucleoside Reverse Transcriptase Inhibitors (NNRTIs)	Bind HIV RT in an alternative site from the DNA-binding pocket, preventing it from performing its enzymatic activities	Etravirine (ETR) Rilpivirine (RPV) Doravirine (DOR)	31-33
Protease Inhibitors (PIs)	Inhibit the HIV enzyme protease which is necessary for the proteolytic maturation of infectious virus particles	Atazanavir (ATV) Darunavir (DRV) Fosamprenavir (FPV)	34-36
Fusion Inhibitors	Block HIV entry by antagonizing the receptors that HIV uses on the surface of target cells	Enfuvirtide (T-20) Maraviroc (MVC)	37,38
Integrase Strand-Transfer Inhibitors (INSTIs)	Impede integration of HIV DNA within the host chromosome by binding and sequestering the viral enzyme integrase	Dolutegravir (DTG) Raltegravir (RAL)	39,40

The use of antiretrovirals in monotherapy quickly revealed that HIV was able to mutate to escape drug recognition[41,42]. The concept of combination antiretroviral therapy (cART) was tested in clinical trials and demonstrated a substantial advantage in overcoming resistance, paving its way swiftly into clinical practice in the mid 1990s[41]. Presently, therapeutic regimens for HIV are still managed as cART, generally comprised of three agents of at least two different drug classes[41]. An increasing number of fixed-dose combination (FDC) pills are on the market, combining several drugs into an all-in-one tablet for ease of dosing and adherence[43]. Although the advent of cART revolutionized what used to be a death sentence into a chronic illness, access, high treatment cost, drug resistance, and unwanted side effects remain important challenges to overcome to reach the UNAIDS 90-90-90 goals.

1.4 HIV-1: Genome Organization

The HIV-1 genome consists of a single-stranded (ss) RNA of positive polarity just over 9 kilobase pairs (kb) in length (shown in figure 1)[44]. Analogous to all other retroviruses, HIV-1 is diploid, signifying there are two copies of the full length vRNA in each virus particle[44]. The HIV-1 genome contains several differential RNA splicing elements to create nine gene products, notably, the polyproteins Gag and Pol, and the proteins Env, Tat, Rev, Vpu, Vpr, Vif, and Nef[45]. The Gag precursor protein ($Pr55^{Gag}$) encodes the viral structural proteins that form the majority of the HIV-1 virion: matrix (MA, p17), capsid (CA, p24), nucleocapsid (NC, p7), and p6, including two spacer peptides SP1 and SP2[44,46]. Pol encodes the three retroviral enzymes: protease (PR), reverse transcriptase (RT), and integrase (IN). Moreover, Env encodes the viral envelope glycoprotein (gp)160 which is then processed by cellular enzymes to generate the mature envelope glycoproteins gp120 and gp41[44,46].

Separate from the quintessential retroviral coding domains *gag*, *pol,* and *env*, HIV-1 also entertains the production of two regulatory proteins and four accessory proteins[46]. The regulatory protein Tat acts as an activator of transcription of the HIV-1 provirus, ensuring its efficient synthesis, and Rev allows nuclear export of intron-containing HIV-1 mRNAs[47,48]. The HIV-1 accessory genes Vpu, Vpr, Vif, and Nef play key roles in antagonizing various intrinsic restriction factors, whilst simultaneously promoting viral infectivity[49].

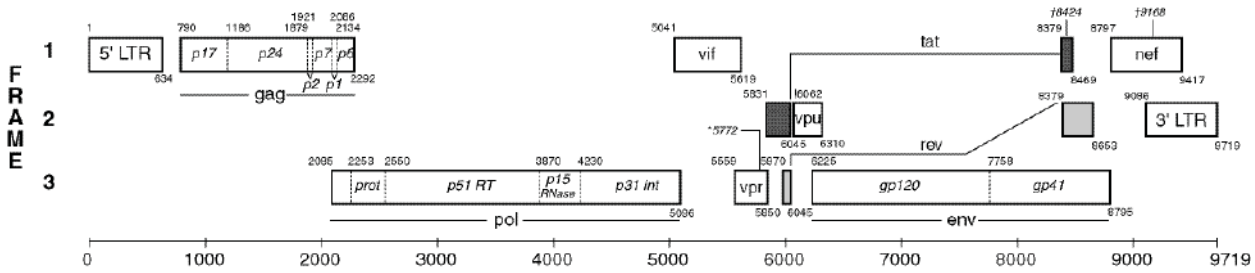

Figure 1: Schematic representation of the HIV-1 genome. The HIV-1 genome is represented as white boxes denoting open reading frames with the gene start position indicated by the number at the upper left-hand corner. The Tat and Rev spliced exons are represented as black and grey rectangles, respectively. The scale is representative of base pairs (bp). Image retrieved from the 2018 HIV Sequence Compendium.

1.5 HIV-1: Viral Pathogenesis

1.5a HIV-1 Replication Cycle - Early Events

HIV-1 exhibits tropism for cells decorated with the CD4 glycoprotein, a member of the immunoglobulin superfamily[50,51]. Cells marked with CD4 include the $CD4^+$ T-cells of the lymphoid lineage of blood cells, as well as macrophages and dendritic cells, derived from a common monocyte myeloid precursor[50]. The key player in cell recognition is the HIV-1 Env glycoprotein complex, consisting of two homotrimers of gp120 and gp41[52,53]. The gp120 trimer is exposed to the extracellular environment, anchored by the transmembrane integrated gp41 subunit[52,53]. Cell attachment to CD4 is governed by gp120 via its CD4-binding-site (CD4bs)[53]. This precise interaction is ultimately followed by a conformational change in the variable 3 (V3) domain of gp120, which is required for binding to a host cell co-receptor, consisting of either the C-X-C chemokine receptor type 4 (CXCR4) or the C-C chemokine receptor type 5 (CCR5)[54]. These co-receptors differentiate X4-tropic viruses (CXCR4) from R5-tropic (CCR5) viruses, the latter being more transmittable and seen earlier in HIV-1 infection[55]. This intricate series of protein-protein interactions draw the viral and host membranes in close proximity, culminating in their hemifusion[56].

Following virus-host membrane hemifusion, the viral capsid core is propelled into the intracellular environment of the target cell, as seen in figure 2[56]. It is at this stage that RT is activated, binding vRNA to initiate reverse transcription within the capsid core[57]. An HIV-1 virion contains an average of 50 RT molecules, enhancing the likelihood of RT-vRNA interactions[58,59]. A host tRNA(Lys3) binds the primer binding side (PBS) in the conserved 5' region of the vRNA, priming minus-strand DNA synthesis by RT[57]. In addition to its RNA- and DNA-dependent DNA polymerase activity (p66), RT contains a nuclease (RNAseH) domain (p51), which effectively induces degradation of RNA species as polymerization is occurring[60]. This includes degradation of

the transient RNA-DNA hybrid species created during reverse transcription to avoid immune detection[60,61]. Reverse transcription yields a full-length double-stranded (ds)DNA species derived from the inbound vRNA, flanked by long terminal repeats (LTRs)[59]. Gradual dismantlement of the capsid core occurs concurrently with reverse transcription[62].

Evolution of the RT-RNA/DNA complex (RTC) into the pre-integration complex (PIC) sets the scene for DNA integration. The PIC consists of the newly synthesized dsDNA bound by the retroviral enzyme IN[63]. The first of two distinct steps of DNA integration occurs in the cytoplasm, and involves the cutting of two nucleotides off each 3' end of the dsDNA to generate staggered ends, entitled 3' end processing[64]. This exposes a free hydroxyl group on each end, necessary to catalyze the chemical reaction of DNA integration[64]. Nuclear import of the PIC is facilitated by the hijacking of various nucleoporins (Nups) that constitute the nuclear pore complexes (NPCs), which regularly serve as nucleus gatekeepers[65]. Within the nucleus, the processed dsDNA is free to attack host chromosomal DNA[66,67]. In this second step, entitled strand transfer, the free 3' hydroxyl groups capture exposed phosphodiester bonds within the genomic DNA in order to covalently integrate and embed their own genetic information within that of the host[66,67].

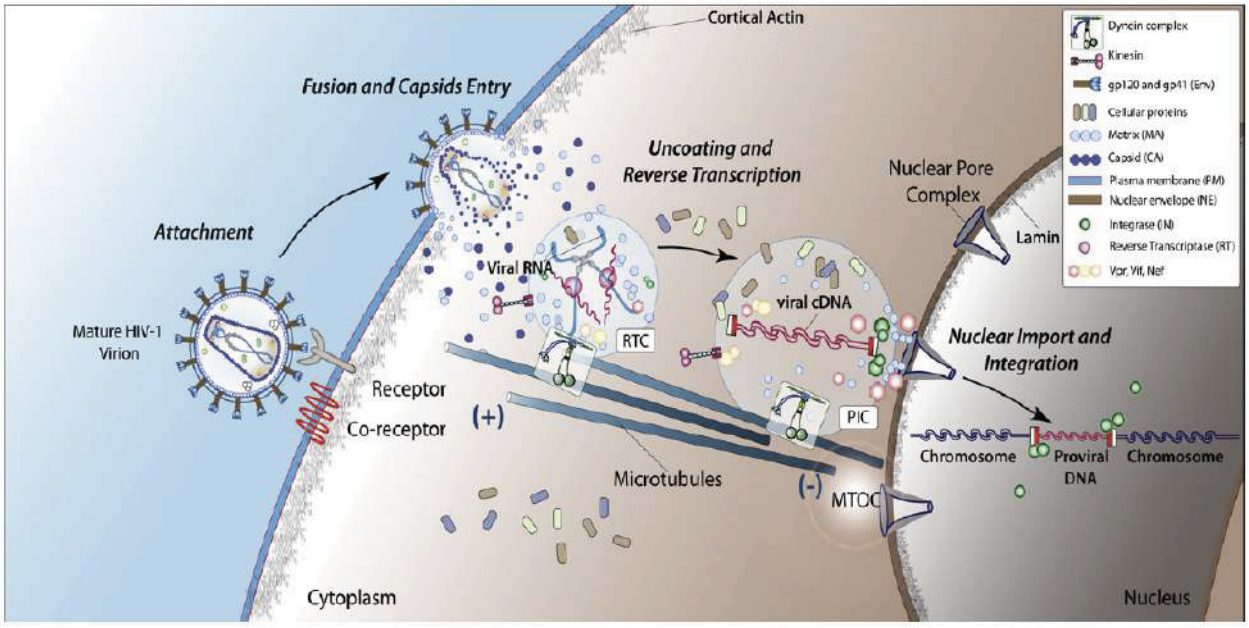

Figure 2: The early steps of the HIV-1 replication cycle. The early steps of the viral life cycle include engagement of the viral glycoproteins with the host cell receptor CD4 and co-receptors (red) on target cells, followed by virus-host lipid membrane hemifusion and introduction of the viral capsid core into the cytoplasm. Reverse transcription of the vRNA to cDNA by the viral enzyme reverse transcriptase (green circle) forms the pre-integration complex (PIC), which begins retrograde-mediated translocation to the nucleus on the microtubules. This is ultimately followed by nuclear import through the nuclear pore complex and integration of the viral cDNA as a provirus (pink) in the host chromosome, catalyzed by the viral enzyme integrase (green circle). Figure obtained with permission from Mouland and Milev in Chapter 22 of King, S. (2011). *Dyneins*. London: Academic Press, pp.560-583.

Paradoxically, the cellular co-factor lens epithelium-derived growth factor (LEDGF) obligingly assists IN-mediated integration of retroviral DNA by tethering the enzyme to the chromatin, therefore boosting integration efficiency[68,69]. This integrated copy of HIV-1 DNA is referred to as the provirus[70]. Selection of target site integration is more or less arbitrary; however, integration is shown to occur preferentially in genomic hubs undergoing active transcription[71]. This is rather fitting as it provides the virus a chance to optimize its own replication concurrently with that of its host[71]. Post-integration, the provirus holds many fates. Active transcription will promote the cell to become a factory of mass production of virus particles or contrarily, epigenetic modifications may instigate the provirus to lie dormant as a latent reservoir[71,72].

1.5b HIV-1 Replication Cycle - Late Events

Following integration within the host genome, the HIV-1 provirus generates short, completely spliced mRNAs, consisting of Tat and Rev[73]. Tat, identified as the *trans*-activator of transcription, binds the *trans*-activation response (TAR) element, a regulatory element located 3' of the HIV-1 promoter[74]. Tat recruits an essential host transcriptional co-factor P-TEFb, dramatically increasing transcription of the provirus by the host RNA polymerase II[74]. Increased signaling through the key immune regulatory NF-κB pathway has also been shown to stimulate Tat-mediated *trans*-activation by virtue of two NF-κB binding sites found within the HIV-1 LTR[75].

HIV-1 is subject to substantial alternative splicing to generate several virus-derived mRNA species that are completely spliced (2kb; Tat, Rev, and Nef), incompletely spliced (4.5kb; Env, Vpu, Vif, and Vpr) and completely unspliced (9.2kb; Gag, Gag-Pol and full-length vRNA)[45,73,76]. Normally, incompletely spliced and unspliced transcripts are degraded in the nucleus as part of an intrinsic RNA surveillance mechanism[77]. To overcome these mechanisms, HIV-1 encodes a factor that enables nuclear export of intron-containing viral mRNA transcripts called Rev[48,78]. Rev does so by binding with high affinity to the Rev response element (RRE) found within *Env*, which is absent in the fully spliced mRNAs[48,78]. Rev facilitates nuclear egress through the NPCs and recycles back to the nucleus for recurring rounds of RNA export[79].

HIV-1 RNA is channeled to the cytoplasm for 3' processing and polyadenylation by cellular RNA binding factors[80,81]. Translation of HIV-1 proteins proceeds on host cytosolic polysomes and the endoplasmic reticulum (ER)[82]. The Env precursor gp160 is co-translationally inserted in the ER

membrane, where it undergoes trimerization as well as *N*- and *O*-linked glycosylation[86]. It is then further trafficked to the Golgi apparatus where it is enzymatically cleaved by cellular furin and furin-like proteases, giving rise to the mature gp41 and gp120[83,84]. These glycoproteins then travel to the plasma membrane, as this is the site of virus assembly[85].

Gag, Gag-Pol, and HIV-1 RNA trafficking and assembly is currently one of the least understood aspects of HIV-1 biology and remains an active area of investigation. Gag and Gag-Pol molecules are synthesized at a stochastic ratio of 20:1[86]. Like all other retroviral proteins, they must relocate to the plasma membrane to begin virion assembly (see figure 3)[85]. Several studies have reported localization of Gag and Gag-Pol within endosomal compartments for trafficking towards the cell periphery and fusion with the plasma membrane[87-90]. Gag molecules have also been shown to bind and sequester full-length vRNA during this intracellular travel, which are to be encapsulated within nascent virions[91,92]. In fact, several studies have shown co-trafficking of vRNA and Gag with host endosomal membranes at the microscopic level[90-93]. Although hitching a ride with anterograde-directed endosomes has been shown to be the preferred working model of Gag trafficking, the mechanistic insights behind Gag, Gag-Pol and vRNA trafficking are largely unknown and their elucidation would provide beneficial information about retroviral biology and cell physiology alike.

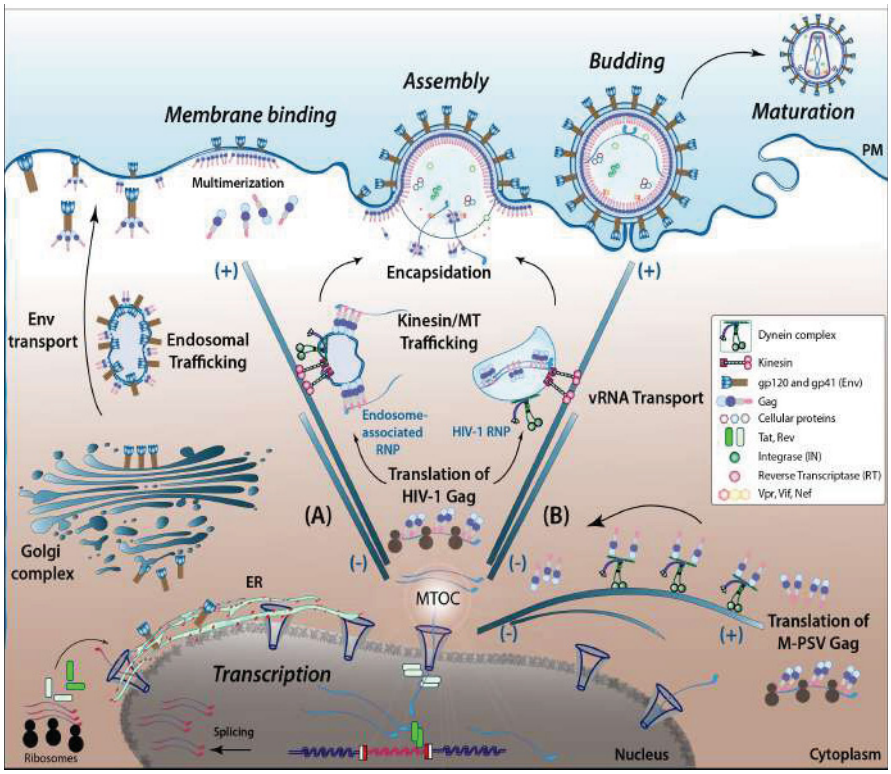

← <u>Figure 3:</u> The late steps of the HIV-1 replication cycle. Transcription of viral proteins Gag and Env as well as full-length unspliced viral mRNA proceeds in the nucleus and the translation of the viral proteins on host ribosomes. The Env glycoprotein is shuttled through the biosynthetic-secretory endosomal pathway to yield the mature surface glycoproteins. Gag associates with vRNA into a ribonucleoprotein (RNP) at a perinuclear region and nucleates travel towards the plasma membrane by utilizing anterograde-directed motor-powered vesicular transport on the microtubules (kinesin/MT trafficking). At the plasma membrane, assembly occurs in lipid-rich microdomains and is arbitrated by Gag multimerization, Env targeting and vRNA encapsidation to form an immature nascent virion. Budding is facilitated by the endosomal complex required for transport (ESCRT) machinery and a maturation step precedes viral egress to create a fully mature and infectious viral particle. Figure obtained with permission from Mouland and Milev in Chapter 22 of King, S. (2011). *Dyneins*. London: Academic Press, pp.560-583.

Assembly of viral components occur in specialized detergent-resistant liquid-ordered plasma membrane microdomains called lipid rafts[94]. Highly concentrated in cholesterol and glycosphingolipids, these rafts provide a lipid-rich shell for viral envelopes[94,95]. Virion assembly begins with the insertion of the MA region of Gag within the lipid rafts using its N-terminal mysristoyl moiety[96]. The membrane lipid phosphatidylinositol 4,5-bisphosphate (PIP_2) plays an important role in anchoring MA to the plasma membrane[95]. In turn, MA guides Env incorporation into the growing viral particle through interaction with the cytoplasmic tail of gp41[97]. Gag multimerization at the assembly site is achieved through binding amongst CA and SP1 domains, which pack Gag and Gag-Pol molecules into a semi-circle, radiating from a common center[98]. At this stage, the highly structured Ψ–site in the vRNA drives vRNA dimerization and encapsidation into growing virus particles through specific interactions with NC[99]. The growing spherical viral shell induces local curvature of the plasma membrane in preparation for retroviral budding.

In order to escape the cell, a nascent virion must form a critical bond with the host tumor susceptibility factor 101 (TSG101), a component of the endosomal sorting complex required for transport (ESCRT) pathway[100-104]. ESCRT-I, together with ESCRT-0, ESCRT-II, ESCRT-III, VPS4-Vta1, and Bro1/ALIX, form the tightly regulated, highly conserved, multi-subunit ESCRT machinery, which sort ubiquitinated cargo for lysosomal degradation[105]. The short late domain "PTAP" of p6 mediates direct binding with TSG101, recruiting the ESCRT machinery to the site of virus assembly[101,102]. In accordance with the role of ubiquitin in ESCRT initiation, ubiquitination of p6 was shown to enhance TSG101 binding 10-fold[104]. p6 also bears another late domain of the YPXL-type, which directly binds the ALG2-interacting protein X (ALIX), an accessory protein of the ESCRT machinery[106]. Numerous sophisticated studies have uncovered the kinetics of the membrane scission reaction, catalyzed by the ESCRT-III component charged MVB protein 4B (CHMP4B) and the vacuolar protein sorting-associated protein 4 (VPS4) ATPase, which constrict the membranous neck of the budding virion to the point of severance, producing a fully enveloped virion[104,105]. Evidently, HIV-1, like all other retroviruses, have evolved to hijack the endosomal protein sorting pathway for virus budding as it does not encode its own membrane fission apparatus[105].

Viral budding and release from the host cell is immediately followed by a maturation step to produce a completely infectious virus particle. This maturation step is mediated by PR, which

cleaves several preordained cleavage sites within Gag and Gag-Pol, yielding their fully processed individual viral components[107]. This step concurrently reorganizes the morphological architecture of the virus[107,108]. The previously radially packed Gag deconstructs to produce a fullerene-like conical viral core made up of CA hexameric rings, housing the NC-bound vRNA[108]. The MA proteins remain anchored to the viral envelope, producing a robust underlying matrix layer[108]. The viral enzymes RT and IN are positioned in proximity to the viral genome within the capsid core[108]. The mature HIV-1 particle is roughly spherical and entertains a diameter of 132 to 146 (nm)[109]. The cytopathic effect of virus will kill the target cell, contributing to the decline of $CD4^+$ T-cell counts characteristic of AIDS[110].

1.5c Circumvention of Host Restriction Factors

The study of HIV-1 has provided a fundamental paradigm for the discovery of virus-host interactions, including host restriction factors. Host restriction factors are interferon (IFN)-induced, germline-encoded proteins that suppress viral infection in a cell-autonomous and dominantly acting fashion[111]. They constitute a key component innate immunity, acting as a first line of defense against invading viruses[111]. Additionally, the presence of these factors within a particular host controls cross-species viral spillover events[111,112]. Nevertheless, HIV-1 has found ways to antagonize and evade these antiviral barriers, relying heavily on the cellular degradation machinery[111]. Several host restriction factors against HIV-1 have been identified and evidence suggest there may be others yet to be elucidated[113]. Examples of HIV-1 host restriction factors are presented in table 2.

Table 2: Human restriction factors antagonizing HIV-1 and mechanisms of circumvention.

Restriction Factors	Stage of Intervention	Mechanism of Restriction	Viral Antagonism	Mechanism of Circumvention	Refs.
Apolipoprotein B mRNA-Editing Enzyme Catalytic Polypeptide-Like 3G (**APOBEC3G**)	RTC Synthesis	As a cytidine deaminase, APOBEC3G removes cytidine residues in retroviral ssDNA causing guanosine-to-adenosine hypermutations in the complementary strand, therefore hampering the genetic integrity of viral information	Vif	Vif recognizes APOBEC3G and sequesters it to be degraded by the cellular ubiquitin-proteasome system	114-117
Tripartite-Motif-Containing 5α (**TRIM5α**)	Capsid Uncoating	TRIM5α recognizes and directly binds incoming retroviral capsids inducing premature disassembly of the capsid and curbing synthesis of retroviral DNA	CA	Human TRIM5α targets retroviruses native to other species such as SIV, but not HIV-1, therefore preventing cross-species transmission	118
Bone Marrow Stromal Cell Antigen 2 (**BST2**)/ **Tetherin**	Virus Budding	Tetherin is a transmembrane protein which hinders budding by physically tethering nascent virions to the plasma membrane	Vpu	Vpu binds tetherin directly and induces its degradation via the cellular ubiquitin-proteasome pathway	119-121
SAM Domain and HD Domain-Containing Protein 1 (**SAMHD1**)	Reverse Transcription	SAMHD1 depletes the intracellular pool of dNTPs for reverse transcription by enzymatically cleaving the phosphate groups off of dNTPs	Vpx	The lentiviral protein Vpx counteracts SAMHD1 by recruiting cellular factors for targeted proteosomal degradation	122-124
Interferon-Induced Transmembrane Proteins (**IFITM**s)	Virus Entry	IFITM1-3 are IFN-sensitive transmembrane proteins that are incorporated into budding progeny virions and impede Env processing and cell-to-cell virus entry	Env	Env is the major determinant of IFITM sensitivity but the mechanism of circumvention is still under investigation	125,126
Myxovirus Resistance Protein B (**MxB**)	DNA Integration	MxB has been shown to impede HIV-1 DNA integration, though whether this occurs prior or after nuclear entry is unclear, however the mechanism is most likely CypA-dependent	CA	CA mutants that are unable to bind CyAp are less sensitive to MxB further suggesting that CA is the specific target for MxB restriction	127-129
Serine Incorporator 5 (**SERINC5**)	Virus Entry	SERINC5 is a transmembrane protein that gets incorporated in budding progeny virions and inhibits subsequent cell-to-cell viral entry by preventing the expansion of the fusion pore	Nef & Env	Nef antagonizes SERINC5 by targeting it for lysosomal degradation, whereas the exact mechanism of SERINC5 antagonism by Env still unknown	130,131

1.5d Establishment of Latency

Shortly after infection, HIV-1 seeds latent viral reservoirs[132]. These reservoirs are largely composed of quiescent, extremely long-lived, memory $CD4^+$ T-cells, but other cell types such as macrophages have been postulated to contribute[132,133]. Latently infected cells contain a dormant provirus, which does not express viral proteins, and thus escapes clearance by the immune system[132]. These cellular sanctuaries allow the virus to persist in the body despite the presence of ART[134]. Of critical importance is the fact that treatment interruption results in virological rebound[134]. Several mechanisms contribute to the maintenance of a latent reservoir. One is the onset of transcriptionally silent heterochromatin and epigenetic alterations of the provirus[135-137]. These include the recruitment of chromatin silencing complexes, increased DNA methylation, histone deacetylation, and the limited availability of positive transcription factors[135-137]. Proviruses may also undergo latency when

submitted to transcriptional interference[138]. This occurs when proviruses integrated in opposite polarity block RNA polymerase II read-through and therefore silence the provirus[138].

1.6 The Quest for an HIV Cure: Strategies and Future Perspectives

1.6a Tackling the Latent Reservoirs

The main barrier to curing HIV-1 is the presence of latent HIV-1 reservoirs[132]. Current HIV/AIDS cure strategies aim to tackle these latent reservoirs. A "functional" HIV-1 cure is defined as a strategy to reduce the size of the reservoirs, thus preventing reactivation and sustaining low viral loads[139]. "Sterilizing" cures aim to completely rid the body of the virus, including latent virus[140].

One cure strategy termed "shock and kill" involves the intentional reactivation of latently infected cells in the hopes of removing their invisibility to the immune system. Reactivation of latent virus is achieved by administering latency-reversing agents (LRAs). LRAs increase viral gene expression[141]. These include the histone deacetylase inhibitors (HDACis), histone and DNA methyltransferase inhibitors, bromodomain inhibitors, and protein kinase C agonists[142]. Cells with increased viral gene expression activate the immune system, which is now being able to flush them out[139,142]. Hence, LRAs constitute the "shock" and immune clearance the "kill". Clinical trials of this approach demonstrated that this technique is unproductive at clearing the viral reservoirs[143-148]. It was shown that although certain LRAs proved successful in reactivating latent virus, none showed a reduction in the amount of infected cells[143-148]. It has been suggested that administering immune activators may help the immune system with the "kill" portion of the strategy[141]. Despite the attention this technique has gained, the preliminary clinical trial data for shock and kill strategies reveal unpromising results and necessitate further evaluation.

Diametrically opposite to "shock and kill" is "block and lock". Instead of reactivating the latent virus, this strategy aims to lock it in a permanent non-expressing state, forever. This is achieved through administration of Tat inhibitors or small interfering (si)RNA targeting the HIV-1 promoter, causing transcriptional gene silencing[149-152]. *In vitro* experiments with these compounds displayed significant silencing of latent virus even in the presence of LRAs[150,152]. Still, block and lock strategies have yet to reach clinical trials. Obvious complications with this strategy are the fact that individuals would still need to take medicines daily and that the HIV-1 provirus would still be

present, threatening to resurface at treatment cessation. Conversely, these drugs may alleviate the inflammatory strain ART is known to cause in some individuals. Also it is recognized that 5 to 8% of human genomes contain transcriptionally silent endogenous retroviruses, therefore a block and lock strategy could perhaps instigate HIV-1 proviruses to become evolutionary genomic passengers such as the endogenous retroviruses[153].

Another arm of the HIV-1 cure field is assigned to gene therapies. Excision of HIV-1 DNA *in situ* has been demonstrated by virtue of gene-editing tools such as the zinc-finger nucleases (ZFNs) and CRISPR-Cas9 (described in section 3)[154-156]. Similarly to shock and kill, these techniques aim to purge viral reservoirs from the body, leading to a sterilizing cure[154-156]. The limitations with gene therapies are finding an appropriate delivery method, targeting the right cellular subtypes, and achieving drug safety[157]. Also, there is always the looming threat of off-target effects with gene therapies[158]. Genetically engineering cells to be refractory to HIV-1 is also widely discussed. This is warranted by the two case studies of one individual and possibly a second whom have been cured of their HIV-1 infection. The Berlin patient and the more recent London patient, whose cure status requires further validation, constitute two previously HIV-1-positive individuals who received bone marrow transplants from donors who were heterozygous for a mutation in CCR5 (CCR5 Δ32) which prevented its cell surface expression[159,160]. Cells received from these donors were thus naturally resistant to CCR5-tropic HIV-1 and lead to HIV-1 remission in the Berlin and London patients[159,160]. Several groups are attempting to recreate this phenomenon *in vitro*; however, this treatment option would not be compatible with most people.

1.6a HIV-1 Vaccine Development

Although not curative, an HIV-1 vaccine could prevent virus transmission in the population at large. Of the several HIV-1 vaccine trials performed thus far, RV 144 (also known as the Thai trial) was the only one to provide supporting evidence of being effective. The initial report demonstrated that the rate of contracting HIV-1 infection amongst individuals who received the vaccine was 31% lower than individuals having received the placebo[161]. Nevertheless, researchers have remained cautiously optimistic about the RV144 vaccine trials.

The obstacles preventing the creation of a successful HIV-1 vaccine include the broad variety of HIV-1 subtypes, its ability to mutate rapidly, and the lack of an animal model that reliably

predicts vaccine efficiency in humans[162]. The current field of HIV-1 vaccinology considers broadly neutralizing antibodies (bnAbs) as an emerging prospective vaccine approach[163]. bnAbs are a type of antibody naturally produced by the body which are able to recognize and block a diverse population of HIV-1 subtypes from entering target cells[163,164]. Their broad target audience is promising, as this would overcome the challenge of developing a traditional vaccine against a small variety of immunogens[163]. Preliminary research conducted in animal models receiving bnAbs through passive transfer is highly optimistic[163]. Many of these studies have reported that the administered bnAbs are able to shepherd the host immune response to activate naïve B-cells to produce fully mature bnAbs, subsequently protecting the animal against HIV-1 challenge[163-167]. The Env fusion peptide is thus far the most promising therapeutic target for the development of bnAbs-based vaccines[163,166,167]. There is widespread consensus in the HIV/AIDS research community that the development of a successful HIV-1 vaccine would be the most promising avenue to eradication of the virus.

2. Membrane Trafficking

2.0 Membrane Trafficking at a Glance

Cellular membrane trafficking is defined as the specific delivery of molecular cargo between subcellular compartments and the plasma membrane. Analogous to a national postal service, cellular membrane trafficking represents a highly regulated delivery system with all the necessary checks and balances to ensure parcels are shipped and tracked appropriately. As such, molecular cargo is continually processed, sorted, and dispatched to specific intracellular locations via membrane-bound vesicles that shuttle along the cellular cytoskeletal highways (see figure 4). Consequently, membrane trafficking is crucial for homeostasis and underlies the fundamental need for cells to meet specific biosynthetic functions such as nutrient uptake, receptor signaling, and macromolecule recycling[168].

2.1 Endocytosis: Imports

Endocytosis is the highly dynamic and intricate process by which extracellular material gains access to an otherwise impermeable intracellular environment using vesicles derived from the invagination of the plasma membrane[168]. Vesicles are formed at the inward expansion of lipid-rich pockets of the plasma membrane, which surround the cargo to be internalized[169]. Through a series of coordinated fusion and fission events, the resulting small vesicle pinches off and is released into the cytoplasm and entered into a highly synchronized endosomal trafficking circuit[169]. The outcomes

are two-fold; the contents are either returned to the plasma membrane or are sorted for proteosomal degradation via a pathway terminating at a highly acidic organelle termed the lysosome[169].

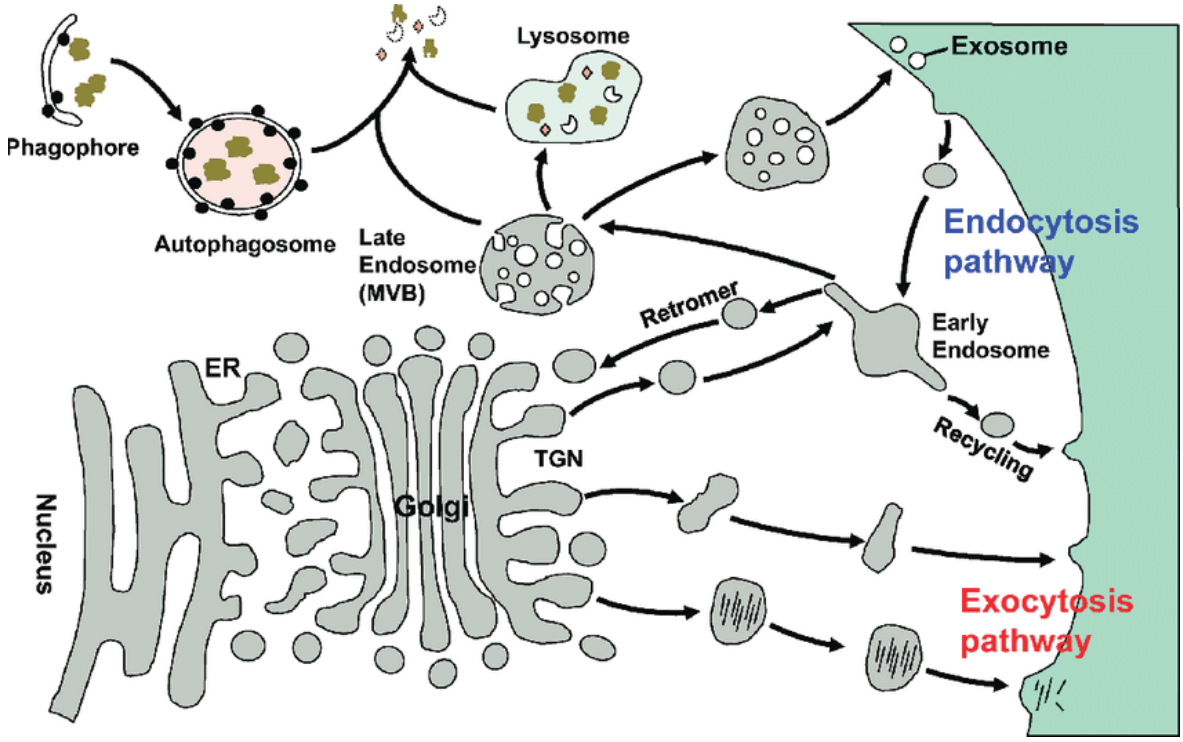

Figure 4: Overview of the membrane trafficking pathway. Membrane trafficking encompasses the endocytosis pathway for entry into the cell, the exocytosis pathway for exit from the cell, the endolysosomal vesicular system, the autophagy pathway and the cytoskeleton. Movement within the membrane trafficking pathway is highly regulated, bidirectional, and sensitive to the metabolic needs of the cell and its dysregulation had been associated to various diseases. Figure obtained from Hasegawa *et al.* [170].

Receptor-mediated endocytosis involves the non-covalent binding of a ligand to its respective cell surface receptor, triggering their internalization[169]. The canonical receptor-mediated endocytosis pathway is clathrin-mediated endocytosis. This type of endocytic internalization utilizes a triskelion-shaped protein named clathrin, found on the intracellular face of the plasma membrane[171]. Its particular geometry allows clathrin to polymerize into a hexagonal lattice-like cage below the membranous bulge containing the receptor-ligand duo[171]. Clathrin-cage initiation is followed by the recruitment of modular clathrin adaptor proteins that regulate the dynamics of vesicular membrane shaping and bending[169]. Caveolae-dependent endocytosis is an alternative mechanism of cellular entry that is clathrin-independent and uses cholesterol- and glycosphingolipid-rich membranous rafts termed caveolae[172]. Caveolae oligomerization causes a local change in membrane morphology that drives the formation of an endocytic vesicle[173,174]. Furthermore, clathrin- and caveolae-independent endocytosis pathways include the RhoA-dependent interleukin 2 (IL-2) receptor endocytosis, the Arf6-associated pathway, and flotillin-mediated endocytosis[175].

Mechanistically, these endocytic pathways differ on the basis of their cargo selection and on the nature of host factors orchestrated to carry out these tasks. Nonetheless, these pathways are collectively characterized by their reorganization of the underlying cortical actin network, the regulation of membrane phospholipid dynamics, the need for dynamin-mediated vesicle pinching and their reliance on the endosomal circuitry for the recycling of endocytic machinery[176].

2.2 Exocytosis: Shipping and Receiving

The opposite function of endocytosis is exocytosis, also called the biosynthetic-secretory pathway. The constitutive biosynthetic-secretory pathway delivers molecules synthesized by the cell to various subcellular compartments or the plasma membrane through highly regulated, sequential, and bidirectional vacuolar transport. Proteins are manufactured in the ER and packaged into budding membrane-enclosed vesicles that are destined for the Golgi apparatus[177]. These vesicles are made up of coat proteins II (COPII), which regulate anterograde-directed transport while protecting and segregating nascent proteins from the cytoplasm[177]. These vesicles fuse with acceptor membranes found at the *cis* "receiving" face of the Golgi, and release their cargo into its membranous folds[177]. The Golgi apparatus plays an important role in the decoration, folding, and sorting of nascent proteins[178]. ER-resident proteins are cycled back to the ER via COPI vesicles[177]. All other proteins are loaded and "shipped" out of the *trans*-Golgi network (TGN) into secretory vesicles called endosomes[179]. Endosomes are born from the TGN, stealing a membranous coat to envelope and isolate cargo[179]. These vesicles traffic to their delivery site along the microtubules and fuse with acceptor membranes to deliver their contents[179].

2.3 Rab GTPases and the Endolysosomal System: Traffic Control

Endosomes are part of a larger, highly dynamic, interconnected, vesicular-tubular network collectively known as the endolysosomal system[180]. This system has four principal components: the early endosome, the recycling endosome, the late endosome, and the lysosome[180]. Rather than existing as independent structures, these compartments are transient, having the ability to metamorphose into one another[180,181]. Coordinating these events is a family of small GTPases called the Ras-related proteins in brain, hereinafter referred to as Rab[181]. There are over 70 members of the Rab family in mammalians, all playing central roles in cell growth and metabolism[181,182]. These small 20-25 kilodalton (kDa) proteins cycle between inactive (GDP-loaded) and active (GTP-loaded) states in order to temporally and spatially organize endosomal vesicle trafficking[181,183]. Moreover,

Rabs communicate with many signaling cascades in order to regulate endosomal biogenesis and trafficking depending on the metabolic needs of the cell[181,183]. Rabs are found in the cytoplasm as soluble prenylated proteins bound to a cognate GDP dissociated inhibitor (GDI)[184,185]. Specific cellular clues will trigger the recruitment of certain Rabs to endosomal membranes where they will encounter their respective guanine nucleotide exchange factor (GEF)[186]. GEFs regulate the molecular switch from GDP to GTP, which in turn stabilizes the Rabs on endosomal surfaces[181,186]. Active Rab-GTP enables the recruitment of a vast array of effector molecules to the membrane[186]. GTPase activation proteins (GAPs) trigger GTP hydrolysis, disembarking the Rab from the endosomal membrane and replacing it with a different Rab[186]. These subtle but intricate Rab switches are what make the Rabs master regulators of intracellular membrane trafficking.

The internalization of ubiquitinated cargo in endocytic vesicles acts as a cellular trigger for the recruitment of Rabex-5, a Rab5-GEF, to the vesicular membrane[187,188]. Rabex-5 will in turn promote the concentration of Rab5 on the membrane, marking these structures as Rab5-positive early endosomes[187,188]. The exchange of Rab5 for Rab11 yields a structural change to a recycling endosome[185,189]. Recycling endosomes loop between early endosomes and the plasma membrane to recycle proteins, such as ion transporters, back to the cell surface for recurring rounds of endocytosis[185,189]. Early endosomes mature into late endosomes, corresponding to a loss of Rab5 concomitant to a gain of Rab7, as illustrated in figure 5[190]. The Rab7-specific GEF Mon1-Ccz1 promotes the Rab5-to-Rab7 conversion into late endosomes[191].

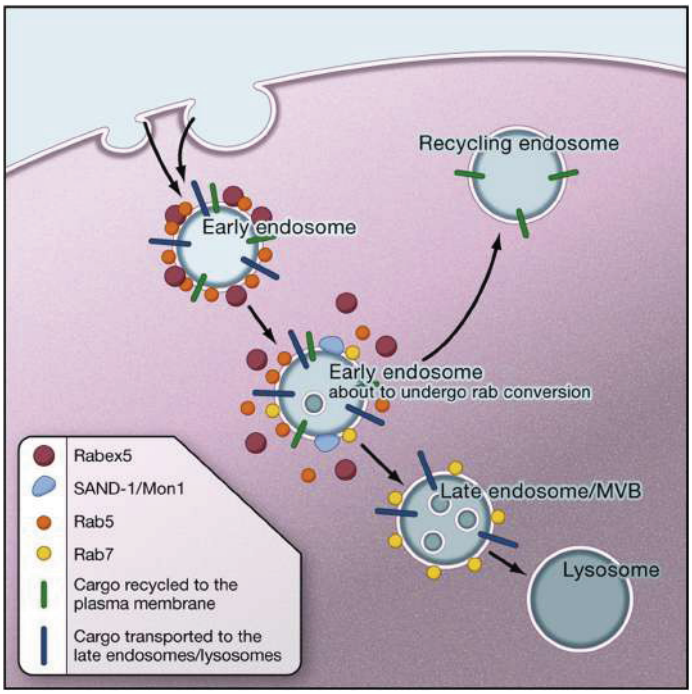

← **Figure 5: The endolysosomal pathway.** The Rab5 GEF Rabex5 recognizes ubiquitinated cargo from endocytosis-derived vesicles, recruiting Rab5 to these early endosomal membranes. The early endosome can either return its cargo to the plasma membrane via recycling endosomes or undergo Rab conversion into late endosomal structures. The conversion is mediated by the release of Rabex5 and Rab5 from the endosome and the concurrent recruitment of the Mon1-Ccz1 (yeast nomenclature: SAND-1/Mon1) and Rab7. Late endosomes deliver their contents to the dead-end organelle, the lysosome, to be recycled as constituent macromolecules back to the cell. Image acquired from Poteryaev *et al.* [190].

Late endosomes fuse with lysosomes, which release hydrolytic enzymes to allow the orderly break down of bulk cargo into macromolecules, providing fresh building blocks for various cellular processes[192]. The presence of proton pumps on endosomal membranes generates a stable pH gradient concurrent with the maturation process[180]. Early endosomes entertain a slightly acidic pH of 6.5 to promote dissociation of receptors from their ligands, late endosomes have a pH of 5.5, and lysosomes are highly acidic with a pH of about 4.5[180]. Like late endosomes, lysosomes are Rab7-positive and cluster in a perinuclear region, complicating their distinction. Thus, they are often coined late endosomes/lysosomes (LE/Lys)[191]. This ambiguity highlights the fluidity and transitory nature of the organelles in this pathway. Rabs are chiefly involved in endolysosomal positioning but have also been shown to play key roles in other cellular processes such as Golgi protein sorting and phospholipid metabolism[181].

2.4 Autophagy: Waste Management and Recycling

Macroautophagy, henceforth called autophagy, is a pathway intimately involved in membrane trafficking, which allows lysosomal degradation and recycling of cellular material. Autophagy occurs at basal levels as a cellular purging mechanism, although it is enhanced during periods of starvation, energy depletion, and cellular stress[193]. In contrast to the ubiquitin-proteasome degradation pathway that ensures the degradation of short-lived proteins, autophagy entails the selective degradation of long-lived proteins and whole organelles[194]. Autophagy can be conceptualized in four steps, shown in figure 6. The process is started in step 1: initiation, with the mechanistic target of rapamycin (mTOR) serving as a sensor of cellular metabolism and physiology, monitoring changes in nutrient depletion and stress and also acting as a negative regulator of autophagy[193,194]. A demand for autophagy will cause inhibition of mTOR through upstream signaling pathways and activation of the autophagy pathway[194]. Step 2: autophagosome formation, which involves two networks of autophagy adaptor proteins, the ULK complex and the PI3K-III complex, that instigate the nucleation of isolated membrane structures originating from the ER[193]. This is followed by step 3: maturation, in which two ubiquitin-like conjugation systems, the Atg12-Atg5-Atg16L complex and the LC3B-PE complex, facilitate the maturation of the isolated membrane into a double-membraned vesicle coined the autophagosome, which engulfs selected material to be degraded[193,194]. Finally in step 4: fusion, the autophagosome merges with the endolysosomal system, fusing with late endosomes to create transitory organelles called amphisomes, or fusing directly with the lysosome for bulk cargo digestion by the lysosomal acid hydrolases[192].

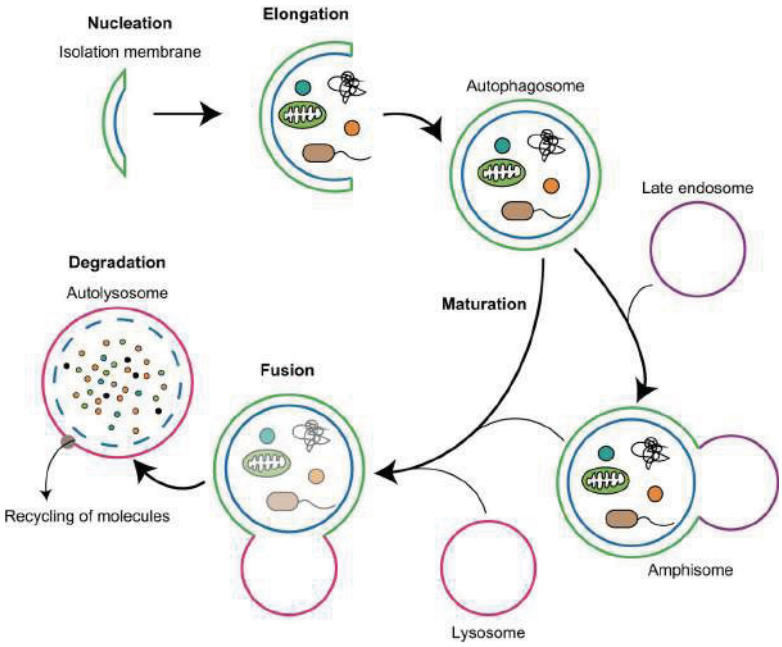

Figure 6: The autophagy pathway. Autophagy is the waste management and recycling facility of the cell. When the cell is in need of nutrients it shuts off mTOR signaling, which in turn activates several networks of autophagy factors to create a double-membraned structure called the autophagosome. This structure matures and sequesters cellular material to be digested. The autophagosome can first fuse with late endosomes to transfer bulk material, or directly fuse with the lysosome for lysosomal-mediated degradation of the engulfed cargo and return of essential nutrients to the cell. Image acquired from Nakamura and Yoshimori[192].

2.5 Cytoskeleton: Intracellular Highways

The cytoskeleton, as the name implies, is the frame-like structure that provides mechanical support to the cell, giving it its shape and internal organization[195]. The cytoskeleton encompasses a network of different filaments, notably, the intermediate filaments, the actin filaments and the microtubules. Intermediate filaments are non-polarized, stable, rope-like fibers, which provide the bulk of the mechanical strength to cells[195]. Actin filaments are found as an elastic meshwork cushion at the cell cortex, predominantly supporting the plasma membrane[196]. Actin filaments are made up of repeated actin subunits, which polymerize into long spiral chains[196]. Actin filaments are polarized filaments meaning they hold a plus (+) and minus (-) end, with ATP-generated polymerization occurring at the (+) end[196].

Like actin filaments, microtubules are also dynamic polarizing structures, which are constantly assembling at their (+) end and disassembling at their (-) end[197]. Moreover, microtubules are composed of dimers of α-tubulin and β-tubulin, which polymerize to form large, hollow, cylindrical structures[197]. The microtubules are the true intracellular highways as they are the tracks for the dynein and kinesin microtubule-associated proteins (MAPs). Kinesins are globular two-headed molecules, which direct anterograde (+) end directed transport from the cell periphery towards the microtubule-organizing center (MTOC)[198]. Kinesins do so by walking their head groups on the microtubules, a process that is ATP-dependent. Due to their directionality, kinesins play important roles in guiding vesicles derived from endocytosis to the cell center[198]. On the other hand,

dyneins regulate retrograde (-) end directed transport from the MTOC to the cell periphery[199]. Like kinesins, dyneins are also dimeric two-headed motor-cargos, with two heavy chains forming the head domains[197]. However, they differ on the basis that they require a myriad of microtubule-binding proteins to activate movement[199]. One such binding partner is dynactin, a hetero-complex of eight subunits including p150^{Glued}, which has been implicated in dynein cargo recruitment[199]. For example, the LE/Lys marker Rab7 interacts directly with p150 ^{Glued} and Rab-interacting lysosomal protein (RILP) linking the endocytic vesicles to the microtubules for controlled (-) end directed movement by dynein[199]. The opposing polarity of kinesin and dynein motors creates a tug-of-war with the winner defining the net direction of movement along the microtubules[200].

2.6 Membrane Trafficking and HIV-1

As non-living and obligate intracellular parasites, viruses have evolved to highjack the cellular membrane trafficking pathway for productive reproduction within their respective host. Due to genome size constraints, viruses cannot encode their own means of intracellular travel; instead they use the host cellular machinery at their disposal. In this way, viruses mediate entry into cells, replication of their viral components, transport of their viral proteins and nucleic acids, and viral budding and egress. To a certain extent, cells have developed an arsenal of methods to counteract the seizure of membrane traffic by viruses. Indeed, studying viruses has underpinned most of our existing knowledge of membrane trafficking and the underlying molecular functions.

HIV-1 interacts substantially with various components of the membrane trafficking pathway. Electron microscopy investigations have revealed HIV-1 co-opting clathrin adaptors to mediate entry into cells through CD4/co-receptor-mediated endocytosis[201-203]. Furthermore, the HIV-1 Env glycoprotein has been shown to traverse the biosynthetic-secretory pathway, utilizing the endocytic recycling pathway to direct incorporation into growing virus particles[204,205]. Several bodies of evidence implicate various Rabs in the replication of HIV-1[204-208], reviewed by Spearman[209]. A study by Caillet *et al.* demonstrates that siRNA silencing of the LE/Lys marker Rab7 (human isotype Rab7a) hinders HIV-1 virion budding[208]. This hindrance was postulated to be due to an observed impediment in the proteolytic maturation of Env gp160 to gp120 and gp41[208]. The specific role of Rab7a in the onset of this particular phenotype has not been explored[208]. The authors note that a defect in virus budding is typical of BST2/tetherin-mediated restriction of virus budding in Vpu-deficient viruses[208]. In fact, results show co-localization of BST2/tetherin with Env-positive patches

on the plasma membrane in HeLa cells, despite the presence of Vpu, further suggesting that HIV-1 depends on Rab7a in the later stages of its replication cycle[208].

HIV-1 has also been proven to interplay with autophagy and lysosomal trafficking. Cinti *et al.* have clearly demonstrated that HIV-1 negatively modulates autophagic flux in T-cells by counteracting the physiological trafficking and acidification of LE/Lys, hindering their eventual fusion with autophagosomes[210]. This impediment of LE/Lys movement benefits HIV-1 survival by blocking the degradation of nascent virions by the autophagosome-lysosome fusion event[210]. Likewise, as mentioned previously, growing bodies of literature report HIV-1 co-localizing with endosomal surfaces, further demonstrating the importance of the endolysosomal pathway in viral production[87-92]. This is supported by the fact that disruption of anterograde-directed endosomal vesicular transport by targeting dynein p150 ^{Glued} significantly reduces virus output (Lehmann *et al.*[90,210]). In fact, HIV-1 has been shown to rely on the polarity of several dynein and kinesin motors to promote capsid uncoating and active transport to the nucleus for import[211-213].

These findings accentuate the fact that HIV-1 has evolved to reprogram intracellular membrane trafficking to facilitate key steps of infection. However, the network of host factors involved in the HIV-1 replication cycle and their mechanisms of action are still unknown. Exploration of these avenues is imperative to understanding the scope of HIV-1 pathogenesis. With recent technological advances, we are better equipped to identify and characterize host factors that are required for HIV-1, including entire cellular pathways such as the membrane trafficking pathway.

3. CRISPR

3.0 CRISPR: Discovery and Characterization

The powerful gene-editing platform that is CRISPR was initially stumbled upon by chance by Ishino and colleagues in 1987. The group reported an array of distinct repetitive DNA elements interspaced by disparate, non-repetitive DNA segments, downstream of their gene of interest, the aminopeptidase *iap* in *Escherichia coli* K12[214]. Following this first encounter, such distinctive loci were subsequently documented in other bacterial and archaeal species as their genomes became available to researchers. More than two decades later, in 2002, these loci were coined the clustered regularly interspaced short palindromic repeats (CRISPR) for the first time[215,216]. The unique fragments of nucleotides found in between the 18-36 bp-long CRISPR elements were termed spacers. Several

research groups simultaneously revealed that these spacers bore perfect homology to the genome of various phages, the viruses that infect prokaryotes[217-219]. Furthermore, the genes located immediately upstream of the CRISPR cassette were found to encode CRISPR-associated (Cas) proteins, which differed in composition amid various species[217,220].

These compelling findings led scientists to believe that the CRISPR-Cas systems may confer resistance to invading genetic material such as phages[220]. This theory was confirmed in 2007, when the bacterium *Streptococcus thermophilus* was able to capture novel spacer sequences from a phage and execute Cas-directed elimination of the phage upon future infection, thus functioning as an adaptive defense system[221]. Soon thereafter, another research group demonstrated that the spacer sequences were actively transcribed into small, non-coding, interfering RNAs, termed CRISPR RNAs (crRNAs)[222,223]. In 2011, French scientist Dr. Charpentier and group discovered a secondary small RNA molecule, called a *trans*-activating CRISPR RNA (tracrRNA), which forms a duplex with the crRNA[224]. This RNA pair was shown to bind and guide the effector protein, Cas, to a complementary genomic location within incoming phages[224]. CRISPR-mediated antiviral immunity constitutes the hallmarks of adaptive immunity, marked by the creation of immunological memory following a first round of infection, culminating in the highly specialized and robust antiviral response upon subsequent encounters with the same pathogen. With its mechanism of viral interference relatively elucidated, the CRISPR-Cas system gained more attention in the science community, leading to its bioengineering for pursuits beyond prokaryotic antiviral immunity.

3.1 CRISPR: Components and Mechanism of DNA Interference

The type II CRISPR-Cas9 system, originating from *Streptococcus pyogenes,* is the best-characterized CRISPR system and constitutes the molecular basis of the CRISPR platforms used in laboratories around the world to date.

3.1a Spacers and Protospacers

Spacers are positioned between repeated CRISPR elements in the prokaryotic genome in chronological order, thus creating a timeline of foregoing infections[219,225]. The corresponding fragment of DNA from which the spacer is derived within the attacking virus or plasmid is called a protospacer, *proto-* meaning precursor. In CRISPR-Cas9 systems, the length of the protospacer is typically 20 nucleotides. Protospacers within invading viral or plasmid DNA are not chosen arbitrarily, but instead are selected upon the presence of a protospacer adjacent motif (PAM)[225,226]. A

PAM consists of a 2-6 bp DNA segment immediately tailing the protospacer sequence, of which the canonical motif is the 3 bp-long 5'-NGG-3' in type II systems[226].

3.1b crRNA Biogenesis

Transcription of the CRISPR locus initially produces a single, long transcript, encompassing the CRISPR repeats and the spacers, coined the pre-crRNA[224,227]. The pre-crRNA is then subsequently digested into smaller fragments, termed crRNAs, by the cellular RNA-specific ribonuclease, RNase III, and Cas9[224]. A typical crRNA includes a homozygous 3' end consisting of 8 bp derived from the CRISPR repeat, and a heterozygous 5' end derivative of the unique neighboring spacer[224].

3.1c tracrRNA Scaffold

Type II CRISPR systems require the presence of a tracrRNA, which is transcribed alongside the pre-crRNA cassette[224]. This small, *trans*-encoded RNA molecule binds to the 3' repeat of the crRNA, forming an RNA duplex[224,228]. The tracrRNA aids in the maturation of the crRNA by recruiting RNase III and Cas9 and helps stabilize the RNA hybrid in the RNP complex[224].

3.1d Cas9 Endonuclease

The elucidation of the *S. pyogenes* Cas9 crystal structure in 2014 demonstrated that the enzyme bears two lobes: the recognition lobe (REC) and the nuclease lobe (NUC)[229]. The REC lobe is further divided into two domains: REC-I and REC-II. REC-I binds the crRNA:tracrRNA heteroduplex, whereas the role of REC-II is still not well understood[229]. The NUC lobe encompasses three domains: RuvC, NHN, and the PAM-interacting (PI) domain[229]. Molded between the two lobes is a positively charged groove that accommodates the complementary single strand of DNA being scanned[229,230]. This allows the PI domain to confer specific recognition of the PAM sequence and initiates binding when it encounters one[229,230]. It is at this point that Cas9 will unwind the bases upstream of the PAM to begin complementary pairing of the crRNA to the target DNA in a zipper-like fashion via Watson-Crick base pairing[229,230]. Once properly bound to the DNA, the NUC-derived RuvC and NHN domains cleave the DNA three nucleotides upstream of the PAM causing a dsDNA break (DSB); the RuvC domain cleaves the non-complementary strand and NHN the complementary strand[229]. With suggested resemblance to the small siRNA pathway[231], the CRISPR-Cas9 system requires the coming together of various components to execute RNA-mediated cleavage of exogenous genomic material.

3.2 Adapting CRISPR-Cas9 From Biology to Biotechnology

The simplicity and accessibility of CRISPR-Cas9 made it an ideal candidate to be artfully bioengineered into a eukaryotic DNA-editing tool. Drs. Charpentier and Doudna collaborated to simplify the crRNA:tracrRNA duplex by fusing them into a single RNA chimera using an artificial tetraloop[228]. This so-called synthetic guide RNA (sgRNA), shown in figure 7, can easily be designed to target any unique, 20 nucleotide-long sequence of interest with the only prerequisite being the presence of an accompanying 3' NGG PAM. There are over 40,000 possible sgRNA target sites in the human genome alone, creating vast possibilities of RNA-programmable genome editing[228]. Likewise, the recombinant *S. pyogenes* Cas9 used in most CRISPR toolboxes nowadays has been mammalian codon-optimized and includes nuclear localization signals (NLSs) for improved nucleus localization[232]. As such, the Cas9 and crRNA:tracrRNA/sgRNA RNP complex compartmentalizes to the nucleus for recognition and cleavage of target chromosomal DNA[232].

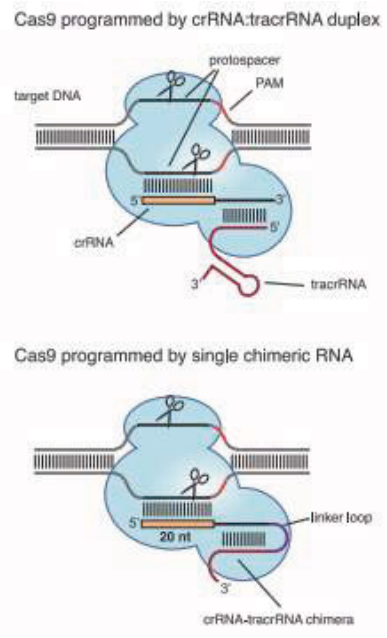

← **Figure 7: Comparison of the RNA duplex and RNA chimera in CRISPR systems.** The upper panel portrays the natural configuration of Cas9 (light blue) complexes with an RNA duplex made up of the crRNA with its cognate tracrRNA. The lower panels displays the duplex simplified into a single RNA chimera by tethering the tracrRNA to the crRNA using an artificial linker loop (purple). The scissors represent the cleavage sites for the Cas9 endonuclease domains. Figure obtained from Jinek *et al.*[228].

Unlike prokaryotic cells, eukaryotes exploit endogenous DNA repair machineries to repair DSBs produced by nucleases, including Cas9. Most often, the nonhomologous end-joining (NHEJ) pathway is employed to repair DSBs. In this pathway, the cellular Ku70-Ku80 heterodimers recognize and bind DSBs, creating a molecular scaffold to aid the recruitment of other NHEJ co-factors[232]. Then, endogenous DNA polymerase fills in the missing gap with the random insertion or deletion of nucleotides, collectively known as indels. These indels cause frameshift mutations, abrogating the normal reading frame of the gene, thus causing a knockout gene (KO). Alternatively, the insertion of a DNA donor oligo template facilitates the introduction of precise genetic modifications, known as homology-directed repair (HDR)[228,232].

3.3 Applications of CRISPR

3.3a CRISPR Therapeutics

Its ability to introduce meticulous tweaks to the genome warrants CRISPR-Cas9 technology a spot in the field of biomedicine. So-called CRISPR therapeutics aim at correcting genetic disorders by fixing gene-level defects though a Cas9 cleavage and HDR sealing mechanism. Another arm of CRISPR biomedicine is allocated to bioengineering cells that are resistant to cancer or viral infections, such as the human $CD4^+$ T-cells which were made resistant to HIV-1 infection by CRISPR-Cas9 removal of the CCR5 co-receptor in 2017[233]. The CRISPR-Cas9 system has also been used to directly target the HIV-1 provirus in order to excise it from chromosomal DNA[234,235]. However, the extraordinary mutability potential of the virus has made targeting it in this way very challenging[234,235]. Shocking news made waves in the science community in November 2018 when claims surfaced announcing a Chinese scientist had genetically engineered human embryos to knockout CCR5 using CRISPR, which were then used to impregnate women through *in vitro* fertilization[236]. Although no scientific reports have yet to be published, these alleged "CRISPR babies" might be the first report of CRISPR being used to genetically engineer humans, sparking many ethical debates around the globe. The CRISPR field is dynamic and has developed immensely over the last six years, leaving much to the imagination of what is to come.

3.3b A New Tool in the Molecular Biology Toolbox

CRISPR has outcompeted its predecessors, the transcription activator-like effector nucleases (TALENs) and ZFNs, by a large margin, particularly in the area of ease of cloning, cost-effectiveness, and ability to multiplex[237]. Moreover, breakthroughs within the field have produced specialized Cas9 mutants and Cas9 fusion proteins providing a versatile assortment of tools to help answer outstanding questions in virtually any field of study[237]. More importantly, the CRISPR-Cas9 system has helped answer fundamental questions about the causal relationship between phenotype and genotype in health and disease when used in a functional genomics screening approach, referred to as a CRISPR screen.

3.3c CRISPR-Cas9 Genetic Screens

Functional genomics is a powerful field that allows precise interrogation of gene and protein function on a global scale, achieved through the introduction of genetic perturbations. When performed in high-throughput screening platforms, functional perturbations can cause loss-of-

function or gain-of-function, depending on the nature of the inquiry. Classically, RNAi-based functional genetic screening platforms have provided useful information; however, the level of mRNA silencing or activation is often inadequate, unreliable, and conducive to off-targets effects. CRISPR-mediated gene editing in a screening approach holds many advantages over its RNAi forerunner. Firstly, CRISPR-Cas9 yields clear-cut genetic perturbations that are user-defined and easily multiplexed, creating many adaptable genotypes[238]. Likewise, CRISPR induces permanent somatic mutations that are retained during DNA replication, thus generating stable cell lines[238]. A single round of transfection is needed to produce a full knockout, in comparison to multiple rounds needed for sustained knockdown using RNAi technologies[238]. Hence, one is left with a more robust genotype and phenotype, which also highlight gene essentiality.

Two types of CRISPR-Cas9 screening platforms have been developed: pooled and arrayed. Pooled screens consist of a mix of predesigned, generally plasmid-bound, guide (g)RNAs supplied to a population of cells in hopes of identifying the genotypic cause underlying a particular phenotype, when combined with next-generation sequencing (NGS)[239]. Pooled screens are often used with genome-scale CRISPR knockout (GeCKO) gRNA libraries, providing a comprehensive and unbiased examination of the genome[240]. By comparison, smaller and more focused gRNA libraries are used for interrogation within a particular gene set. These libraries are principally used in arrayed screening platforms, whereby a single gene perturbation occurs per well in 96- or 386-well plates[241]. In contrast to the pooled approach, arrayed screens are high-throughput and thus easier to multiplex with a range of phenotypic readouts and overcome the need the decipher hits using NGS[240,241]. Both screening platforms have proved to be powerful tools amongst various disciplines, the adoption of either platform depending largely on the user and the nature of the query.

3.4 CRISPR-Cas9 Screens as a Tool to Investigate the Virus-Host Interaction Network

The advent of CRISPR screens quickly preceded its implementation in the complex investigation of virus-host interactions. Through complete ablation of their gene targets, GeCKO screens have identified host factors that are indispensable for the replication of several viruses of clinical importance, including HIV-1, Hepatitis C virus, Zika virus, West Nile virus, and Dengue virus[242-245]. These screens have enabled the systematic analysis of viral host dependency factors (HDFs)[242]. HDFs are cellular gene products that are dispensable for cellular viability but necessary for the survival and spread of the virus within its host[242]. HDFs reflect the crucial role of certain

host factors in the replication of viruses while posing as attractive antiviral drug targets, seeing as their elimination has minimal cellular toxicity.

3.5 HIV-1 CRISPR Screens

The field of HIV-1-host interactions has benefitted greatly from the advent of CRISPR genetic screens. So far, three major CRISPR screens have been performed in relation to HIV-1 infection (outlined in table 3); two reported the CD4 receptor and the CCR5 co-receptor as HDFs, in agreement with earlier reports in the literature[233,242,246]. The first HIV-1 CRISPR screen performed by Hultquist *et al.* employed a focused gRNA library to screen for host factors involved in integration[246]. In addition to CD4 and CCR5, this study validated two previously known HIV-1 co-factors, LEDGF and transportin 3 (TNPO3), as essential cofactors for HIV-1 integration[246]. A second study performed by Park *et al.* aimed to elucidate novel candidate HDFs which make cells refractory to HIV-1 infection[242]. They discovered two genes: *SLC35B2* and *TPST2*, involved in the sulfation of CCR5 and its transport to the cell surface, respectively[242]. These elegant and innovative studies are limited by their exclusive analysis of the early events of the HIV-1 replication cycle. This limitation is owed to their method of analysis. Both studies used cell models that express a Tat-dependent green fluorescent protein (GFP) as a measure of HIV-1 infection, monitored at the single-cell level by flow cytometry[157,161]. Tat is expressed prior to unspliced vRNA export and viral trafficking and assembly and thus these crucial steps are not captured by their approaches[157,161].

Another CRISPR screen performed by Jin *et al.* uncovered two novel genes involved in the maintenance of HIV-1 latency: *TSC1* and *DEPDC5*[247]. These authors performed a genome-wide screen in a specialized T-cell model containing latently integrated HIV-1 that expresses GFP upon reactivation[247]. Gene knockouts that led to virus reactivation represented genes that may play a part in the homeostatic conservation of latent reservoirs, therefore uncovering potential therapeutic targets[247]. Their hits, *TSC1* and *DEPDC5*, encode gene products that individually suppress key steps of the mTOR signaling cascade, a pathway previously reported to be involved in latency[247,248]. In contrast to the two previous major CRISPR screens, the study by Jin *et al.* revealed cellular factors that contribute to HIV-1 pathogenesis post-integration[247]. Similarly, the authors note that the mTOR pathway is highly dependent on autophagy and LE/Lys degradation, and as such, these cellular processes may contribute significantly to the maintenance of HIV-1 latency, further convincing us to focus on these pathways[247].

Table 3: Published genome-wide CRISPR screens in HIV-1 infection

CRISPR Screen	Purpose of Screen	Cell Line Used	Phenotypic Analysis	Screen Hits	Notes
Hultquist *et al.* **Oct 2016** Cell Reports	Identification of HIV-1 IN co-factors using a novel RNP electroporation technique	Primary human $CD4^+$ T-cells	Intracellular single-cell monitoring of GFP expression via flow cytometry and intracellular staining of p24	*CXCR4, CCR5, LEDGF, TNPO3*	These authors performed a rather exclusive refinement of screen hits focusing on HIV-1 IN, which would be ideal candidates for drug development
Park *et al.* **Feb 2017** Nature Genetics	Identification of genome-wide HIV-1 HDFs in a physiologically relevant cell system	Primary $CD4^+$ T-cells Coined "*GXRCas9*"; expresses GFP during productive HIV-1 infection.	Single-cell monitoring of GFP expression via flow cytometry	*CD4, CCR5, TPST2, SLC35B2, ALCAM*	Candidate genes relate to the processing of CCR5 for presentation on T-cells, with the exception of *ALCAM*, which may or may not play a role in the function of CCR5
Jin *et al.* **Aug 2018** Emerging Microbes and Infections	Identification of HIV-1 HDFs involved in the maintenance of latent reservoirs	HIV-1 latently infected Jurkat T-cell line (C11) with integrated GFP reporter expressed upon reactivation of latent provirus	Monitoring of latent GFP reactivation via flow cytometry	*TSC1, DEPDC5*	*DEPDC5* is involved in the amino acid signaling pathway of mTOR, which is closely linked to LE/Lys trafficking, although this was not explored in the article

As highlighted previously, a knowledge gap exists in the identification of host factors usurped by HIV-1 in the later stages of the retroviral life cycle, including those potentially involved in the trafficking of viral proteins and RNA for virus assembly. Late-stage HDFs have been overlooked in previous CRISPR screens due to methods of phenotypic analysis as well as the overall aim to identify factors that when knocked-out, make cells resistant to HIV-1 infection. Therefore, there is an unprecedented need to illuminate the mechanistic events occurring in the later stages of the viral life cycle, providing opportunities to answer outstanding questions about virus trafficking and to identify novel areas for antiviral drug intervention. The CRISPR screen platform provides an ideal approach to identify such cofactors when paired with the ideal phenotypic readouts.

4. CRISPR-Cas9 Analysis of the Interactions Between HIV-1 and the Cellular Membrane Trafficking Pathway

There is substantial evidence hinting at the fact that HIV-1 co-opts the membrane trafficking pathway during various stages of its replication cycle. We hypothesize that HIV-1 targets this pathway to reprogram intracellular trafficking routes to benefit its own replication and survival. Nevertheless, the mechanisms by which HIV-1 arbitrates its hold on the cellular membrane trafficking pathway remain to be elucidated. Uncovering and understanding the virus-host relationships between HIV-1 and the membrane trafficking pathway will likely help to resolve areas of HIV-1 pathogenesis that are not currently understood, such as Gag/vRNA trafficking. The

emergence of precise gene-editing technologies such as CRISPR-Cas9 provides new ways to tackle these long-standing biological questions. By completely depleting cells of certain endosomal factors and trafficking factors, we can potentially identify which ones are hijacked by HIV-1 during its intracellular movement. Conversely, by such means we could also identify novel host restriction factors that, when eliminated, provide the virus with a chance to flourish and replicate more productively compared to wild type settings. Outlined below are our two specific aims in the investigation of the specific relationships between HIV-1 and cellular membrane trafficking.

4.1 Aim 1: CRISPR Screen of the Membrane Trafficking Pathway

In this study, we employed an arrayed CRISPR-Cas9 screening platform paired with an arrayed library of genes involved in intracellular membrane trafficking to identify novel HIV-1 HDFs. To monitor the effect of gene knockout on HIV-1 infection we used a viral infectivity assay to probe the early events of HIV-1 replication and a virus production assay to uncover defects in virus output. Using these methods, we are able to investigate which genes facilitate or restrict virus production, data of which may be confirmatory of genes previously identified to be implicated in HIV-1.

A library of predesigned crRNAs of 140 membrane trafficking genes was employed, with four crRNAs per gene in an arrayed format for functional gene knockout analysis. A HeLa-based HIV-1 reporter cell line, named TZM-bl, was used to conduct the CRISPR-Cas9 screen. This cell line expresses both HIV-1 co-receptors and contains a Tat-responsive HIV-1 LTR driving firefly luciferase, allowing the measurement of HIV-1 infectivity[249,250]. We transfected these cells with a plasmid to express the mammalian codon-optimized Cas9 endonuclease protein. The success of this transfection was confirmed by Western blotting. Stable, Cas9-expressing TZM-bl cells were seeded into 96-well plates and transfected with the membrane trafficking library. After assessment of cell viability, we challenged the genetically edited cells with HIV-1 and examined the effects on luciferase reporter gene expression and virus production. A natural extension of the project will be to validate candidate hits received from the screen as stable knockouts in a biologically relevant T-cell model such as the SUP-T1 cells. This will aid in deciphering the underlying molecular mechanisms driving the anticipated phenotype. Microscopic techniques such as immunofluorescence (IF) and fluorescence *in situ* hybridization (FISH) will be useful techniques to monitor intracellular trafficking events.

4.2 Aim 2: Probing Rab7a Function in HIV-1 Infection Through CRISPR-Cas9 Gene-Editing

We are interested in furthering the investigation of the function of the various steps of autophagy in HIV-1. With pivotal roles at the interface of autophagy and LE/Lys trafficking, Rab7a is an ideal target for HIV-1 to hijack to control intracellular trafficking. Previous studies have suggested a role for Rab7a in the maturation and infectivity of HIV-1 particles; however, the mechanistic insights by which HIV-1 interacts with Rab7a are still pending elucidation.

Rab7a, which is not included in our screen in aim 1, was knocked-out using an RNA-programmable CRISPR-Cas9 system. By depleting these cells of Rab7a, we are able to study the consequence of Rab7a knockout on HIV-1 replication. We expected that gene editing out Rab7a will thwart virus infectivity and propagation, in agreement to the siRNA studies by Caillet *et al.* [208]. We believe this phenotype is due to HIV-1 hijacking the Rab traffic regulators for the relocation of viral proteins and vRNA to the cell periphery. These hypotheses are warranted by the fact that HIV-1 has been previously documented to displace Rab7-positive LE/Lys compartments to the plasma membrane (Cinti *et al.*)[210]. In like manner, the key role of Rab7a in autophagy, a pathway known to crosstalk substantially with HIV-1, adds a layer of complexity to the story. We expected that a Rab7a knockout will not only disrupt regular autophagic flux, but may also severely curtail HIV-1 replication because of its reliance on this pathway. The aim of our work is to further the current knowledge of HIV-1 reprogramming of autophagy and LE/Lys trafficking by revisiting this trafficking phenotype in the context of the Rab GTPases. While riding on the heels of previously published and undercurrent work in the lab, our investigations may help shed new light on the mechanisms by which HIV-1 co-opts major cell machineries to benefit its replication whilst synchronously evading host defense mechanisms. Elucidation of these mechanisms may also provide new knowledge to support viral interactions with host Rab GTPases.

We designed three gRNAs targeting Rab7a. SUP-T1 cells and TZM-bl cells were used to create Rab7a knockout cell lines. The gRNAs and Cas9 were transfected into SUP-T1 and TZM-bl cells using a one-vector system, called lentiCRISPRv2. Gene editing efficiency and viability were assessed in a similar manner as in aim 1. In viable cells, we examined the consequence of Rab7a knockout on HIV-1 infectivity and virus production using the TZM-bl infectivity assay and virus production assays, respectively, in accordance to aim 1. Furthermore, defects in LE/Lys trafficking,

viral protein trafficking, vRNA trafficking, and autophagic flux will be visualized using the aforementioned microscopic techniques.

Ultimately, the exploration of the roles of membrane trafficking genes using the latest gene-editing technology should yield novel information on HIV-1-host interactions controlling intracellular trafficking, and at the same time, potentially uncover new cellular targets for antiviral drug intervention.

CHAPTER 2: MATERIALS AND METHODS

1. Cell Culture Maintenance

HEK293T and TZM-bl cells were grown in Dulbecco's Modified Eagle's medium (DMEM) (Life Technologies) supplemented with 10% fetal bovine serum (FBS) (Invitrogen) and 1% penicillin and streptomycin (Invitrogen). TZM-bl cells (NIH AIDS Reagent Program, Cat #8129) are a HeLa-derived cell line that express CD4, CCR5, and CXCR4, and have a luciferase gene cassette driven by the HIV-1 LTR[249,250]. SUP-T1 cells are derived from human T-cell lymphoblast and grown in Roswell Park Memorial Institute (RPMI) (Life Technologies) medium supplemented with L-glutamine (Sigma-Aldrich), 10% FBS and 1% penicillin and streptomycin. All cell lines were maintained in a 37°C incubator with 5% carbon dioxide (CO_2).

2. Lentiviral Delivery of Cas9 Nuclease to TZM-bl Cells

LentiCas9-Blast (Addgene plasmid #52962) contains a mammalian-codon optimized *S. pyogenes* Cas9 protein with a C-terminal FLAG tag and resistance to blasticidin. HEK293T cells were plated in a 10cm dish (4×10^6 cells) and co-transfected with LentiCas9-Blast, *Indiana vesiculovirus* G protein (VSV-G) (Addgene plasmid #14888), and psPAX2 (Addgene plasmid #12260) using 1ug/μL polyethylenimine (PEI) (Polysciences). Viral supernatants were harvested at 48 hours post-transfection and used to transduce TZM-bl cells with 10μg/mL polybrene (Sigma-Aldrich). At 48 hours post-transduction, TZM-bl cells were subjected to positive selection using DMEM containing 5ng/μL blasticidin (InvivoGen), and continued for 2 weeks.

3. LentiGuide-Puro Delivery

TZM-bl-Cas9 and wild-type (WT) TZM-bl cells were plated at a density of 1.5×10^5 cells/well in 6-well plates and then transiently transfected with either the lentiGuide-Puro vector (Addgene plasmid #52963) containing a 20-mer sgRNA or an empty LentiGuide-Puro vector using jetPRIME® transfection reagent (Polyplus). At 2 days post-transfection, cells were positively selected with 3μ/mL puromycin for 4 days.

4. Intracellular Staining of Cas9-FLAG

TZM-bl-Cas9 cells were pelleted at 1,500rpm for 5 minutes and the supernatant was removed. Cells were re-suspended in phosphate-buffered saline (PBS) (Life Technologies) with 2%

FBS at a concentration of 1×10^6 cells and pelleted again before fixation in 2% paraformaldehyde (PFA) diluted in PBS for 20 minutes at room temperature. Cells were centrifuged and incubated in conjugated FLAG antibody (1:1,000 dilution) (Rockland, Cat #200-343-383) in BD Perm/Wash™ buffer (BD Biosciences) and incubated for 1 hour in obscurity. The cells were then pelleted and washed 3 times in BD Perm/Wash™ buffer prior to flow cytometry. Results were acquired on a BD LSRFortessa™ cell analyzer (BD Biosciences) and analysis was conducted using the FlowJo V10 software (Treestar).

5. Arrayed Screening of the Membrane Trafficking Library

The crRNA library consists of a panel of 140 human membrane trafficking genes (4 crRNAs per gene and 1 non-targeting control (NTC) crRNA) in an arrayed 96-well plate format for one-gene-per-well analysis (Dharmacon™ Edit-R crRNA Library, Cat #GC-005505-01) (see appendix for complete list of crRNAs). Each crRNA and the associated tracrRNA were resuspended in 10mM Tris-HCl buffer pH7.4 (Dharmacon™) to generate 10μM RNA stock solutions which were stored at -20°C. 1μM aliquots were made for each crRNA plate with 10mM Tris-HCl buffer pH7.4 and stored at -20°C. On day 1, TZM-bl-Cas9 cells were plated in flat-bottom 96-well plates at a density of 5×10^3 cells/well in serum-free RPMI and triplicates were made for each plate (see appendix for plate layouts). On day 2, a round-bottom 96-well transfection plate was used and 1:1 ratios of 25nM crRNA and tracrRNA were dispensed per well and mixed with 0.2μL/well of DharmaFECT 1 transfection reagent (Dharmacon™). Serum-free RPMI was used as a dilution medium. After a 10 minute incubation period, TZM-bl-Cas9 cells were transfected with 20μL of the transfection mix and incubated at 37°C with 5% CO_2 for 24 hours. After 24 hours (day 3), the serum-free RPMI was changed to complete media.

6. Cellular Viability Determination

Cellular viability was determined at 72 hours post-transfection of the crRNA library using the LIVE/DEAD™ Fixable Near-IR Dead Cell Stain Kit (ThermoFisher Scientific, Cat #L10119). Following centrifugation of the 96-well plates at 1,000rpm for 5 minutes at room temperature, media was removed and the cells were washed with PBS. The cells were pelleted again, re-suspended in a 1:4 dilution of the LIVE/DEAD™ Fixable Near-IR molecular probe and incubated for 30 minutes at room temperature in obscurity. The plates were then centrifuged again as above, the supernatant removed, and 50μl of trypsin added to each well and incubated for 2 minutes at 37°C.

The cells were pelleted and 4% PFA (Millipore Sigma) was added to each well to fix the cells for 15 minutes at room temperature, protected from light. The plates were then centrifuged again and washed thrice with PBS before being stored with 150µl PBS/well at 4°C until analysis. Results and cell population statistics were acquired on a BD LSRFortessa™ cell analyzer (BD Biosciences).

7. gRNA Design

Three gRNAs were designed for *RAB7A* using the Off-Spotter algorithm for CRISPR-Cas design created by the Jefferson Computational Medicine Center (https://cm.jefferson.edu/Off-Spotter/) (see table 4). Each gRNA is 20 nucleotides in length, has a NGG PAM, has zero predicted mismatches, and is located within the first 1,000 nucleotides of the protein-encoding sequence to ensure a complete knockout. Each gRNA was chemically synthesized by Invitrogen and rehydrated in double-distilled water.

Table 4: Rab7a gRNA characteristics

Gene Target	gRNA Name	Start Site (bp)	Strand	gRNA Sequence	Reverse Complement	Length (nt)	PAM
RAB7A (624 bp)	gRNA-1	204	+	ACGGTTCCAGTCTCTCGGTG	CACCGAGAGACTGGAACCGT	20	TGG
	gRNA-2	237	+	AGGTGCAGACTGCTGCGTTC	GAACGCAGCAGTCTGCACCT	20	TGG
	gRNA-3	337	-	GGGAAGTTTTCAGGATCTCG	CGAGATCCTGAAAACTTCCC	20	GGG

8. CRISPR Editing of SUP-T1 Cells

gRNAs were cloned into the lentiCRISRPRv2 vector (Addgene plasmid #52961), which expresses a mammalian codon-optimized *S. pyogenes* Cas9 and confers resistance to puromycin. HEK293T cells were plated in a 10cm dish (4×10^6 cells) and co-transfected with LentiCRISPRv2, VSV-G, and psPAX2 using 1ug/µL PEI. Viral supernatants were harvested at 48 hours post-transfection and used to spinoculate SUP-T1 cells in 24-well plates (2×10^6 cells/well) with 8ug/mL polybrene at 1,800rpm for 45 minutes at room temperature. 48 hours post-spinoculation cells were expanded in 6-well plates and positively selected with 2ug/mL puromycin (Invivogen) for 2 weeks.

9. HIV-1 NL4.3 Viral Stocks and Infection

NL4.3 virus particles were produced by transfecting HEK293T cells with the HIV-1 NL4.3 provirus-encoding plasmid pNL4.3 using the jetPRIME® transfection reagent. Supernatants were collected 48 hours post-transfection, filtered through a 0.45µm pore-sized filter (Pall Corporation) and ultra-centrifuged at 20,000rpm for 1 hour at 4°C. The virus-containing pellet was collected, re-

suspended in RPMI media and stored at -80°C. The viral multiplicity of infection (MOI) was quantified using the X-gal staining assay in TZM-bl indicator cells as described previously in the literature[251]. TZM-bl-Cas9 cells were infected with NL4.3 with an MOI of 1 using 6μg/mL polybrene by spinoculation at 1,800rpm for 30 minutes at room temperature. The cells were incubated with the viruses for 2.5 hours and then washed once with PBS and replenished with complete media. Cell extracts and cell-free supernatants were collected for analysis at 48 hours post-spinoculation.

10. Viral Infectivity

Viral Infectivity was measured quantitatively by infecting TZM-bl cells and measuring luciferase production. *Arrayed Screen (96-Well Plate Format):* At 48 hours post-infection with NL4.3, the cell-free supernatant was removed from the plates and the cells were washed twice with PBS. The cells were lysed with 1X active lysis buffer (Brij®58, 1M Tris Acetate, 200mM $Mg(C_2H_3O_2)_2$, 20mM EGTA, 10M NaOH) and frozen at -80°C for at least 1 hour to release cell contents and enable luciferase detection. Cell lysates were mixed with 1X luciferase substrate (1M KPO_4, 1M $MgSO_4$, 1M DTT, 100mM ATP, 10X Luciferin) and luciferase activity was measured in relative light units (RLUs) using a MicroBeta® TriLux luminescence counter (PerkinElmer). *24-Well Plate Format*: Wild-type TZM-bl indicator cells were plated in 24-well plates (4×10^4 cells/well) and infected the next day with viral cell-free supernatant from infected cells. At 48 hours post-infection, TZM-bl indicator cells were washed with PBS and cell extracts were obtained with 1X active lysis buffer, as mentioned previously. Cell lysates were mixed with 1X luciferase substrate and luciferase RLUs was measured using the GloMax 20/20® luminometer (Promega).

11. Virus Production

Cell-free viral supernatants were collected 48h post-infection with NL4.3 and frozen at −20°C. Virus production was measured by extracellular HIV-1 capsid (p24) levels quantified using an enzyme-linked immunosorbent assay (ELISA) (PerkinElmer) or by measuring reverse transcriptase activity, according to the manufacturer's protocol.

12. Western Immunoblotting

Cells were lysed in NP40 lysis buffer (50mM Tris pH7.4, 150mM NaCl, 0.5mM EDTA, 0.5% NP40). Protein concentration for each cell lysate was quantified by Bradford assay (Bio-Rad). Equal amounts of protein (20μg) were separated by sodium dodecyl sulfate-polyacrylamide gel electrophoresis (SDS-PAGE) and transferred to a nitrocellulose membrane (Bio-Rad). Blocking was performed using 5% non-fat milk in Tris-buffered saline (pH7.4) with 0.1% Tween 20 (TBST) for 1 hour at room temperature. Membranes were probed with conjugated primary antibodies at the respective dilutions (see table 5) overnight at 4°C. The membranes were then washed thrice with TBST and incubated with the corresponding horseradish peroxidase-conjugated secondary antibodies (Rockland Immunochemicals) at a dilution of 1:10,000 for 1 hour at room temperature. Protein detection was performed using Western Lightning Plus-ECL (PerkinElmer). Signal intensities were analyzed by densitometry using ImageJ software (NIH, Bethseda, USA).

Table 5: Western immunoblotting antibody information

Peptide/Protein Target	Antibody Name	Dilution Used	Species Raised	Manufacturer	Cat #
Rab7a	Rab7 (B-3)	1:500	Rabbit	Santa Cruz Biotechnology	Sc-376362
Cas9	Cas9 (7A9-3A3)	1:1,000	Mouse	Cell Signaling Technologies	14697
LC3B	LC3	1:1,000	Rabbit	Cell Signaling Technologies	2775S
p62	SQSTM1/p62	1:1,000	Rabbit	Cell Signaling Technologies	5114S
mTOR	mTOR (7C10)	1:1,000	Rabbit	Cell Signaling Technologies	2983
Phospho-mTOR (Ser2481)	Phospho-mTOR (Ser2481)	1:1,000	Rabbit	Cell Signaling Technologies	2974
S6K	p70 S6 Kinase	1:1,000	Rabbit	Cell Signaling Technologies	9202S
Phospho-S6K (Ser371)	P-p70 S6 Kinase (Ser371)	1:1,000	Rabbit	Cell Signaling Technologies	9208P
HIV-1 p24	Anti-HIV-1 p24	1:10,000	Mouse	NIH AIDS Reagents Program	526
HIV-1 gp160	Anti-HIV-1 IIIB gp160 (HT3)	1:1,000	Goat	NIH AIDS Reagents Program	188
β-Actin	Anti-Beta Actin	1:5,000	Rabbit	Abcam	Ab8227
eIF2α	eIF2α	1:1,000	Mouse	Cell Signaling Technologies	2103
Phospho-eIF2α (Ser51)	Eif2S1 (phospho S51) [E90]	1:1,000	Rabbit	Abcam	Ab32157
GAPDH	GAPDH (PA1-987)	1:3,000	Rabbit	ThermoFisher Scientific	PA1-987

13. Statistical Analysis

Statistical calculations were performed using Graph-Pad Prism 6 and Microsoft Excel 2011 software. For multiple comparisons, one-way analysis of variance (ANOVA) was used in conjunction with Turkey post hoc test. p values lower or equal to 0.05 were considered significant (*$p \leq 0.05$, **$p \leq 0.01$, ***$p \leq 0.001$, and ****$p \leq 0.0001$).

Aim 1: CRISPR Screen of a Membrane Trafficking Library

1.0 Gene Ontology of the crRNA Library

The crRNA library supplied by Dharmacon™ contains 140 different genes classified as having a function in membrane trafficking. The Protein Analysis Through Evolutionary Relationships (PANTHER) gene ontology (GO) tool was used to perform enrichment analysis of the gene set and visualize groups of genes that participate in similar molecular functions. PANTHER ontology classifications result from experimental and computational data curated from the literature. Based on these analyses, the majority of the genes in our crRNA library assume catalytic functions (40% of gene set), such as the Rab GTPases, and binding functions (39% of gene set), such as the clathrin adaptors (figure 8). This is in agreement with the fact that enzymatic reactions (catalytic activity) and protein-protein interactions (binding) is necessary to generate intracellular movement and organization. A significant proportion of the gene set is involved in the maintenance of the cytoskeleton and actin remodeling (structural molecular activity; 10% of gene set), also in accordance with the their fundamental roles in membrane trafficking. Based on our gene annotations, our library contains a broad array of genes entertaining diverse molecular functionalities in membrane trafficking, which coincide with what is suggested to be usurped by viruses to complete their replication cycle within a host cell.

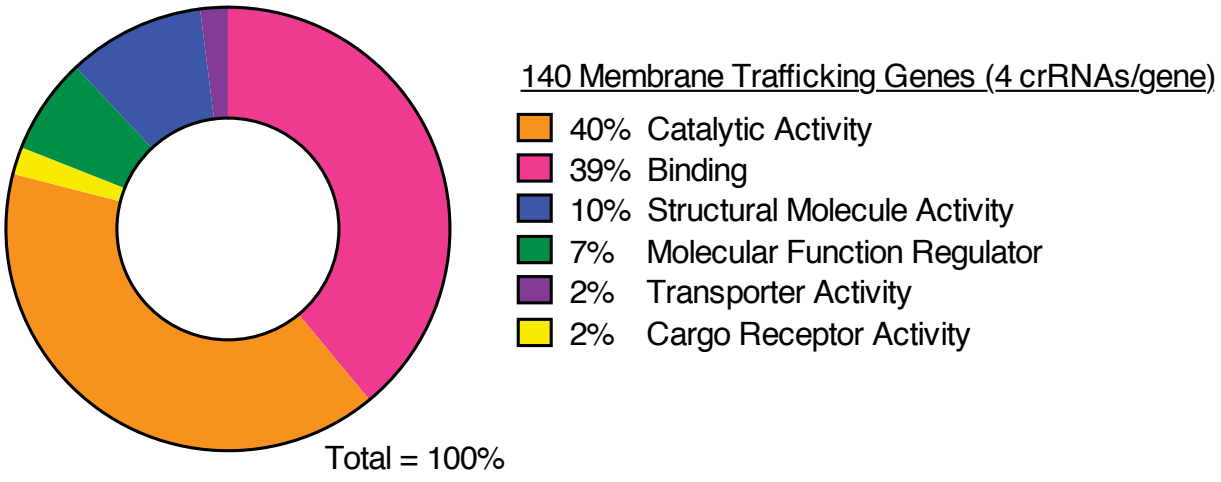

Figure 8: GO annotation of the membrane trafficking crRNA library. Gene enrichment analysis was performed on 140 membrane trafficking genes using the PANTHER 14.1 Classification System with the GO-Slim molecular function tool. Chart percentage (%) is representative of the number of gene hits against the total number of genes in the gene set.

1.1. Creation and Validation of a Cas9-Expressing TZM-bl Cell Line

To enable functional CRISPR screening of the membrane trafficking library we require a cell line that constitutively and stably expresses the Cas9 endonuclease. The HeLa-derived TZM-bl cell line was used as a parental cell line for the screen. We chose these cells due to their high permissibility to HIV-1 infection, their amenability to transfection and confocal imaging, and the presence of an intrinsic luciferase cassette that is driven by a Tat-responsive integrated HIV-1 LTR. The latter provides a means to quantitatively measure HIV-1 viral infectivity in relative light units (RLUs). In order for these TZM-bl cells to constitutively express Cas9 we used a lentiviral vector containing the wild-type *S. pyogenes* Cas9 protein that is C-terminal FLAG-tagged and confers blasticidin resistance, called lentiCas9-Blast (figure 9 A). Various volumes of lentiCas9-Blast from 50µl to 1,000µl were used transduce TZM-bl cells to determine which optimal amount of lentivirus was needed for a robust expression of Cas9. Based our Western blots, the 300µl treatment of lentiCas9 provided the greatest expression of Cas9 without being toxic to the cells (figure 9 A and B). Likewise, this treatment was shown to possess a homogenous population of Cas9-positive cells (99.6%) when gating with a FLAG antibody via flow cytometry (figure 9 C). Altogether, these results show that we have successfully created a cell line that constitutively and stably expresses Cas9 protein using a lentiviral vector. This cell line will thus herein be referred to as TZM-bl-Cas9.

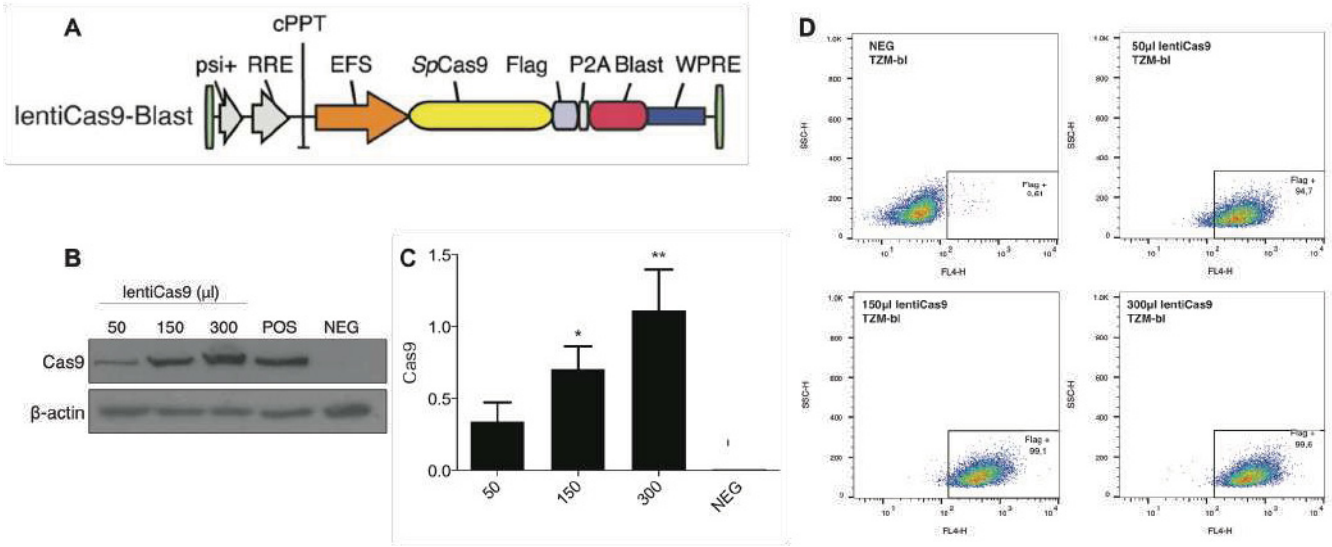

Figure 9: Generation of TZM-bl-Cas9. (**A**) Schematic representation of the lentiCas9-Blast vector. (**B**) Western blot of TZM-bl cells transduced with various volumes of lentiCas9-Blast after two weeks of selection with blasticidin. (**C**) Levels of Cas9 normalized to loading control. (**D**) Flow cytometry of C-terminal FLAG-tagged Cas9 endonuclease. Representative of three independent experiments. One-Way ANOVA; * $p \leq 0.05$, ** $p \leq 0.01$.

To ensure the Cas9 endonuclease in TZM-bl-Cas9 cells can effectively target and cleave the correct genomic targets, we designed an sgRNA targeting a conserved region in the HIV-1 LTR, identical to the one present within the TZM-bl genome. We chose to target the NF-κB binding site within the HIV-1 LTR as this site is highly conserved and is required for provirus transcription initiation or in this case, expression of the luciferase gene cassette. Successful targeting and cleavage of this region would theoretically abrogate luciferase production when the cells are subject to HIV-1 infection. Thus, as an initial test of our approach, we cloned the sgLTR362, named for its targeted nucleotide position, within the lentiGuide-Puro vector (figure 10 A). We then transduced this lentivirus in the TZM-bl-Cas9 cells alongside an empty vector control and challenged the cells to HIV-1 infection with the NL4.3 molecular clone at an MOI of 1. Results indicate effective targeting and abrogation of the sgRNA target site, warranted by the 20–fold decrease ($p \leq 0.0001$) in luciferase production between untreated TZM-bl-Cas9 cells and TZM-bl-Cas9 cells with sgLTR362 (figure 10 B and C). Furthermore, the empty vector control offered only a modest decrease in luciferase production when compared to the untreated control, indicating the 20-fold decrease was mediated by the sgRNA and not by the vector itself. These results not only indicate the presence of Cas9 protein but also verify its functionality in recognizing and cleaving the appropriate genomic targets when supplied with an RNA guide.

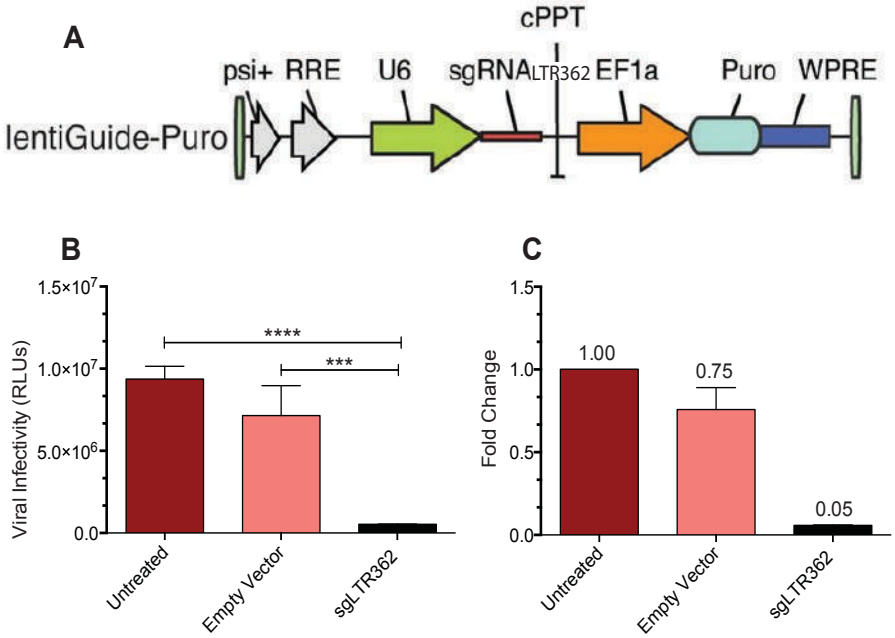

Figure 10: Validation of TZM-bl Cas9 target site binding and cleavage efficiency. (**A**) Schematic representation of the lentiGuide-Puro vector containing a 20-mer sgRNA targeting the LTR362 genomic region. (**B**) Untreated, empty vector and sgRNA treated cells were challenged with HIV-1 NL4.3 and viral infectivity was measured as luciferase production in relative light units (RLUs). (**C**) Fold change relative to the untreated control. Representative of three independent experiments. One-Way ANOVA; *** $p \leq 0.001$, **** $p \leq 0.0001$.

1.2. An Arrayed CRISPR Screening Platform in TZM-bl-Cas9 Cells

We performed three independent arrayed screens using our library of 140 membrane trafficking genes in TZM-bl-Cas9 cells to uncover genes that may hold crucial roles in the replication cycle of HIV-1. Figure 11 A represents a diagram of the CRISPR screening platform we employed. We used a non-targeting crRNA as a negative control. The crRNA library was transfected in the TZM-bl-Cas9 at a 1:1 ratio with the respective tracrRNA. Three days after transfection of the crRNA library in the TZM-bl-Cas9 cells we assessed the viability of the genetically edited cells. Cellular viability was evaluated by discriminating single live cells versus dead cells via a flow cytometry gating method, outlined in figure 11 B. Under normal cell culture conditions, over 70% of our gene targets displayed 75% or higher cellular viability after gene perturbation, which is optimal for using them in further experimental investigations. In line with what we expected, our non-transfected and non-targeting controls possessed the highest cellular viability percentages (≥ 90%) and proliferated at rates comparable to wild-type cells. Seven gene knockouts proved to be detrimental to cellular viability, determined by a cellular viability percentage lower than 60% (shown in the boxed inlet in the legend of figure 11 C). These genes entertain crucial roles in cell homeostasis and survival, highlighting their cellular essentiality. Due to this compromise in cellular viability, these seven knockout cell lines will be removed from future experiments and figures; however, this does not eliminate their potential roles as cofactors in HIV-1 infection.

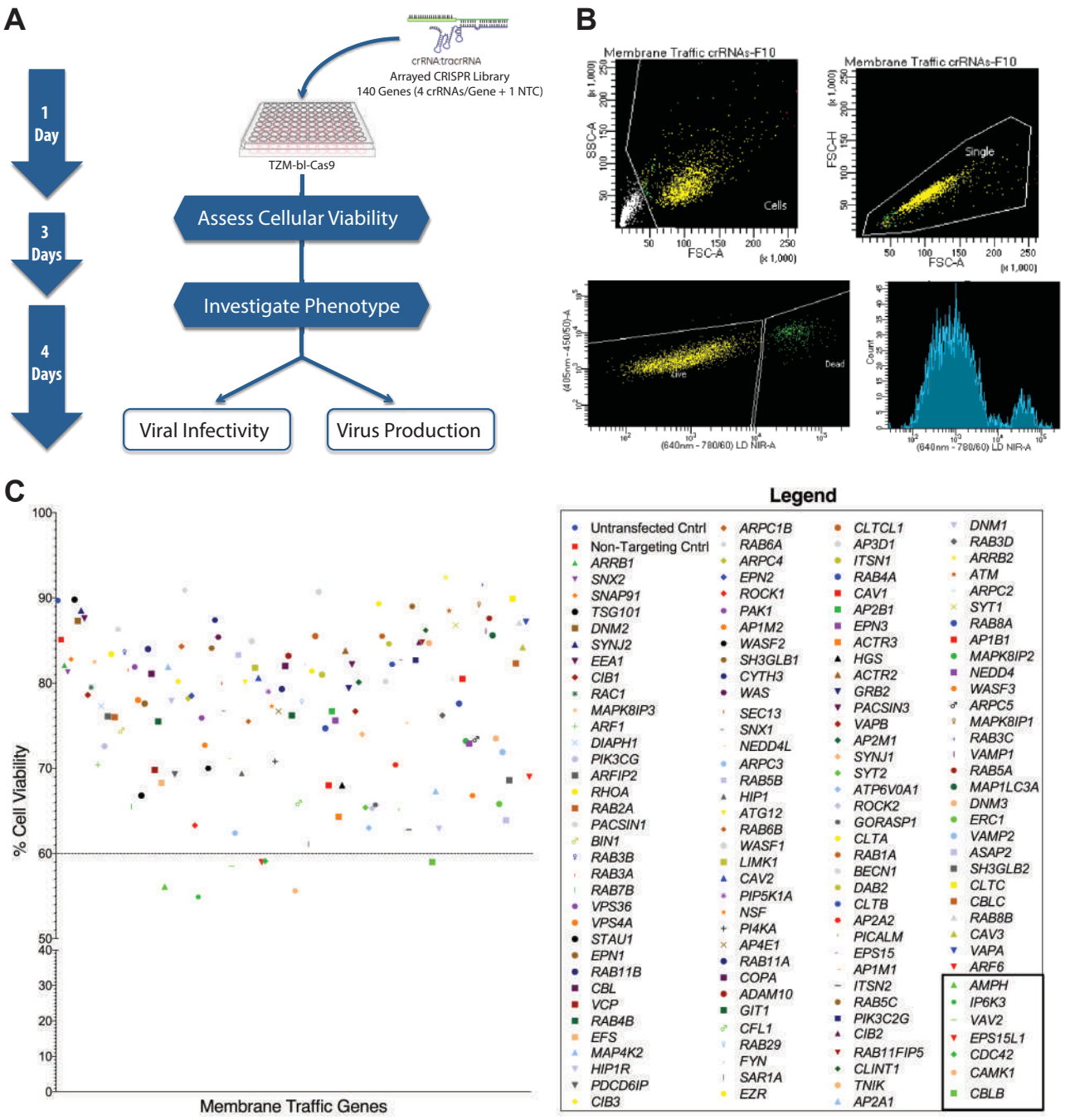

Figure 11: Arrayed CRISPR screen targeting 140 membrane trafficking genes in TZM-bl-Cas9 cells. (**A**) Schematic representation of the arrayed CRISPR screen protocol. (**B**) Live versus dead flow cytometry gating strategy performed on the arrayed CRISPR screen knockouts. Forward and side scatter (FSC-A vs. SSC-A) gating identifies cells, forward area versus height (FSC-A vs. FSC-H) differentiates singlets from doublets, and the spectrum intensity of the amine-binding probe differentiates live versus dead cells, also shown as two peaks in a histogram. (**C**) Cellular viability of CRISPR screen knockouts is represented as a percentage of single live cells to total single cell population. Knockouts entertaining 60% cellular viability or lower are found boxed in the bottom right hand corner of the legend.

1.3. A CRISPR Screen of Membrane Trafficking Factors Unveils Crucial HIV-1 Modulators

In each screen replicate, we infected the cells with HIV-1 NL4.3 at an MOI of 1 72 hours following CRISPR-Cas9 gene editing. We then collected the cell lysates and viral supernatants to evaluate HIV-1 viral infectivity and virion production, respectively. We used the TZM-bl luciferase assay to measure viral infectivity by virtue of the intrinsic LTR-driven luciferase cassette present within our TZM-bl-Cas9 cells. Firstly, we had to optimize this assay to be performed in arrayed 96-well plate format, thus providing a high-throughout method of analyzing viral infectivity following CRISPR-Cas9 gene editing. To ensure the luciferase assay was compliant with our TZM-bl-Cas9 cells, we compared our cells to the wild-type TZM-bl cells and found no significant difference in luciferase readings when both were subjected to HIV-1 infection (figure 12 A). Likewise, as demonstrated in figure 12 B, there was no significant difference between the untransfected, mock transfected (transfection reagent only), and non-targeting controls treatments in our TZM-bl-Cas9 cells, signifying the luciferase assay was amenable to our modified cell type. Therefore, we could use this assay to compare viral infectivity levels between our different membrane trafficking gene knockouts and analyze which ones presented significant decreases or increases in infectivity compared to our baseline non-targeting control crRNA treatment. Figure 12 C displays the luciferase readings from our three screen replicates, the fold change of which is calculated in figure 12 D.

Nine gene knockouts consistently displayed greater than a 2-fold decrease in infectivity compared to the non-targeting controls throughout three screen replicates (shown as bolded columns in figure 12 D). These genes (with associated fold decrease) are: *AP2B1* (0.28-fold), *SYT2* (0.32-fold), *ERC1* (0.33-fold), *MAPK8IP2* (0.36-fold), *PICALM* (0.37-fold), *VAPB* (0.37-fold), *VAMP2* (0.38-fold), *PACSIN3 (*0.38-fold*)*, and *ACTR2 (*0.39-fold*)*. A threshold of 2-fold decrease or higher in viral infectivity levels compared to non-targeting control was chosen based on what is reported as significant in the literature. These results suggest that these nine genes may play crucial roles in the replication cycle of HIV-1, predominantly in the early stages of the cycle. This is warranted by the fact that their absence significantly curtails virus infectivity by more than 2-fold. Thus, these genes merit further investigation as potential viral modulators in the early steps of the HIV-1 replication cycle.

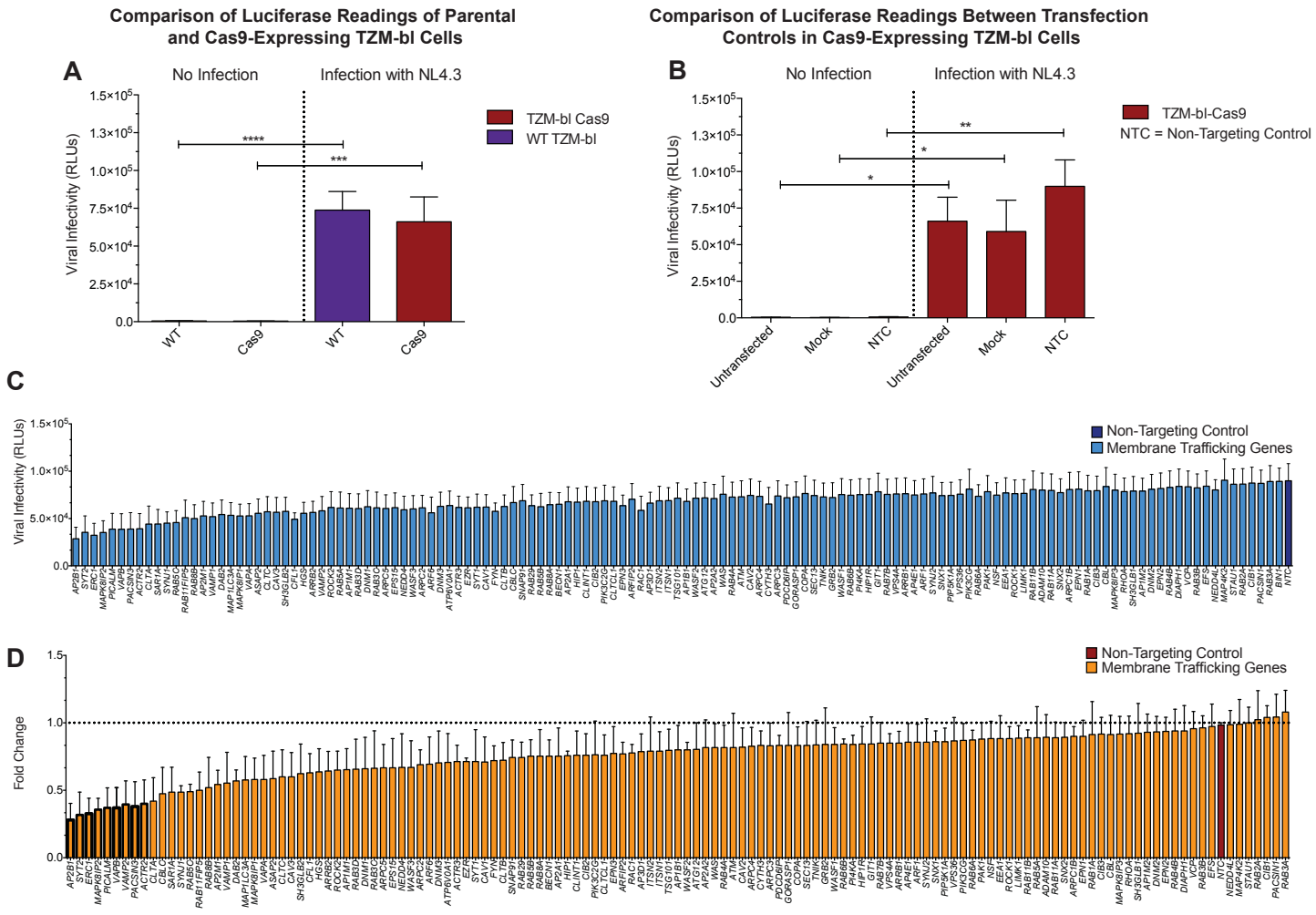

<u>Figure 12:</u> Viral infectivity of membrane trafficking CRISPR screen knockouts. (A) Wild-type (WT) TZM-bl and TZM-bl-Cas9 were infected with NL4.3 or left uninfected and luciferase activity was measured. **(B)** TZM-bl-Cas9 were transfected with a non-targeting control crRNA (NTC), with transfection reagent only (mock), or left untransfected and either infected with NL4.3 or not infected and luciferase activity was measured. **(C)** Viral infectivity of CRISPR screen knockouts infected with NL4.3 measured using the TZM-bl luciferase assay. **(D)** Plot summarizing the fold change of knockouts compared to the NTC (dark red) from three independent experiments. The dotted line is representative of the averaged NTC. One-Way ANOVA; * $p \leq 0.05$, ** $p \leq 0.01$ ***, $p \leq 0.001$, **** $p \leq 0.0001$.

To supplement our viral infectivity data, we measured virus production of our CRISPR screen knockouts. We used a p24 antigen enzyme-linked immunosorbent assay that captures extracellular capsid protein, therefore providing a measure of released viral particle numbers across our membrane trafficking gene knockouts. We used the cell-free viral supernatant complementary with the cell lysates used for infectivity measurements. Similarly to the luciferase assay, the p24 capsid assay was also performed in arrayed 96-well format, which needed to be optimized for our TZM-bl-Cas9 cells. As shown in figure 13 A, no disparities exist between untransfected, mock transfected, and non-targeting controls, implying our assay is complementary with our modified cell type. Thus, we can use this assay to assess differences in released viral particles amongst our

membrane trafficking gene knockouts in comparison with our baseline non-targeting control crRNA. Displayed in figure 13 B are the relative extracellular p24 measurement compared to the non-targeting control, the fold change of which is plotted in figure 13 C. Our results reveal that one gene, *VPS36* (known also under its mammalian nomenclature, *EAP45*), consistently exhibited more than a 2-fold decrease in extracellular p24 compared to our non-targeting control treatment (shown as a bolded column in figure 13 C). These results imply a key function for *VPS36* in the later virus production steps of the HIV-1 replication cycle, as highlighted by the severe defects in proper virus production when it is genetically eliminated. In all, this gene alongside the nine aforementioned genes should be investigated further as our CRISPR screen has phenotypically identified them as having key roles in the replication cycle of HIV-1.

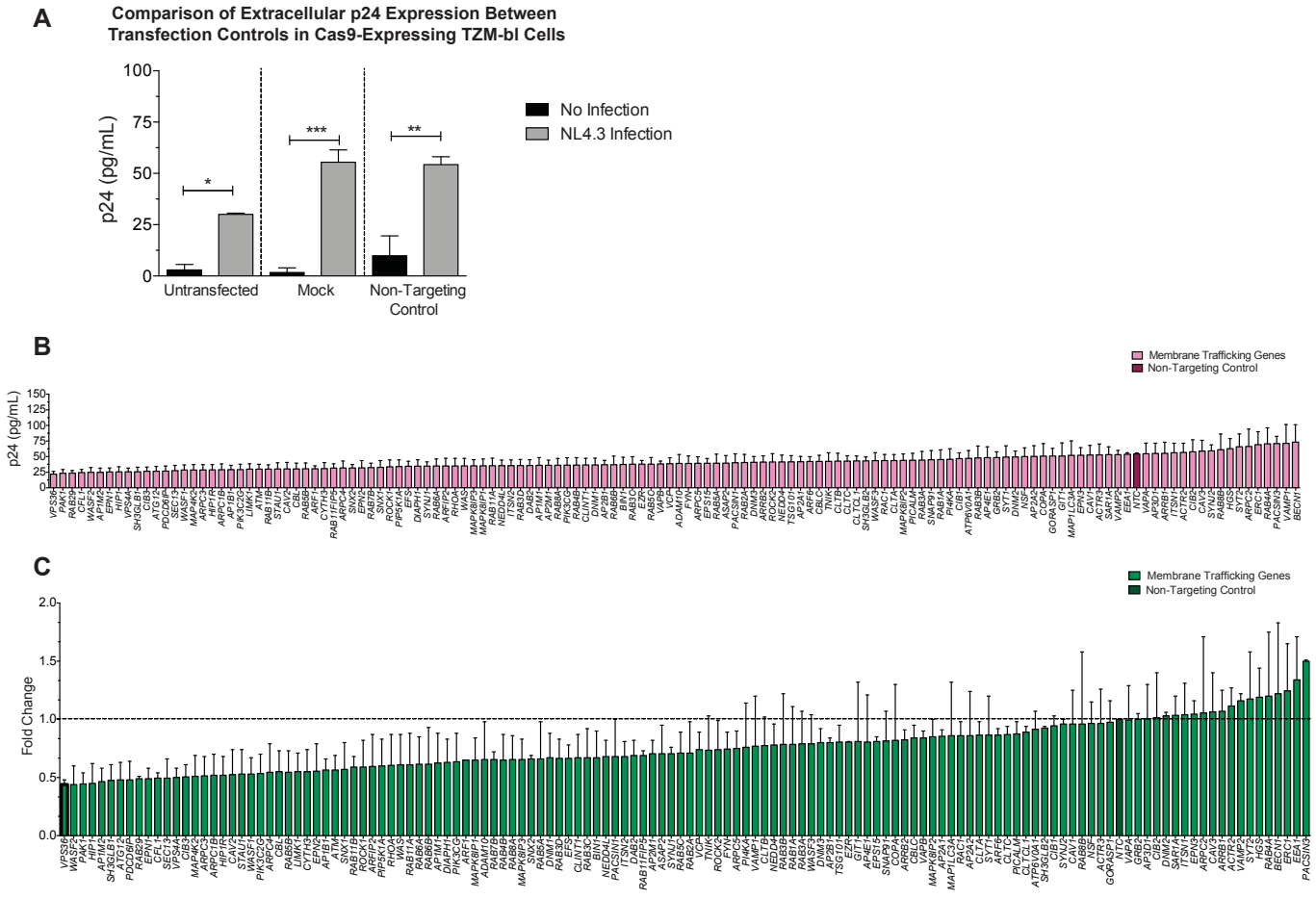

Figure 13: Production of viral particles of membrane trafficking CRISPR screen knockouts. (A) TZM-bl-Cas9 were transfected with a non-targeting control crRNA (NTC), with transfection reagent only (mock), or left untransfected and either infected with NL4.3 or not infected and extracellular p24 was measured. **(B)** Released virus particles of CRISPR screen knockouts infected with NL4.3 measured using the extracellular p24 antigen enzyme-linked immunosorbent assay. **(C)** Plot summarizing the fold change of knockouts compared to the NTC (dark green). Representative of two independent experiments. The dotted line is representative of the averaged NTC. One-Way ANOVA; * $p \leq 0.05$, ** $p \leq 0.01$ ***, $p \leq 0.001$.

1.4 Interaction Networks of CRISPR Screen Hits Uncovers a Dependence on Clathrin-Mediated Endocytosis

Our screen identified ten genes as necessary cofactors for HIV-1. We used the Search Tool for the Retrieval of Interacting Genes (STRING) to analyze and predict interaction networks amongst our identified hits. This database curates known protein-protein interactions documented in the literature and uses this information to predict interaction networks amongst queried genes. Genes are visualized as nodes and the thickness of the connecting edges is representative of the confidence and strength of the data supporting protein-protein associations. The associations determined by STRING are illustrative of proteins that co-participate in a shared molecular function but does not necessarily mean they directly interact with one another. Our analysis reveals a cluster of seven genes amongst our ten identified hits, highlighted in the grey bubble in figure 14. This cluster is enriched in genes encoding factors that jointly contribute to clathrin-mediated endocytosis. The thick edges connecting the clustered genes suggest that these genes entertain very similar molecular functions. These results imply that HIV-1 may depend on the coordinated actions of all these gene products, such that the depletion of one significantly impedes the pathway as a whole. Our STRING results confirm that over 70% of our hits are involved in the clathrin-mediated endocytosis pathway, further advocating the fact that HIV-1 may target this particular pathway. Thus, future hypothesis-based experimental analyses should refocus on this particular category of membrane trafficking to uncover the molecular events leading to the dependence on HIV-1 on clathrin-mediated endocytosis.

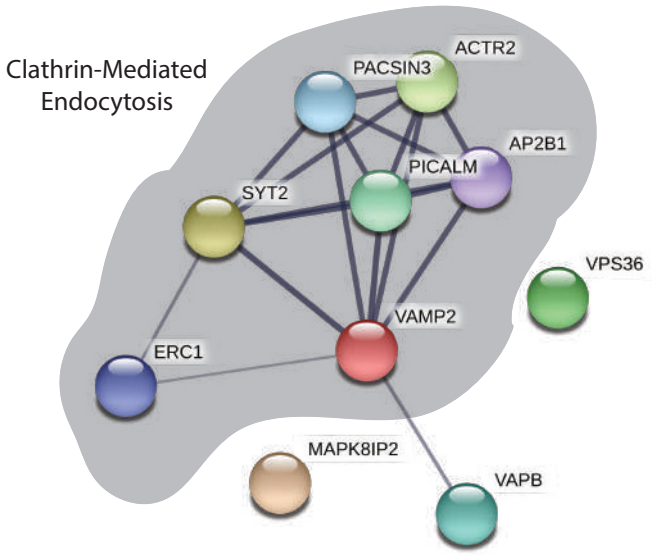

← **Figure 14: Protein interaction network of CRISPR screen hits.** The network of protein-protein interactions was visualized with STRING 11.0 using a recommended confidence interaction score of 0.400. Genes are represented as colourful nodes and the thickness of the edges coincide with the strength of data supporting these associations. Genes clustering in clathrin-mediated endocytosis are denoted in the grey bubble.

Aim 2: Probing Rab7a Function in HIV-1 Infection Through CRISPR-Cas9 Gene Editing

2.0. Creation of TZM-bl and SUP-T1 Rab7a Knockout Cell Lines

To explore the effect of Rab7a in the HIV-1 replication cycle, we genetically altered the *RAB7A* to abrogate its cellular expression using the CRISPR-Cas9 system. We made Rab7a knockouts in HeLa-based TZM-bl cells, described above, and in the T lymphoblast SUP-T1 cell line. Three sgRNAs targeting human *RAB7A* were designed in-house (sgRNA-1, sgRNA-2, and sgRNA-3) and cloned into the lentiCRISPRv2 vector, which encodes the mammalian-codon optimized *S. pyogenes* Cas9 endonuclease. Rab7a abrogation was confirmed by Western blot analysis of the cells (figure 14). In TZM-bl cells, we used two dilutions (1:3 and 1:5) for the lentiviral delivery of each sgRNA. In these TZM-bl cells, complete Rab7a knockout proved efficient and specific, and did not affect cellular viability. In SUP-T1 cells, only a 1:5 lentiviral delivery was used. In these cells, sgRNA-2 proved non-viable, yet sgRNA-1 and sgRNA-3 displayed complete abrogation of Rab7a without compromising cellular viability. In both cell types, Rab7a knockouts and wild-type cells proliferated at a comparable manner (data not shown). Therefore, our results in figure 14 confirm that we have created stable Rab7a knockout cells lines in both TZM-bl and SUP-T1 cell types, which can be used to investigate the effect of Rab7a knockout on HIV-1 infection.

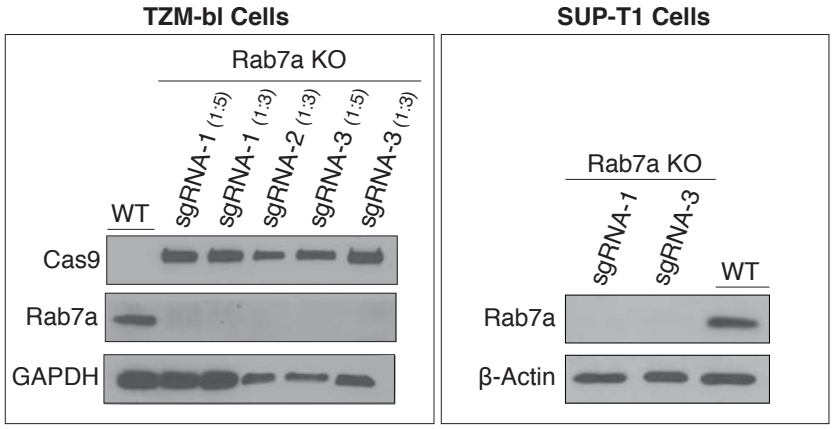

Figure 15: Generation of Rab7a knockout TZM-bl and SUP-T1 cell lines. TZM-bl cells (left panel) and SUP-T1 cells (right panel) were used to create Rab7a knockout (KO) cells lines. Three lentiCRISPv2 vectors, each containing a unique sgRNA targeting the *RAB7A* gene (denoted as sgRNA-1, sgRNA-2 and sgRNA-3) were transfected using two titers (1:3 and 1:5) in TZM-bl cells and one titer (1:5) in SUP-T1 cells. Complete Rab7a knockout was confirmed in both cell types using a specific antibody targeting the 23kDa Human Rab7a protein. WT: wild-type cells.

2.1 SUP-T1 Rab7a KO Cells Display Deficiencies in HIV-1 Infectivity and Virus Production

We explored whether our more physiologically relevant Rab7a knockout T-cell line, SUP-T1, exhibited the same HIV-1 phenotype seen in HeLa cells as in the literature[208]. We challenged them to HIV-1 infection and measured viral infectivity of the cell-free viral supernatant using the luciferase assay in TZM-bl indicator cells. In support of what is described in the literature in HeLa cells, our SUP-T1 Rab7a knockout cells display a significant deficiency in the infectivity of released viral particles. Indeed, our results show a 20–fold decrease in infectivity in comparison to the parental SUP-T1 cells, as seen in figure 14 A. To confirm whether the lowered infectivity corresponded to a decreased number of released viral particles, we measured the RT activity of the cell-free viral supernatant. As shown in figure 14 B, there is a 2–fold decrease in RT activity in Rab7a knockout cells compared to wild type. These results provide a more concrete Rab7a phenotype due to the complete ablation of the *RAB7A* gene using CRISPR-Cas9, in comparison to the moderate siRNA gene knockdown studies found in the literature. In addition of supporting previous studies, our results suggest a major role for the small GTPase Rab7a in the infectivity and egress of HIV-1 from T-cells.

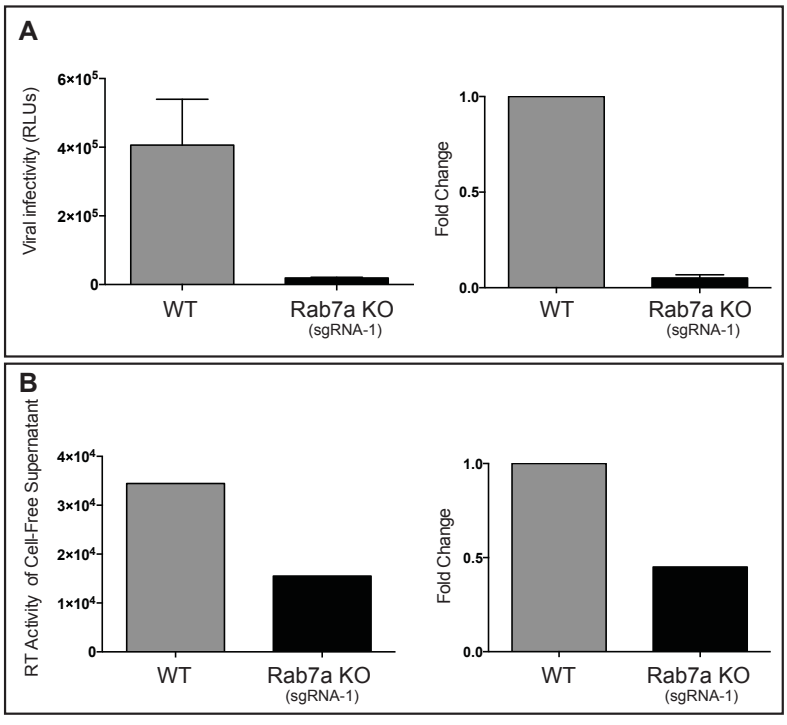

Figure 16: Viral infectivity and RT activity of virus particles released from Rab7a knockout T-cells. (A) Viral infectivity levels of viral supernatant from Rab7a genetically edited SUP-T1 cells and wild-type (WT) SUP-T1 cells using the TZM-bl luciferase assay with associated fold inhibition. **(B)** Reverse transcriptase activity of cell-free viral supernatant from Rab7a knockout (KO) SUP-T1 cells and WT cells with associated fold inhibition.

2.2 Selective Inhibition of HIV-1 Protein Processing in TZM-bl Rab7a Knockouts

The apparent Rab7a phenotype suggested severe defects at the later steps of the replication cycle of HIV-1 after the synthesis of viral proteins. We sought to explore where exactly in the series of events this blockade may be happening. We investigated the intracellular levels of Env and Gag polyproteins to examine whether there were defects in the quantities or maturity levels of these proteins, which may contribute to the phenotype observed. In TZM-bl Rab7a knockout cells, we detected a high level of full-length precursor envelope glycoprotein gp160 compared to wild-type cells, when observed via Western blot (figure 15). This phenotype is recapitulated across all three Rab7a knockouts, further confirming a deficit in the processing of immature gp160 to the mature gp120 and gp41 Env glycoproteins. A similar phenotype is seen in Gag processing, as there is a clear presence of the Gag intermediate p41 in the Rab7a sgRNA-1 and sgRNA-2 knockouts but not in the wild type. These results insinuate a clear blockage in viral protein maturation and processing in Rab7a knockout conditions. This block may be due to direct or indirect role for Rab7a in maturation process of the HIV-1 glycoproteins Env and Gag. Moreover, in the same Western blot, we see an increase in Gag and Env present in Rab7a knockouts compared to the wild type. This may be suggestive of increasing intracellular Gag levels that are not released in nascent virions. These results are illustrative that Rab7a plays a part in the processing of viral proteins, whether that be a direct role in the proteolytic processing of viral precursors or in the trafficking of viral precursors to the site of proteolytic maturation still needs to be illuminated.

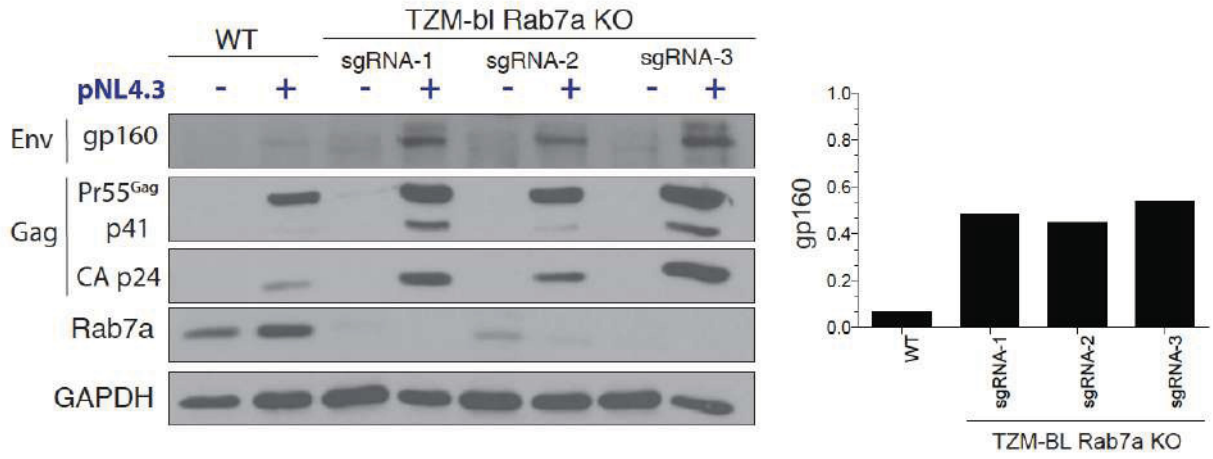

Figure 17: HIV-1 Env and Gag processing intermediates in Rab7a knockout TZM-bl cells. Western blot of Rab7a knockout and wild type (WT) TZM-bl cells infected with HIV-1 pNL4.3 for 48 hours. Quantified levels of Env gp160 across all cell lines is displayed on the right hand side.

2.3 Autophagosome-Lysosome Fusion is Blocked in Infected Rab7a Knockout Cells

Rab7a is well established to facilitate autophagosome-lysosome fusion. Thus, the absence of Rab7a should interfere with regular autophagosome-lysosome fusion and lysosome regeneration. To investigate the consequence of Rab7a knockout on autophagy in TZM-bl cells, we immunoblotted for two well-known indicators of autophagic flux, LC3 and p62. The microtubule-associated protein light chain 3 (LC3) is recruited to the exterior and interior of nucleating autophagosomal membranes. Prior to recruitment, the cytosolic form of the protein termed LC3-I is irreversibly conjugated to phosphatidylethanolamine to form LC3-II, which is membrane-bound. Conjugation of LC3-I to II shifts its molecular weight, which is visible on a Western blot and therefore provides a visual measurement of autophagosome maturation. p62 or sequestosome 1 (SQSTM1) is an autophagic substrate found in the lumen of autophagosomes and is degraded concurrently with enclosed cargo, thus providing a measurement of autophagic degradation.

We infected our Rab7a knockouts with HIV-1 NL4.3 and investigated intracellular levels of these two autophagy markers via Western blot. Figure 16 reveals similar presence of LC3-I and LC3-II between infected and non-infected treatments in the Rab7a knockouts, whereas the wild type displays no presence of these proteins. This is suggestive of augmented autophagic flux in Rab7a knockout cells compared to wild type cells. This increase in autophagy is likely a direct effect of the Rab7a knockout, as HIV-1 infection does not significantly alter the intracellular levels of LC3-I or LC3-II. Furthermore, there is a clear accumulation of p62 in the Rab7a knockout, providing evidence of obstruction during the autophagosome-lysosome fusion stage, which is not present in wild type cells. A blockage at the level of autophagosome-lysosome fusion is in agreement with the key role of the small GTPase in this step and highlights its essentiality in autophagy. However, it is not yet clear whether autophagy is increased due to stress from the Rab7a knockout itself or by a cellular mechanism aiming to clear the accumulated autophagosomes that are not being degraded and regenerated. Interestingly, it is not yet clear whether Rab7a plays a role in the crosstalk between HIV-1 and autophagy, however; these results are a clear indication that the last step of autophagy is disrupted when Rab7a is depleted.

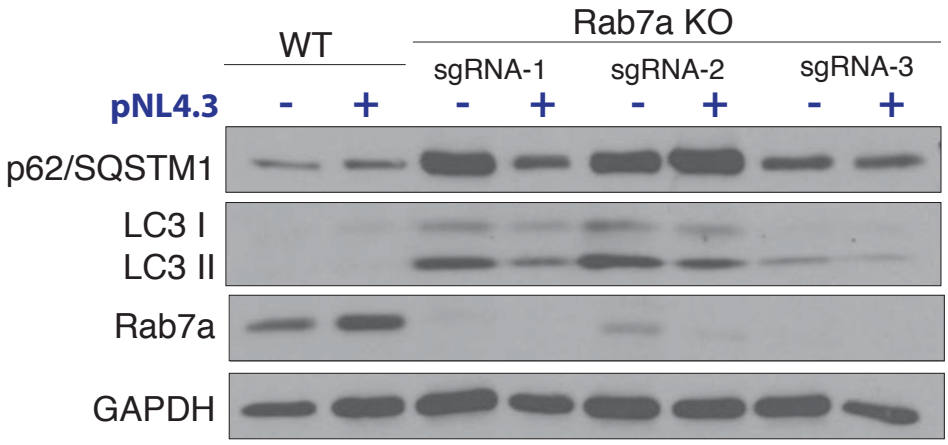

Figure 18: Disruption of autophagic flux in Rab7a knockout TZM-bl cells. Western blot of Rab7a KO and WT TZM-bl cells infected with HIV-1 pNL4.3 for 48 hours and probed for intracellular autophagic flux indicators LC3-I/LC3-II and p62/SQSTM1.

CHAPTER 4: DISCUSSION

Discerning the complex HIV-1-host interaction network is imperative to understanding mechanisms of viral pathogenesis and elucidating previously underappreciated steps of HIV-1 replication. To uncover these viral-host interactions, we used a CRISPR screen in which 140 cellular genes involved in membrane trafficking were systematically assayed for their effect on HIV-1 replication. Of the 140 queried cellular genes, our CRISPR screen has identified ten genes that when completely ablated, have major consequences on HIV-1 replication and survival. The majority of our hit genes have not yet been documented in HIV-1 biology, making them worthy of further investigation.

Surprisingly, a protein interaction analysis revealed that an overwhelming majority of our hits (7/10) are well-known cofactors of clathrin-mediated endocytosis. These findings highlight the importance of clathrin-mediated endocytosis in the HIV-1 replication cycle, likely for facilitating cell ingress. Unlike many enveloped RNA viruses, HIV-1 entry has been determined to be pH-independent, relying instead on direct hemifusion with the plasma membrane for access to the cytoplasm[56]. Nonetheless, several lines of evidence support the fact that in certain cell types, HIV-1 may require endocytic support for cellular entry. Indeed, HIV-1 has been shown to engage in vesicular-mediated endocytosis when observed by electron microscopy in macrophages[252] and T-cells[201], and later in HeLa cells[203] using time-resolved imaging analyses of single virions. Additional studies reinforced this observation using dominant mutants, short-hairpin (sh)RNA knockdowns, or chemical disruption of various endocytosis adaptors in macrophages[253-255], dendritic cells[256], T-cells[257-259], and HeLa cells[202,203,259,260]. Likewise, inhibition of endosomal acidification was shown to increase viral entry and infection, presumably due to viral evasion of lysosomal degradation[261-263]. Numerous lines of evidence argue that endocytic entry of HIV-1 is favourable for cell-free viral entry, though not for cell-to-cell transmission, which would predominantly rely on hemifusion[264,265]. The field of HIV-1 endocytosis remains highly controversial as it is still unclear what cellular players take part in the process. Evidence put forward leads to the idea that endocytosis of HIV-1 is likely cell-type specific and circumstantial[264,265]. Our study provides additional support for a mechanism of cell entry that is dependent on endocytosis in HeLa-based cells. Also, our screen results broaden our knowledge of clathrin cofactors that may contribute to this mechanism.

Of our ten hits, the adaptor protein complex 2 (AP-2) has previously been heavily documented in HIV-1 infection (a thorough literature review of our ten hits can be found in Table 6). AP-2 is a heterotetrameric complex of two large α- and β-subunits, a medium μ-subunit, and a small σ-subunit and functions in cargo selection and transport of clathrin-coated vesicles. Strong evidence confirms direct binding of endogenously synthesized Env with the μ-subunit of AP-2, supporting its role in membrane targeting and Env internalization during virion assembly[266-269]. Gag has also been shown to bind directly to μ-AP-2 at its MA-CA junction, interactions of which are temporally exclusive to the late steps of the viral cycle[270]. Likewise, it is well recognized that HIV-1 Nef downregulates cell surface expression of CD4 through interactions with the α- and σ-subunits of AP-2[271,272]. Despite the abundance of reports evidencing HIV-1 interactions with the α-, μ- and σ-subunits of AP-2, our own results appear to be well supportive of a role for the β-subunit of AP-2 (*AP2B1)* in the early phase of HIV-1 infection. AP-2 is also known to regulate the endocytosis of G-protein coupled receptors (GCPRs)[273]. The fact that the HIV-1 co-receptors CXCR4 and CCR5 are GCPRs could explain the inhibitory effect of AP-2 knockout on HIV-1 infectivity. These results propose a putative role for AP-2 at the level of Env/co-receptor engagement[274-276]. An alternative explanation for this phenotype could be due to exogenous secretion of HIV-1 Tat to bystander cells via AP-2-dependent clathrin-mediated endocytosis[277-279]. Studies show that inhibition of clathrin adaptors using siRNAs greatly reduced Tat internalization in neighbouring T-cells[277]. Our method of phenotypic analysis involves a luciferase reporter gene that is *trans*-activated under the control Tat binding to the LTR. Thus, the lowered luciferase readings could be explained by the absence of AP-2 clathrin adaptors necessary for Tat uptake.

To further corroborate a role for AP-2 in HIV-1 infectivity, another one of our hits, *PICALM*, encodes the phosphatidylinositol-binding clathrin assembly protein (PICALM, also as known as CALM) that is required for AP-2-dependent clathrin-mediated endocytosis. The PICALM/AP-2 complex regulates clathrin-coated vesicle assembly and maturation[280]. PICALM is targeted by several viral glycoproteins that use clathrin-mediated endocytosis as a means of cellular entry, such as the Ebola virus glycoprotein[276]. However, interactions between HIV-1 and PICALM in the early stages of replication have not yet been reported. We believe the inhibitory effect of PICALM knockout on HIV-1 infectivity is related to AP-2, further highlighting the dependence of the virus on this pathway. Interestingly, an siRNA screen identified PICALM as a cofactor in

retroviral assembly and release[281]. Evidently, HIV-1 seems to target endocytic adaptors, supported by the extensive diversity of published interactions between HIV-1 and endocytosis, specifically clathrin-mediated endocytosis. Thus, it is not entirely surprising to anticipate an alleged role for AP-2 and PICALM in the early stages of HIV-1 infection alongside their well-established roles in the late stages of HIV-1. Another one of our hits, *ACTR2,* encodes the actin related protein 2 (Arp2), also documented to function in lentiviral infection. Arp2 is a constituent of the Arp2/3 complex situated on the cytoplasmic face of the plasma membrane[282]. Arp2/3 is required for cortical actin filament nucleation and polymerization[282]. It is well acknowledged that the actin filament network is distorted to allow HIV-1 access to the cytoplasm[282,283]. Indeed, siRNA knockdown of Arp2 in H9 T-cells was shown to block HIV-1 infection[282]. Our results concur well with evidence indicating that HIV-1 is dependent on Arp2/3 for viral entry, further validating of our experimental approach.

Our other hit involved in endocytosis ERC1 encodes the ELKS/Rab6-interacting/CAST family member 1 protein (ERC1). ERC1 is a multifaceted protein, taking part in Rab6-mediated early endosome-to-TGN trafficking and regulation of the IKK/NF-κB pathway[284,285]. As of yet, no putative role is documented for ERC1 in HIV-1 replication; though, a high-throughput yeast two-hybrid screen identified ERC1 to be of importance for the replication of Dengue virus[286]. Likewise, it is known that the IKK/NF-κB pathway is important in HIV-1 infection and our results from CRISPR-targeting of the NF-κB binding site on the HIV-1 LTR further corroborate this. The regulatory role of ERC1 in the IKK/NF-κB pathway may thus play a role in the inhibitory effect of its knockdown on HIV-1 infectivity.

Table 6: Background information about CRISPR screen hits

	Hit Gene	Protein Name	Cellular Role	Previously Known Interaction(s) with HIV-1	Interaction(s) with Other Hit Gene(s)	Refs.
Involved in Endocytosis	*AP2B1*	Adaptor Protein Complex 2 (**AP-2**)	- Functions in cargo selection and transport of clathrin-coated vesicles - Heterotetrameric complex of two large α- and β-subunits, a medium μ-subunit, and a small σ-subunit	- HIV-1 Env with the μ-subunit of AP-2 during membrane targeting and internalization in virion assembly - HIV-1 Gag in direct binding to μ-AP-2 at its MA-CA junction during virion assembly - HIV-1 Nef downregulates cell surface expression of CD4 through interactions with the α- and σ-subunits of AP-2	- Forms a complex with **PICALM** to regulate clathrin-coated vesicle assembly and maturation	266-272
	PICALM	Phosphatidylinositol-Binding Clathrin Assembly Protein (**PICALM**)	- Functions as an adaptor protein in clathrin-mediated endocytosis of cell surface receptors	- None	- Forms a complex with **AP-2** to regulate clathrin-coated vesicle assembly and maturation	280
	ACTR2	Actin Related Protein 2 (**Arp2**)	- Part of the Arp2/3 complex involved in cortical actin filament nucleation and polymerization	- siRNA knockdown of Arp2 in H9 T-cells blocks productive HIV-1 entry and infection	- No direct links but cortical actin plays a significant role in clathrin-mediated endocytosis	282,283
	PACSIN3	Protein Kinase C and Casein Kinase Substrate in Neurons 3 (**PACSIN3**)	- Interacts with PACSIN1 and PACSIN2 to connect the actin cytoskeleton to endocytic vesicle formation	- A study identified PACSIN3, a well-known extracellular vesicle marker, in urinary samples from HIV-1-positive individuals but not in HIV-1-negative individuals	- No direct links but is a member of the actin and endocytosis gene families	287
	ERC1	ELKS/Rab6-Interacting/CAST Family Member 1 Protein (**ERC1**)	- Regulatory subunit in the IKK/NF-κB pathway involved in the regulation of neurotransmitter release and Rab6-mediated endosome to Golgi transport	- None	- No direct links with other hit genes	284,285
	SYT2	Synaptotagmin 2	- Regulates trafficking of synaptic vesicles in a calcium-dependent manner	- None	- Collaborates with **VAMP-2** to control synaptic vesicle fusion and transport	288
	VAMP2	Vesicle-Associated Membrane Protein 2 (**VAMP-2**)	- Regulates docking and fusion of synaptic vesicle transmission	- None	- Collaborates with **synaptogamin 2** to control synaptic vesicle fusion and transport	288
	MAPK8IP2	Mitogen-Activated Protein Kinase 8 Interacting Protein 2 (**MAPK8IP2**)	- Interacts with JNK-signalling components to regulate vesicle transport and protein motors	- None	- No direct links with other hit genes	289
	VAPB	Vesicle-Associated Membrane protein-Associated Protein B (**VAPB**)	- Participates in the ER unfolded protein response	- None	- No direct links with other hit genes	290
	VPS36/ EAP45	Vacuolar Protein-Sorting-Associated Protein 36 (**Vps36**) also known as EAP45	- A ESCRT-II component that interacts with Vps22 and Vps25 and is recruited to the site of endosomal vesicle formation and budding on the plasma membrane	- Reduced HIV-1 virion export in Vps36 CRISPR-knockout and shRNA-knockdown HAP1 cells - Vps36 shown to be involved in HIV-1 vRNA trafficking alongside Staufen1	- No direct links with other hit genes but is a member of the ESCRT pathway	291-293

Our virion production assay hit *VPS36* encodes the vacuolar protein-sorting-associated protein 36 (Vps36), alternatively known as EAP45. Vps36 is a component of ESCRT-II alongside Vps22 and Vps25, which are recruited to the site of endosomal vesicle formation and budding on the plasma membrane[291]. The ESCRT machinery, as mentioned previously, is hijacked by HIV-1 in the late phase of infection to facilitate release of nascent enveloped virions from host cells. ESCRT-II plays a central role in bridging ESCRT-I and ESCRT-III during ESCRT formation and is also able to bind ubiquitinated proteins for cargo selection[291-293]. There is considerable literature implicating Vps36 in the late stage assembly of HIV-1 virions, which corroborates with the inhibitory effect of Vps36 knockout on extracellular Gag levels[291-293]. Meng *et al.* reported reduced HIV-1 virion export in Vps36 CRISPR-knockout and shRNA-knockdown HAP1 cells[293]. Our lab has previously revealed an additional role for ESCRT-II in the trafficking of vRNA to the budding site through interactions with the RNA-binding protein Staufen1[292]. The results from our work substantiate the findings reported by Meng *et al.* and Ghoujal *et al.* and further supports the role of VPS36 in efficient virion biogenesis, vRNA trafficking, and export. Interestingly, the other ESCRT adaptor included in our screen, *TSG101*, did not significantly reduce viral output despite its established role in HIV-1 budding. Potential reasons attributed to this observation may be due to incomplete *TSG101* knockout, which could be assessed in validation studies in stable *TSG101* knockout cells or the fact that TSG101 may not be absolutely required for virion budding.

Intriguingly, none of our infectivity hits overlap with our virion production hits. We expected that the genes with low luciferase readings would also exhibit low virion production results due to reduced virus infection in these cells. Despite these unexpected observations, several reasons could be attributed to this outcome. One is the fact that our two methods of analysis quantify two different stages of the life cycle and thus are not comparable measurements. Also, despite the fact that some gene knockouts would impede virus infectivity, some virus would still be able to integrate within the genome of the cells and go on to productively carry out the late stages of the viral life cycle unencumbered. This would lead to the production of near-normal virus production titers as seen in our study.

Our screen focused mostly on gene knockouts that inhibited HIV-1 infectivity and viral production; however, several gene knockouts amplified infectivity and virus output relative to our non-targeting control. Although not significant (*i.e.* $\geq$ 2-fold change), these phenotypes may be of

interest to explore further as they could represent factors that naturally restrict virus replication. This would not be unexpected, as many established host restriction factors are known to rely heavily on the lysosomal degradation system, a pathway in which membrane trafficking factors overlap with greatly.

Our study has inherent limitations. The first is the several drawbacks associated to CRISPR-Cas9 technology. CRISPR-Cas9 gene editing has been shown to produce off-target mutations due to imperfect gRNA binding at genomic locations other than the intended site, although the frequency of these off-target effects is much lower than RNAi technologies[294]. Additionally, many researchers have sounded a note of caution with regards to CRISPR-mediated gene editing as it induces the cellular p53-mediated DNA damage response and consequently selects for cells with a non-functional p53 pathway[295]. The latter is incredibly important in the context of CRISPR screening in cancer research but should still be taken into account as the p53 pathway plays a significant role in viral infections[296,297]. Furthermore, cellular viability is affected when genetically perturbing a vital gene, thus limiting our ability to investigate whether such a gene product would entertain a role in HIV-1 infection. Another limitation is the fact that our results are likely cell-type specific. Our screen was performed in HeLa-derived TZM-bl cells, whereas major HIV-1 GeCKO screens used T-cell subtypes including patient-isolated $CD4^+$ T-cells. Therefore, these data need to be interpreted with caution as it is recognized that HIV-1 infection landscapes differ greatly amongst cell subtypes; the contradictory reports about HIV-1 endocytosis exemplify this observation.

Our future work will consist of validating our phenotypic findings in more biologically relevant cell types such as T-cells and macrophages. Further investigations in these cell types may help elucidate the functional link of certain endocytic proteins in HIV-1 infection. Such investigations will require stable knockout cell lines in which gene knockout is confirmed by way of protein expression and target sequencing. $CD4^+$ T-cell derivatives, such as the SUP-T1 cells would be an optimal cell line as they represent a more physiologically relevant T-cell model than TZM-bl cells. We anticipate that our endocytic factor knockout cell lines would inhibit HIV-1 infectivity in accordance to our screen results, keeping in mind that others have reported differently[298]. Experimental approaches that will aid in dissecting what is occurring at the molecular level include the HIV-1 fusion assays using a β-lactamase-vpr marker to monitor virion-cell fusion events and electron microscopy of entry events. Future work with the other hits that are not involved in

endocytosis will notably follow different hypothesis-driven paths. IF and FISH are helpful tools to track differences in trafficking pathways and investigate the locality of viral proteins and vRNA.

Our work with the small GTPase Rab7a stands as a point-of-concept for our future experiments with the CRISPR screen hits. We generated viable and stable Rab7a knockouts in two different cell lines: SUP-T1 and TZM-bl using the CRISPR-Cas9 system. These cell lines were used to further our investigation of the function of Rab7a in HIV-1 infection. Our preliminary results recapitulate the Rab7a HIV-1 knockdown phenotype reported earlier by Caillet *et al*[208]. We were able to visualize similar defects in Env and Gag processing and maturation. In agreement with Caillet *et al.*[208], we believe that the high presence of these immature viral proteins may prevent HIV-1 assembly and exit from the cell[208]. This lends support to the fact that Rab7a directly or indirectly aids the production of infectious HIV-1 virus particles, though the mechanism by which this occurs is still unclear. Going beyond what was performed by Caillet *et al.*[208] we investigated the inhibitory effect of Rab7a knockout on autophagy and lysosomal trafficking as we believe it is through these two pathways that Rab7a functions in HIV-1 replication.

Rab7a serves as the master regulator of autophagy and endolysosomal trafficking independently, while also linking these two processes together. In autophagy, Rab7a is reported to facilitate the fusion of autophagosomes with late endosomes and lysosomes at the MTOC in the perinuclear region. Our results document this well, as we observe a high presence of p62 in the Rab7a knockouts, which is indicative of a block in lysosomal degradation of autophagosomal p62-tagged cargo. Interestingly, recent findings in Rab7a knockout MDCK-II cells repute Rab7a's role in the fusion step of autophagy[299]. Instead, the authors of this study suggest that mammalian Rab7a functions in the maturation process of autophagosome-lysosome units in nutrient-rich conditions and further stating that fusion of these compartments is Rab7a-independent[299]. However, the study in question did not investigate intracellular levels of p62, instead they based their results on autophagosome clearance by IF[299]. Our results are well supportive of a fusion block in Rab7a-negative cells, which is backed up by ample literature as well as the fact that Rab7a already mediates the fusion of late endosomes with lysosomes[181,299]. As a suggestion for future work, treating Rab7a-positive and Rab7a-negative cells with bafilomycin A1, a drug that completely inhibits the fusion step by affecting lysosomal acidification[300], may be useful for deciphering Rab7a's role in the fusion event. Furthermore, we were surprised by the fact that there was no significant difference in

autophagic flux between HIV-1-infected cells and uninfected cells in both the Rab7a knockout and wild type. This is unexpected, as HIV-1 is known to alter autophagic flux in T-cells. It would be interesting to see if this phenotype is retained when repeating these experiments with the bafilomycin A1 treatment.

In addition to autophagy, Rab7a also controls LE/Lys trafficking. Our previous work (Cinti *et al.* 2017) revealed for the first time that LE/Lys trafficking is disturbed in HIV-1-infected T-cells[210]. These defects are visually evident as Rab7a-positive LE/Lys organelles compartmentalize in a peripheral locality and remain there despite arsenite treatment, which normally shepherds LE/Lys back to the MTOC[210]. Alongside the LE/Lys trafficking deficits, endosomal acidification was also inhibited[300]. Indeed, Rab7a binds its effector RILP to govern dynein (-)-end travel, but this interaction also nucleates v-ATPase assembly, which in turn allows acidification of endosomal comparments[181]. Our recommendation for future work in the Rab7a project consists of using confocal microscopy to investigate defects in endolysosomal trafficking and acidification in Rab7a knockout cells. Lysosomal compartments are easily distinguishable using a marker for lysosome-associated membrane glycoprotein 1 (LAMP1) and Rab7a can be confirmed absent using a Rab7a probe. To investigate the locality of viral protein and RNA trafficking we will use probes for HIV-1 Gag and vRNA using FISH. We hypothesize that there will be defects in Gag and vRNA trafficking to the plasma membrane. We expect to see aggregates of Gag- and vRNA-positive puncta at the juxtanuclear region, presumably having missed their ride on anterograde-directed endolysosomal compartments. Endosomal acidification defects can be visualized with specialized pH-sensitive dyes. Our preliminary Rab7a results are encouraging and will be validated by forthcoming experiments to help decipher the exact function of Rab7a in the HIV-1 replication cycle. Nevertheless, we have shown that Rab7a plays an integral role in HIV-1 infectivity and virus production, which supports its consideration as a potential therapeutic target.

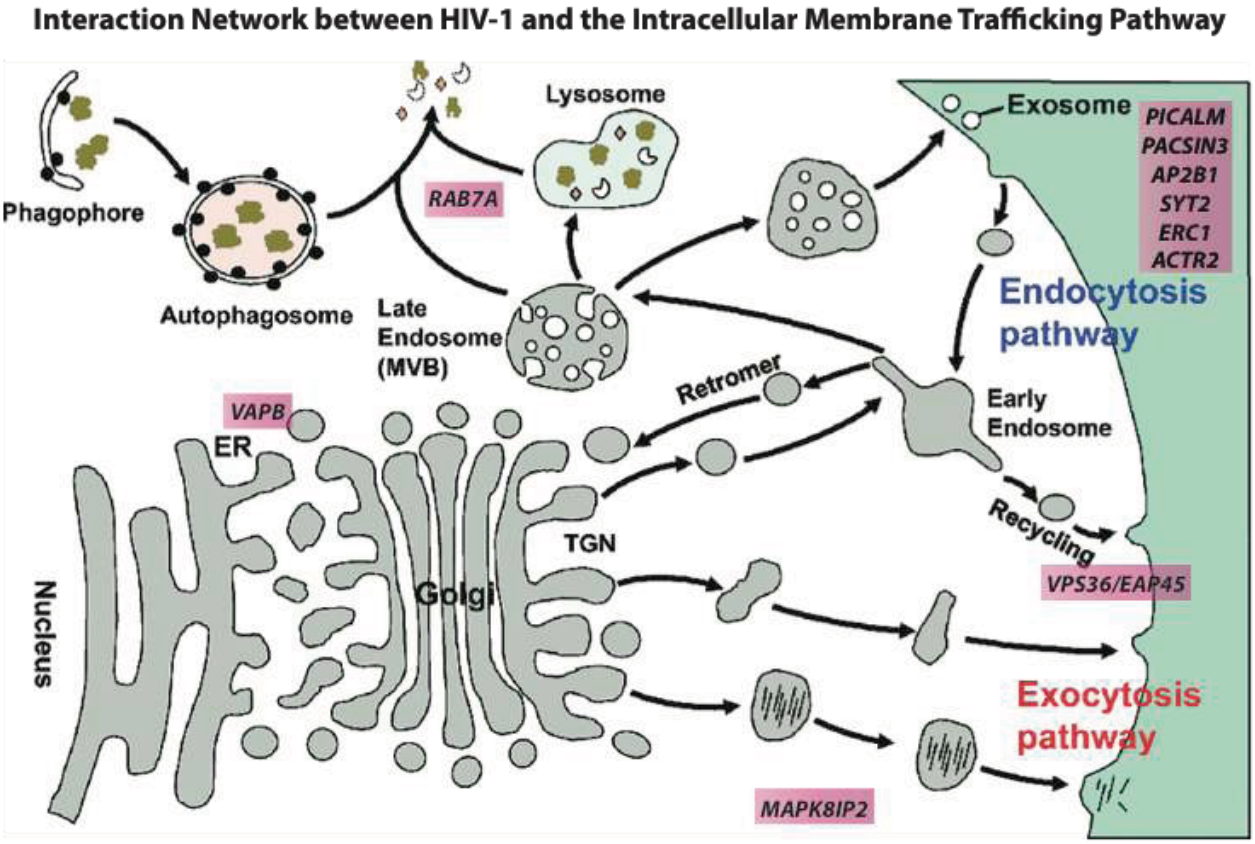

Figure 19: Working model of the virus-host interactions between HIV-1 and the intracellular membrane trafficking pathway. Candidate genes with putative roles in the HIV-1 replication cycle are denoted by pink rectangles at their established subcellular location.

CHAPTER 5: SUMMARY AND CONCLUSION

HIV-1 co-opts host cellular machineries to ensure an environment that allows efficient replication of its viral components. One of the ways by which HIV-1 accomplishes this is by reprogramming the intracellular membrane trafficking routes to arbitrate its own travel to and fro various subcellular compartments. Indeed, HIV-1 has been evidenced to touch each sub-category of what is defined as membrane trafficking. The means by which HIV-1 exerts its hold on the trafficking pathway are pending elucidation. We have helped define these virus-host interactions by using a cutting-edge functional genomic approach based on the CRISPR-Cas9 technology. We used an arrayed CRISPR-Cas9 screen to question the role of 140 cellular genes involved in membrane trafficking in HIV-1 infection in HeLa-based TZM-bl cells. Gene knockouts displaying compromises in HIV-1 infection were identified using two different methods of analysis: the TZM-bl infectivity assay and the extracellular p24 antigen capture assay.

Of our library of 140 genes, we identified 10 that caused inhibition of HIV-1 infectivity and virus production, enlisting these genes as potential HDFs. The majority of these hits function in endocytosis, suggesting HIV-1 targets this particular sub-category of membrane trafficking. Others were confirmatory of data already published in the literature, endorsing the validity of our approach. Hit validation and analysis in SUP-T1 T-cells is currently ongoing. In parallel, we studied the function of the membrane trafficking factor Rab7a in HIV-1 infection, acting as a proof-of-concept prototype for our novel CRISPR screen hits. Our preliminary results with Rab7a confirm its importance in HIV-1, as infectivity and RT activity of released virus particles was severely inhibited. Likewise, we observed defects in autophagy persuading us to further our investigation in Rab7a's possible role behind of the LE/Lys trafficking defects in HIV-1 that our lab has previously reported.

Returning to the hypothesis posed at the beginning of this study, it is now possible to state that HIV-1 targets membrane trafficking factors to facilitate key replication steps. Further inquisition into the exact function of the membrane trafficking HDFs we uncovered will contribute to knowledge about HIV-1 intracellular trafficking and potentially illuminate new avenues of opportunity for therapeutic intervention. While broadly inhibiting the membrane trafficking pathway is not a reasonable consideration, targeted disruptions of specific interactions between HIV-1 proteins and host trafficking factors could be leveraged in a beneficial way.

BIBLIOGRAPHY

1 Gottlieb, M. S. *et al.* Pneumocystis carinii pneumonia and mucosal candidiasis in previously healthy homosexual men: evidence of a new acquired cellular immunodeficiency. *The New England journal of medicine* **305**, 1425-1431, doi:10.1056/nejm198112103052401 (1981).

2 Kaposi's sarcoma and Pneumocystis pneumonia among homosexual men--New York City and California. *MMWR. Morbidity and mortality weekly report* **30**, 305-308 (1981).

3 Update on acquired immune deficiency syndrome (AIDS)--United States. *MMWR. Morbidity and mortality weekly report* **31**, 507-508, 513-504 (1982).

4 Possible transfusion-associated acquired immune deficiency syndrome (AIDS) - California. *MMWR. Morbidity and mortality weekly report* **31**, 652-654 (1982).

5 Barre-Sinoussi, F. *et al.* Isolation of a T-lymphotropic retrovirus from a patient at risk for acquired immune deficiency syndrome (AIDS). *Science (New York, N.Y.)* **220**, 868-871 (1983).

6 Popovic, M., Sarngadharan, M. G., Read, E. & Gallo, R. C. Detection, isolation, and continuous production of cytopathic retroviruses (HTLV-III) from patients with AIDS and pre-AIDS. *Science (New York, N.Y.)* **224**, 497-500 (1984).

7 Case, K. Nomenclature: human immunodeficiency virus. *Annals of internal medicine* **105**, 133 (1986).

8 Fischl, M. A. *et al.* The efficacy of azidothymidine (AZT) in the treatment of patients with AIDS and AIDS-related complex. A double-blind, placebo-controlled trial. *The New England journal of medicine* **317**, 185-191, doi:10.1056/nejm198707233170401 (1987).

9 Nobel Prizes 2008. *Angewandte Chemie (International ed. in English)* **47**, 8556, doi:10.1002/anie.200804933 (2008).

10 Sharp, P. M. & Hahn, B. H. Origins of HIV and the AIDS pandemic. *Cold Spring Harbor perspectives in medicine* **1**, a006841, doi:10.1101/cshperspect.a006841 (2011).

11 Faria, N. R. *et al.* HIV epidemiology. The early spread and epidemic ignition of HIV-1 in human populations. *Science (New York, N.Y.)* **346**, 56-61, doi:10.1126/science.1256739 (2014).

12 Hemelaar, J., Gouws, E., Ghys, P. D. & Osmanov, S. Global and regional distribution of HIV-1 genetic subtypes and recombinants in 2004. *AIDS* **20**, W13-23, doi:10.1097/01.aids.0000247564.73009.bc (2006).

13 Shaw, G. M. & Hunter, E. HIV transmission. *Cold Spring Harbor perspectives in medicine* **2**, doi:10.1101/cshperspect.a006965 (2012).

14 Fox, J. & Fidler, S. Sexual transmission of HIV-1. *Antiviral research* **85**, 276-285, doi:10.1016/j.antiviral.2009.10.012 (2010).

15 Des Jarlais, D. C. *et al.* 30 Years on Selected Issues in the Prevention of HIV among Persons Who Inject Drugs. *Advances in preventive medicine* **2013**, 346372, doi:10.1155/2013/346372 (2013).

16 Dosekun, O. & Fox, J. An overview of the relative risks of different sexual behaviours on HIV transmission. *Current opinion in HIV and AIDS* **5**, 291-297, doi:10.1097/COH.0b013e32833a88a3 (2010).

17 Ahmed, N. Most at-risk populations: contextualising HIV prevention programmes targeting marginalised groups in Zanzibar, Tanzania. *Afr J AIDS Res* **13**, 205-213, doi:10.2989/16085906.2014.952645 (2014).

18 *Guidance on Pre-Exposure Oral Prophylaxis (PrEP) for Serodiscordant Couples, Men and Transgender Women Who Have Sex with Men at High Risk of HIV: Recommendations for Use in the Context of Demonstration Projects*. World Health Organization. (2012).
19 Sarma, H. & Oliveras, E. Implementing HIV/AIDS education: impact of teachers' training on HIV/AIDS education in Bangladesh. *J Health Popul Nutr* **31**, 20-27 (2013).
20 Gray, R. H. *et al.* Increased risk of incident HIV during pregnancy in Rakai, Uganda: a prospective study. *Lancet* **366**, 1182-1188, doi:10.1016/s0140-6736(05)67481-8 (2005).
21 Wariki, W. M. V. *et al.* Interventions for preventing mother-to-child HIV transmission: protocol of an overview of systematic reviews. *BMJ open* **7**, e014332, doi:10.1136/bmjopen-2016-014332 (2017).
22 John, T. J. Towards zero transmission of HIV through blood transfusion. *The Indian journal of medical research* **134**, 746-748 (2011).
23 Petroll, A. E., Galletly, C. L., Havens, P. L., Kwiecinski, M. F. & Pinkerton, S. D. Updated CDC guidelines for HIV testing: a review for Wisconsin practitioners. *WMJ : official publication of the State Medical Society of Wisconsin* **107**, 84-90 (2008).
24 Clarke, C. M. *et al.* Implementation of HIV treatment as prevention strategy in 17 Canadian sites: immediate and sustained outcomes from a 35-month Quality Improvement Collaborative. *BMJ quality & safety* **25**, 345-354, doi:10.1136/bmjqs-2015-004269 (2016).
25 Cohen, M. S. *et al.* Prevention of HIV-1 infection with early antiretroviral therapy. *The New England journal of medicine* **365**, 493-505, doi:10.1056/NEJMoa1105243 (2011).
26 Taylor, D. *et al.* Probability of a false-negative HIV antibody test result during the window period: a tool for pre- and post-test counselling. *International journal of STD & AIDS* **26**, 215-224, doi:10.1177/0956462414542987 (2015).
27 Kilby, D. L., Major, C. J., Steben, M. H., Sutherland, W. D. & Bally, G. A. Point-of-care HIV testing using simple/rapid HIV test kits: guidance for health-care professionals. *Canada communicable disease report = Releve des maladies transmissibles au Canada* **26**, 49-59 (2000).
28 Napierala Mavedzenge, S., Baggaley, R. & Corbett, E. L. A review of self-testing for HIV: research and policy priorities in a new era of HIV prevention. *Clinical infectious diseases : an official publication of the Infectious Diseases Society of America* **57**, 126-138, doi:10.1093/cid/cit156 (2013).
29 De Clercq, E. Clinical potential of the acyclic nucleoside phosphonates cidofovir, adefovir, and tenofovir in treatment of DNA virus and retrovirus infections. *Clinical microbiology reviews* **16**, 569-596 (2003).
30 Coates, J. A. *et al.* The separated enantiomers of 2'-deoxy-3'-thiacytidine (BCH 189) both inhibit human immunodeficiency virus replication in vitro. *Antimicrobial agents and chemotherapy* **36**, 202-205 (1992).
31 Schiller, D. S. & Youssef-Bessler, M. Etravirine: a second-generation nonnucleoside reverse transcriptase inhibitor (NNRTI) active against NNRTI-resistant strains of HIV. *Clinical therapeutics* **31**, 692-704, doi:10.1016/j.clinthera.2009.04.020 (2009).
32 Domingo, P. & Ribera, E. [Data on rilpivirine in treatment-naive patients. Lessons from ECHO, THRIVE and STaR]. *Enfermedades infecciosas y microbiologia clinica* **31 Suppl 2**, 20-29, doi:10.1016/s0213-005x(13)70139-3 (2013).
33 Cote, B. *et al.* Discovery of MK-1439, an orally bioavailable non-nucleoside reverse transcriptase inhibitor potent against a wide range of resistant mutant HIV viruses. *Bioorganic & medicinal chemistry letters* **24**, 917-922, doi:10.1016/j.bmcl.2013.12.070 (2014).
34 Colonno, R. J., Thiry, A., Limoli, K. & Parkin, N. Activities of atazanavir (BMS-232632) against a large panel of human immunodeficiency virus type 1 clinical isolates resistant to

one or more approved protease inhibitors. *Antimicrobial agents and chemotherapy* **47**, 1324-1333 (2003).
35 Ghosh, A. K., Dawson, Z. L. & Mitsuya, H. Darunavir, a conceptually new HIV-1 protease inhibitor for the treatment of drug-resistant HIV. *Bioorganic & medicinal chemistry* **15**, 7576-7580, doi:10.1016/j.bmc.2007.09.010 (2007).
36 Wire, M. B., Shelton, M. J. & Studenberg, S. Fosamprenavir : clinical pharmacokinetics and drug interactions of the amprenavir prodrug. *Clinical pharmacokinetics* **45**, 137-168, doi:10.2165/00003088-200645020-00002 (2006).
37 Matthews, T. *et al.* Enfuvirtide: the first therapy to inhibit the entry of HIV-1 into host CD4 lymphocytes. *Nature reviews. Drug discovery* **3**, 215-225, doi:10.1038/nrd1331 (2004).
38 Veljkovic, N. *et al.* Preclinical discovery and development of maraviroc for the treatment of HIV. *Expert opinion on drug discovery* **10**, 671-684, doi:10.1517/17460441.2015.1041497 (2015).
39 Hazuda, D. J. *et al.* Inhibitors of strand transfer that prevent integration and inhibit HIV-1 replication in cells. *Science (New York, N.Y.)* **287**, 646-650 (2000).
40 Lennox, J. L. *et al.* Safety and efficacy of raltegravir-based versus efavirenz-based combination therapy in treatment-naive patients with HIV-1 infection: a multicentre, double-blind randomised controlled trial. *Lancet* **374**, 796-806, doi:10.1016/s0140-6736(09)60918-1 (2009).
41 Hammer, S. M. *et al.* A trial comparing nucleoside monotherapy with combination therapy in HIV-infected adults with CD4 cell counts from 200 to 500 per cubic millimeter. AIDS Clinical Trials Group Study 175 Study Team. *The New England journal of medicine* **335**, 1081-1090, doi:10.1056/nejm199610103351501 (1996).
42 Larder, B. A., Kemp, S. D. & Harrigan, P. R. Potential mechanism for sustained antiretroviral efficacy of AZT-3TC combination therapy. *Science (New York, N.Y.)* **269**, 696-699 (1995).
43 Boyd, M. A., Cooper, D. A. & Gilks, C. F. Towards a universal second-line fixed-dose combination ART. *The lancet. HIV* **5**, e3-e5, doi:10.1016/s2352-3018(17)30180-7 (2018).
44 Muesing, M. A. *et al.* Nucleic acid structure and expression of the human AIDS/lymphadenopathy retrovirus. *Nature* **313**, 450-458 (1985).
45 Borg, K. T., Favaro, J. P. & Arrigo, S. J. Involvement of human immunodeficiency virus type-1 splice sites in the cytoplasmic accumulation of viral RNA. *Virology* **236**, 95-103, doi:10.1006/viro.1997.8726 (1997).
46 Gallo, R., Wong-Staal, F., Montagnier, L., Haseltine, W. A. & Yoshida, M. HIV/HTLV gene nomenclature. *Nature* **333**, 504, doi:10.1038/333504a0 (1988).
47 Kao, S. Y., Calman, A. F., Luciw, P. A. & Peterlin, B. M. Anti-termination of transcription within the long terminal repeat of HIV-1 by tat gene product. *Nature* **330**, 489-493, doi:10.1038/330489a0 (1987).
48 Najera, I., Krieg, M. & Karn, J. Synergistic stimulation of HIV-1 rev-dependent export of unspliced mRNA to the cytoplasm by hnRNP A1. *Journal of molecular biology* **285**, 1951-1964, doi:10.1006/jmbi.1998.2473 (1999).
49 Strebel, K. HIV accessory proteins versus host restriction factors. *Current opinion in virology* **3**, 692-699, doi:10.1016/j.coviro.2013.08.004 (2013).
50 Wu, H., Kwong, P. D. & Hendrickson, W. A. Dimeric association and segmental variability in the structure of human CD4. *Nature* **387**, 527-530, doi:10.1038/387527a0 (1997).
51 Ryu, S. E. *et al.* Crystal structure of an HIV-binding recombinant fragment of human CD4. *Nature* **348**, 419-426, doi:10.1038/348419a0 (1990).
52 Lu, M., Blacklow, S. C. & Kim, P. S. A trimeric structural domain of the HIV-1 transmembrane glycoprotein. *Nature structural biology* **2**, 1075-1082 (1995).

53 Kwong, P. D. *et al.* Structure of an HIV gp120 envelope glycoprotein in complex with the CD4 receptor and a neutralizing human antibody. *Nature* **393**, 648-659, doi:10.1038/31405 (1998).
54 Starcich, B. R. *et al.* Identification and characterization of conserved and variable regions in the envelope gene of HTLV-III/LAV, the retrovirus of AIDS. *Cell* **45**, 637-648 (1986).
55 Kozak, S. L. *et al.* CD4, CXCR-4, and CCR-5 dependencies for infections by primary patient and laboratory-adapted isolates of human immunodeficiency virus type 1. *J Virol* **71**, 873-882 (1997).
56 Ashkenazi, A., Viard, M., Wexler-Cohen, Y., Blumenthal, R. & Shai, Y. Viral envelope protein folding and membrane hemifusion are enhanced by the conserved loop region of HIV-1 gp41. *FASEB journal : official publication of the Federation of American Societies for Experimental Biology* **25**, 2156-2166, doi:10.1096/fj.10-175752 (2011).
57 Isel, C. *et al.* Specific initiation and switch to elongation of human immunodeficiency virus type 1 reverse transcription require the post-transcriptional modifications of primer tRNA3Lys. *The EMBO journal* **15**, 917-924 (1996).
58 Julias, J. G., Ferris, A. L., Boyer, P. L. & Hughes, S. H. Replication of phenotypically mixed human immunodeficiency virus type 1 virions containing catalytically active and catalytically inactive reverse transcriptase. *J Virol* **75**, 6537-6546, doi:10.1128/jvi.75.14.6537-6546.2001 (2001).
59 Hu, W. S. & Hughes, S. H. HIV-1 reverse transcription. *Cold Spring Harbor perspectives in medicine* **2**, doi:10.1101/cshperspect.a006882 (2012).
60 Lightfoote, M. M. *et al.* Structural characterization of reverse transcriptase and endonuclease polypeptides of the acquired immunodeficiency syndrome retrovirus. *J Virol* **60**, 771-775 (1986).
61 Purohit, V., Roques, B. P., Kim, B. & Bambara, R. A. Mechanisms that prevent template inactivation by HIV-1 reverse transcriptase RNase H cleavages. *J Biol Chem* **282**, 12598-12609, doi:10.1074/jbc.M700043200 (2007).
62 Stremlau, M. *et al.* Specific recognition and accelerated uncoating of retroviral capsids by the TRIM5alpha restriction factor. *Proceedings of the National Academy of Sciences of the United States of America* **103**, 5514-5519, doi:10.1073/pnas.0509996103 (2006).
63 Bowerman, B., Brown, P. O., Bishop, J. M. & Varmus, H. E. A nucleoprotein complex mediates the integration of retroviral DNA. *Genes & development* **3**, 469-478 (1989).
64 Fujiwara, T. & Craigie, R. Integration of mini-retroviral DNA: a cell-free reaction for biochemical analysis of retroviral integration. *Proceedings of the National Academy of Sciences of the United States of America* **86**, 3065-3069 (1989).
65 Monette, A., Pante, N. & Mouland, A. J. HIV-1 remodels the nuclear pore complex. *The Journal of cell biology* **193**, 619-631, doi:10.1083/jcb.201008064 (2011).
66 Brown, P. O., Bowerman, B., Varmus, H. E. & Bishop, J. M. Correct integration of retroviral DNA in vitro. *Cell* **49**, 347-356 (1987).
67 Bushman, F. D., Fujiwara, T. & Craigie, R. Retroviral DNA integration directed by HIV integration protein in vitro. *Science (New York, N.Y.)* **249**, 1555-1558 (1990).
68 Llano, M. *et al.* An essential role for LEDGF/p75 in HIV integration. *Science (New York, N.Y.)* **314**, 461-464, doi:10.1126/science.1132319 (2006).
69 Shun, M. C. *et al.* LEDGF/p75 functions downstream from preintegration complex formation to effect gene-specific HIV-1 integration. *Genes & development* **21**, 1767-1778, doi:10.1101/gad.1565107 (2007).
70 Temin, H. M. The DNA provirus hypothesis. *Science (New York, N.Y.)* **192**, 1075-1080 (1976).

71 Wang, G. P., Ciuffi, A., Leipzig, J., Berry, C. C. & Bushman, F. D. HIV integration site selection: analysis by massively parallel pyrosequencing reveals association with epigenetic modifications. *Genome research* **17**, 1186-1194, doi:10.1101/gr.6286907 (2007).
72 Khan, S., Iqbal, M., Tariq, M., Baig, S. M. & Abbas, W. Epigenetic regulation of HIV-1 latency: focus on polycomb group (PcG) proteins. *Clinical epigenetics* **10**, 14, doi:10.1186/s13148-018-0441-z (2018).
73 Watts, J. M. *et al.* Architecture and secondary structure of an entire HIV-1 RNA genome. *Nature* **460**, 711-716, doi:10.1038/nature08237 (2009).
74 Tahirov, T. H. *et al.* Crystal structure of HIV-1 Tat complexed with human P-TEFb. *Nature* **465**, 747-751, doi:10.1038/nature09131 (2010).
75 Nabel, G. & Baltimore, D. An inducible transcription factor activates expression of human immunodeficiency virus in T cells. *Nature* **326**, 711-713, doi:10.1038/326711a0 (1987).
76 Stoltzfus, C. M. Chapter 1. Regulation of HIV-1 alternative RNA splicing and its role in virus replication. *Advances in virus research* **74**, 1-40, doi:10.1016/s0065-3527(09)74001-1 (2009).
77 Lemieux, C. *et al.* A Pre-mRNA degradation pathway that selectively targets intron-containing genes requires the nuclear poly(A)-binding protein. *Molecular cell* **44**, 108-119, doi:10.1016/j.molcel.2011.06.035 (2011).
78 Malim, M. H., Hauber, J., Le, S. Y., Maizel, J. V. & Cullen, B. R. The HIV-1 rev trans-activator acts through a structured target sequence to activate nuclear export of unspliced viral mRNA. *Nature* **338**, 254-257, doi:10.1038/338254a0 (1989).
79 Henderson, B. R. & Percipalle, P. Interactions between HIV Rev and nuclear import and export factors: the Rev nuclear localisation signal mediates specific binding to human importin-beta. *Journal of molecular biology* **274**, 693-707, doi:10.1006/jmbi.1997.1420 (1997).
80 Gilmartin, G. M., Fleming, E. S., Oetjen, J. & Graveley, B. R. CPSF recognition of an HIV-1 mRNA 3'-processing enhancer: multiple sequence contacts involved in poly(A) site definition. *Genes & development* **9**, 72-83 (1995).
81 Das, A. T., Klaver, B. & Berkhout, B. A hairpin structure in the R region of the human immunodeficiency virus type 1 RNA genome is instrumental in polyadenylation site selection. *J Virol* **73**, 81-91 (1999).
82 Swanson, C. M., Sherer, N. M. & Malim, M. H. SRp40 and SRp55 promote the translation of unspliced human immunodeficiency virus type 1 RNA. *J Virol* **84**, 6748-6759, doi:10.1128/jvi.02526-09 (2010).
83 Earl, P. L., Doms, R. W. & Moss, B. Oligomeric structure of the human immunodeficiency virus type 1 envelope glycoprotein. *Proceedings of the National Academy of Sciences of the United States of America* **87**, 648-652 (1990).
84 Hallenberger, S. *et al.* Inhibition of furin-mediated cleavage activation of HIV-1 glycoprotein gp160. *Nature* **360**, 358-361, doi:10.1038/360358a0 (1992).
85 Gelderblom, H. R. Assembly and morphology of HIV: potential effect of structure on viral function. *Aids* **5**, 617-637 (1991).
86 Jacks, T. *et al.* Characterization of ribosomal frameshifting in HIV-1 gag-pol expression. *Nature* **331**, 280-283, doi:10.1038/331280a0 (1988).
87 Molle, D. *et al.* Endosomal trafficking of HIV-1 gag and genomic RNAs regulates viral egress. *J Biol Chem* **284**, 19727-19743, doi:10.1074/jbc.M109.019844 (2009).
88 Ono, A. HIV-1 Assembly at the Plasma Membrane: Gag Trafficking and Localization. *Future virology* **4**, 241-257, doi:10.2217/fvl.09.4 (2009).
89 Nydegger, S., Foti, M., Derdowski, A., Spearman, P. & Thali, M. HIV-1 egress is gated through late endosomal membranes. *Traffic (Copenhagen, Denmark)* **4**, 902-910 (2003).

90 Lehmann, M. *et al.* Intracellular transport of human immunodeficiency virus type 1 genomic RNA and viral production are dependent on dynein motor function and late endosome positioning. *J Biol Chem* **284**, 14572-14585, doi:10.1074/jbc.M808531200 (2009).
91 Levesque, K. *et al.* Trafficking of HIV-1 RNA is mediated by heterogeneous nuclear ribonucleoprotein A2 expression and impacts on viral assembly. *Traffic (Copenhagen, Denmark)* **7**, 1177-1193 (2006).
92 Poole, E., Strappe, P., Mok, H. P., Hicks, R. & Lever, A. M. HIV-1 Gag-RNA interaction occurs at a perinuclear/centrosomal site; analysis by confocal microscopy and FRET. *Traffic (Copenhagen, Denmark)* **6**, 741-755, doi:10.1111/j.1600-0854.2005.00312.x (2005).
93 Mouland, A. J. *et al.* RNA trafficking signals in human immunodeficiency virus type 1. *Molecular and cellular biology* **21**, 2133-2143, doi:10.1128/mcb.21.6.2133-2143.2001 (2001).
94 Ono, A. & Freed, E. O. Plasma membrane rafts play a critical role in HIV-1 assembly and release. *Proceedings of the National Academy of Sciences of the United States of America* **98**, 13925-13930, doi:10.1073/pnas.241320298 (2001).
95 Chan, R. *et al.* Retroviruses human immunodeficiency virus and murine leukemia virus are enriched in phosphoinositides. *J Virol* **82**, 11228-11238, doi:10.1128/jvi.00981-08 (2008).
96 Saad, J. S. *et al.* Structural basis for targeting HIV-1 Gag proteins to the plasma membrane for virus assembly. *Proceedings of the National Academy of Sciences of the United States of America* **103**, 11364-11369, doi:10.1073/pnas.0602818103 (2006).
97 Yu, X., Yuan, X., McLane, M. F., Lee, T. H. & Essex, M. Mutations in the cytoplasmic domain of human immunodeficiency virus type 1 transmembrane protein impair the incorporation of Env proteins into mature virions. *J Virol* **67**, 213-221 (1993).
98 Wright, E. R. *et al.* Electron cryotomography of immature HIV-1 virions reveals the structure of the CA and SP1 Gag shells. *The EMBO journal* **26**, 2218-2226, doi:10.1038/sj.emboj.7601664 (2007).
99 D'Souza, V. & Summers, M. F. How retroviruses select their genomes. *Nature reviews. Microbiology* **3**, 643-655, doi:10.1038/nrmicro1210 (2005).
100 Gottlinger, H. G., Dorfman, T., Sodroski, J. G. & Haseltine, W. A. Effect of mutations affecting the p6 gag protein on human immunodeficiency virus particle release. *Proceedings of the National Academy of Sciences of the United States of America* **88**, 3195-3199 (1991).
101 VerPlank, L. *et al.* Tsg101, a homologue of ubiquitin-conjugating (E2) enzymes, binds the L domain in HIV type 1 Pr55(Gag). *Proceedings of the National Academy of Sciences of the United States of America* **98**, 7724-7729, doi:10.1073/pnas.131059198 (2001).
102 Demirov, D. G., Ono, A., Orenstein, J. M. & Freed, E. O. Overexpression of the N-terminal domain of TSG101 inhibits HIV-1 budding by blocking late domain function. *Proceedings of the National Academy of Sciences of the United States of America* **99**, 955-960, doi:10.1073/pnas.032511899 (2002).
103 Martin-Serrano, J., Zang, T. & Bieniasz, P. D. HIV-1 and Ebola virus encode small peptide motifs that recruit Tsg101 to sites of particle assembly to facilitate egress. *Nature medicine* **7**, 1313-1319, doi:10.1038/nm1201-1313 (2001).
104 Garrus, J. E. *et al.* Tsg101 and the vacuolar protein sorting pathway are essential for HIV-1 budding. *Cell* **107**, 55-65 (2001).
105 Carlton, J. G. & Martin-Serrano, J. Parallels between cytokinesis and retroviral budding: a role for the ESCRT machinery. *Science (New York, N.Y.)* **316**, 1908-1912, doi:10.1126/science.1143422 (2007).
106 Fujii, K. *et al.* Functional role of Alix in HIV-1 replication. *Virology* **391**, 284-292, doi:10.1016/j.virol.2009.06.016 (2009).

107 Wlodawer, A. & Erickson, J. W. Structure-based inhibitors of HIV-1 protease. *Annual review of biochemistry* **62**, 543-585, doi:10.1146/annurev.bi.62.070193.002551 (1993).
108 Li, S., Hill, C. P., Sundquist, W. I. & Finch, J. T. Image reconstructions of helical assemblies of the HIV-1 CA protein. *Nature* **407**, 409-413, doi:10.1038/35030177 (2000).
109 Gentile, M. *et al.* Determination of the size of HIV using adenovirus type 2 as an internal length marker. *Journal of virological methods* **48**, 43-52 (1994).
110 Alimonti, J. B., Ball, T. B. & Fowke, K. R. Mechanisms of CD4+ T lymphocyte cell death in human immunodeficiency virus infection and AIDS. *The Journal of general virology* **84**, 1649-1661, doi:10.1099/vir.0.19110-0 (2003).
111 Malim, M. H. & Bieniasz, P. D. HIV Restriction Factors and Mechanisms of Evasion. *Cold Spring Harbor perspectives in medicine* **2**, a006940, doi:10.1101/cshperspect.a006940 (2012).
112 Kirmaier, A., Krupp, A. & Johnson, W. E. Understanding restriction factors and intrinsic immunity: insights and lessons from the primate lentiviruses. *Future virology* **9**, 483-497, doi:10.2217/fvl.14.25 (2014).
113 Ghimire, D., Rai, M. & Gaur, R. Novel host restriction factors implicated in HIV-1 replication. *The Journal of general virology* **99**, 435-446, doi:10.1099/jgv.0.001026 (2018).
114 Sheehy, A. M., Gaddis, N. C., Choi, J. D. & Malim, M. H. Isolation of a human gene that inhibits HIV-1 infection and is suppressed by the viral Vif protein. *Nature* **418**, 646-650, doi:10.1038/nature00939 (2002).
115 Harris, R. S. *et al.* DNA deamination mediates innate immunity to retroviral infection. *Cell* **113**, 803-809 (2003).
116 Mangeat, B. *et al.* Broad antiretroviral defence by human APOBEC3G through lethal editing of nascent reverse transcripts. *Nature* **424**, 99-103, doi:10.1038/nature01709 (2003).
117 Yu, X. *et al.* Induction of APOBEC3G ubiquitination and degradation by an HIV-1 Vif-Cul5-SCF complex. *Science (New York, N.Y.)* **302**, 1056-1060, doi:10.1126/science.1089591 (2003).
118 Stremlau, M. *et al.* The cytoplasmic body component TRIM5alpha restricts HIV-1 infection in Old World monkeys. *Nature* **427**, 848-853, doi:10.1038/nature02343 (2004).
119 Neil, S. J., Zang, T. & Bieniasz, P. D. Tetherin inhibits retrovirus release and is antagonized by HIV-1 Vpu. *Nature* **451**, 425-430, doi:10.1038/nature06553 (2008).
120 Van Damme, N. *et al.* The interferon-induced protein BST-2 restricts HIV-1 release and is downregulated from the cell surface by the viral Vpu protein. *Cell host & microbe* **3**, 245-252, doi:10.1016/j.chom.2008.03.001 (2008).
121 McNatt, M. W., Zang, T. & Bieniasz, P. D. Vpu binds directly to tetherin and displaces it from nascent virions. *PLoS pathogens* **9**, e1003299, doi:10.1371/journal.ppat.1003299 (2013).
122 Laguette, N. *et al.* SAMHD1 is the dendritic- and myeloid-cell-specific HIV-1 restriction factor counteracted by Vpx. *Nature* **474**, 654-657, doi:10.1038/nature10117 (2011).
123 Lahouassa, H. *et al.* SAMHD1 restricts the replication of human immunodeficiency virus type 1 by depleting the intracellular pool of deoxynucleoside triphosphates. *Nature immunology* **13**, 223-228, doi:10.1038/ni.2236 (2012).
124 Hofmann, H. *et al.* The Vpx lentiviral accessory protein targets SAMHD1 for degradation in the nucleus. *J Virol* **86**, 12552-12560, doi:10.1128/jvi.01657-12 (2012).
125 Lee, W. J., Fu, R. M., Liang, C. & Sloan, R. D. IFITM proteins inhibit HIV-1 protein synthesis. *Scientific reports* **8**, 14551, doi:10.1038/s41598-018-32785-5 (2018).
126 Yu, J. *et al.* IFITM Proteins Restrict HIV-1 Infection by Antagonizing the Envelope Glycoprotein. *Cell Rep* **13**, 145-156, doi:10.1016/j.celrep.2015.08.055 (2015).
127 Liu, Z. *et al.* The interferon-inducible MxB protein inhibits HIV-1 infection. *Cell host & microbe* **14**, 398-410, doi:10.1016/j.chom.2013.08.015 (2013).

128 Goujon, C. *et al.* Human MX2 is an interferon-induced post-entry inhibitor of HIV-1 infection. *Nature* **502**, 559-562, doi:10.1038/nature12542 (2013).
129 Kane, M. *et al.* MX2 is an interferon-induced inhibitor of HIV-1 infection. *Nature* **502**, 563-566, doi:10.1038/nature12653 (2013).
130 Shi, J. *et al.* HIV-1 Nef Antagonizes SERINC5 Restriction by Downregulation of SERINC5 via the Endosome/Lysosome System. *J Virol* **92**, doi:10.1128/jvi.00196-18 (2018).
131 Beitari, S., Ding, S., Pan, Q., Finzi, A. & Liang, C. Effect of HIV-1 Env on SERINC5 Antagonism. *J Virol* **91**, doi:10.1128/jvi.02214-16 (2017).
132 Dahabieh, M. S., Battivelli, E. & Verdin, E. Understanding HIV latency: the road to an HIV cure. *Annual review of medicine* **66**, 407-421, doi:10.1146/annurev-med-092112-152941 (2015).
133 Jordan, A., Bisgrove, D. & Verdin, E. HIV reproducibly establishes a latent infection after acute infection of T cells in vitro. *The EMBO journal* **22**, 1868-1877, doi:10.1093/emboj/cdg188 (2003).
134 Pierson, T., McArthur, J. & Siliciano, R. F. Reservoirs for HIV-1: mechanisms for viral persistence in the presence of antiviral immune responses and antiretroviral therapy. *Annual review of immunology* **18**, 665-708, doi:10.1146/annurev.immunol.18.1.665 (2000).
135 Duverger, A. *et al.* Determinants of the establishment of human immunodeficiency virus type 1 latency. *J Virol* **83**, 3078-3093, doi:10.1128/jvi.02058-08 (2009).
136 Tyagi, M., Pearson, R. J. & Karn, J. Establishment of HIV latency in primary CD4+ cells is due to epigenetic transcriptional silencing and P-TEFb restriction. *J Virol* **84**, 6425-6437, doi:10.1128/jvi.01519-09 (2010).
137 Verdin, E., Paras, P., Jr. & Van Lint, C. Chromatin disruption in the promoter of human immunodeficiency virus type 1 during transcriptional activation. *The EMBO journal* **12**, 3249-3259 (1993).
138 Han, Y. *et al.* Orientation-dependent regulation of integrated HIV-1 expression by host gene transcriptional readthrough. *Cell host & microbe* **4**, 134-146, doi:10.1016/j.chom.2008.06.008 (2008).
139 Davenport, M. P. *et al.* Functional cure of HIV: the scale of the challenge. *Nature reviews. Immunology* **19**, 45-54, doi:10.1038/s41577-018-0085-4 (2019).
140 Xu, W. *et al.* Advancements in Developing Strategies for Sterilizing and Functional HIV Cures. *BioMed research international* **2017**, 6096134, doi:10.1155/2017/6096134 (2017).
141 Kim, Y., Anderson, J. L. & Lewin, S. R. Getting the "Kill" into "Shock and Kill": Strategies to Eliminate Latent HIV. *Cell host & microbe* **23**, 14-26, doi:10.1016/j.chom.2017.12.004 (2018).
142 Rasmussen, T. A. & Lewin, S. R. Shocking HIV out of hiding: where are we with clinical trials of latency reversing agents? *Current opinion in HIV and AIDS* **11**, 394-401, doi:10.1097/coh.0000000000000279 (2016).
143 Archin, N. M. *et al.* Administration of vorinostat disrupts HIV-1 latency in patients on antiretroviral therapy. *Nature* **487**, 482-485, doi:10.1038/nature11286 (2012).
144 Elliott, J. H. *et al.* Short-term administration of disulfiram for reversal of latent HIV infection: a phase 2 dose-escalation study. *The lancet. HIV* **2**, e520-529, doi:10.1016/s2352-3018(15)00226-x (2015).
145 Elliott, J. H. *et al.* Activation of HIV transcription with short-course vorinostat in HIV-infected patients on suppressive antiretroviral therapy. *PLoS pathogens* **10**, e1004473, doi:10.1371/journal.ppat.1004473 (2014).
146 Gutierrez, C. *et al.* Bryostatin-1 for latent virus reactivation in HIV-infected patients on antiretroviral therapy. *Aids* **30**, 1385-1392, doi:10.1097/qad.0000000000001064 (2016).

147 Rasmussen, T. A. *et al.* Panobinostat, a histone deacetylase inhibitor, for latent-virus reactivation in HIV-infected patients on suppressive antiretroviral therapy: a phase 1/2, single group, clinical trial. *The lancet. HIV* **1**, e13-21, doi:10.1016/s2352-3018(14)70014-1 (2014).
148 Sogaard, O. S. *et al.* The Depsipeptide Romidepsin Reverses HIV-1 Latency In Vivo. *PLoS pathogens* **11**, e1005142, doi:10.1371/journal.ppat.1005142 (2015).
149 Mousseau, G. *et al.* The Tat Inhibitor Didehydro-Cortistatin A Prevents HIV-1 Reactivation from Latency. *mBio* **6**, e00465, doi:10.1128/mBio.00465-15 (2015).
150 Ahlenstiel, C. *et al.* Novel RNA Duplex Locks HIV-1 in a Latent State via Chromatin-mediated Transcriptional Silencing. *Molecular therapy. Nucleic acids* **4**, e261, doi:10.1038/mtna.2015.31 (2015).
151 Mendez, C., Ledger, S., Petoumenos, K., Ahlenstiel, C. & Kelleher, A. D. RNA-induced epigenetic silencing inhibits HIV-1 reactivation from latency. *Retrovirology* **15**, 67, doi:10.1186/s12977-018-0451-0 (2018).
152 Suzuki, K. *et al.* Closed chromatin architecture is induced by an RNA duplex targeting the HIV-1 promoter region. *J Biol Chem* **283**, 23353-23363, doi:10.1074/jbc.M709651200 (2008).
153 Griffiths, D. J. Endogenous retroviruses in the human genome sequence. *Genome biology* **2**, Reviews1017 (2001).
154 Zhu, W. *et al.* The CRISPR/Cas9 system inactivates latent HIV-1 proviral DNA. *Retrovirology* **12**, 22, doi:10.1186/s12977-015-0150-z (2015).
155 Qu, X. *et al.* Zinc-finger-nucleases mediate specific and efficient excision of HIV-1 proviral DNA from infected and latently infected human T cells. *Nucleic acids research* **41**, 7771-7782, doi:10.1093/nar/gkt571 (2013).
156 Karpinski, J. *et al.* Directed evolution of a recombinase that excises the provirus of most HIV-1 primary isolates with high specificity. *Nature biotechnology* **34**, 401-409, doi:10.1038/nbt.3467 (2016).
157 Haworth, K. G., Peterson, C. W. & Kiem, H. P. CCR5-edited gene therapies for HIV cure: Closing the door to viral entry. *Cytotherapy* **19**, 1325-1338, doi:10.1016/j.jcyt.2017.05.013 (2017).
158 Aryal, N. K., Wasylishen, A. R. & Lozano, G. CRISPR/Cas9 can mediate high-efficiency off-target mutations in mice in vivo. *Cell death & disease* **9**, 1099, doi:10.1038/s41419-018-1146-0 (2018).
159 Hutter, G. *et al.* Long-term control of HIV by CCR5 Delta32/Delta32 stem-cell transplantation. *The New England journal of medicine* **360**, 692-698, doi:10.1056/NEJMoa0802905 (2009).
160 Gupta, R. K. *et al.* HIV-1 remission following CCR5Delta32/Delta32 haematopoietic stem-cell transplantation. *Nature* **568**, 244-248, doi:10.1038/s41586-019-1027-4 (2019).
161 Rerks-Ngarm, S. *et al.* Vaccination with ALVAC and AIDSVAX to prevent HIV-1 infection in Thailand. *The New England journal of medicine* **361**, 2209-2220, doi:10.1056/NEJMoa0908492 (2009).
162 Ensoli, B., Cafaro, A., Monini, P., Marcotullio, S. & Ensoli, F. Challenges in HIV Vaccine Research for Treatment and Prevention. *Frontiers in immunology* **5**, 417, doi:10.3389/fimmu.2014.00417 (2014).
163 Burton, D. R. Advancing an HIV vaccine; advancing vaccinology. *Nature reviews. Immunology* **19**, 77-78, doi:10.1038/s41577-018-0103-6 (2019).
164 Jardine, J. G. *et al.* HIV-1 broadly neutralizing antibody precursor B cells revealed by germline-targeting immunogen. *Science (New York, N.Y.)* **351**, 1458-1463, doi:10.1126/science.aad9195 (2016).

165 Xu, K. *et al.* Epitope-based vaccine design yields fusion peptide-directed antibodies that neutralize diverse strains of HIV-1. *Nature medicine* **24**, 857-867, doi:10.1038/s41591-018-0042-6 (2018).
166 Duan, H. *et al.* Glycan Masking Focuses Immune Responses to the HIV-1 CD4-Binding Site and Enhances Elicitation of VRC01-Class Precursor Antibodies. *Immunity* **49**, 301-311.e305, doi:10.1016/j.immuni.2018.07.005 (2018).
167 Pauthner, M. G. *et al.* Vaccine-Induced Protection from Homologous Tier 2 SHIV Challenge in Nonhuman Primates Depends on Serum-Neutralizing Antibody Titers. *Immunity* **50**, 241-252.e246, doi:10.1016/j.immuni.2018.11.011 (2019).
168 Herrmann, J. M. & Spang, A. Intracellular parcel service: current issues in intracellular membrane trafficking. *Methods in molecular biology (Clifton, N.J.)* **1270**, 1-12, doi:10.1007/978-1-4939-2309-0_1 (2015).
169 Kaksonen, M. & Roux, A. Mechanisms of clathrin-mediated endocytosis. *Nature reviews. Molecular cell biology* **19**, 313-326, doi:10.1038/nrm.2017.132 (2018).
170 Hasegawa, T., Sugeno, N., Kikuchi, A., Baba, T. & Aoki, M. Membrane Trafficking Illuminates a Path to Parkinson's Disease. *The Tohoku journal of experimental medicine* **242**, 63-76, doi:10.1620/tjem.242.63 (2017).
171 Pearse, B. M. Clathrin: a unique protein associated with intracellular transfer of membrane by coated vesicles. *Proceedings of the National Academy of Sciences of the United States of America* **73**, 1255-1259 (1976).
172 Nabi, I. R. & Le, P. U. Caveolae/raft-dependent endocytosis. *The Journal of cell biology* **161**, 673-677, doi:10.1083/jcb.200302028 (2003).
173 Fra, A. M., Williamson, E., Simons, K. & Parton, R. G. De novo formation of caveolae in lymphocytes by expression of VIP21-caveolin. *Proceedings of the National Academy of Sciences of the United States of America* **92**, 8655-8659 (1995).
174 Kiss, A. L. & Botos, E. Endocytosis via caveolae: alternative pathway with distinct cellular compartments to avoid lysosomal degradation? *Journal of cellular and molecular medicine* **13**, 1228-1237, doi:10.1111/j.1582-4934.2009.00754.x (2009).
175 Hansen, C. G. & Nichols, B. J. Molecular mechanisms of clathrin-independent endocytosis. *Journal of cell science* **122**, 1713-1721, doi:10.1242/jcs.033951 (2009).
176 Meinecke, M. *et al.* Cooperative recruitment of dynamin and BIN/amphiphysin/Rvs (BAR) domain-containing proteins leads to GTP-dependent membrane scission. *J Biol Chem* **288**, 6651-6661, doi:10.1074/jbc.M112.444869 (2013).
177 Scales, S. J., Pepperkok, R. & Kreis, T. E. Visualization of ER-to-Golgi transport in living cells reveals a sequential mode of action for COPII and COPI. *Cell* **90**, 1137-1148 (1997).
178 Bonfanti, L. *et al.* Procollagen traverses the Golgi stack without leaving the lumen of cisternae: evidence for cisternal maturation. *Cell* **95**, 993-1003 (1998).
179 Gu, F., Crump, C. M. & Thomas, G. Trans-Golgi network sorting. *Cellular and molecular life sciences : CMLS* **58**, 1067-1084, doi:10.1007/pl00000922 (2001).
180 Hu, Y. B., Dammer, E. B., Ren, R. J. & Wang, G. The endosomal-lysosomal system: from acidification and cargo sorting to neurodegeneration. *Translational neurodegeneration* **4**, 18, doi:10.1186/s40035-015-0041-1 (2015).
181 Langemeyer, L., Frohlich, F. & Ungermann, C. Rab GTPase Function in Endosome and Lysosome Biogenesis. *Trends in cell biology* **28**, 957-970, doi:10.1016/j.tcb.2018.06.007 (2018).
182 Colicelli, J. Human RAS superfamily proteins and related GTPases. *Science's STKE : signal transduction knowledge environment* **2004**, Re13, doi:10.1126/stke.2502004re13 (2004).

183 Wandinger-Ness, A. & Zerial, M. Rab proteins and the compartmentalization of the endosomal system. *Cold Spring Harbor perspectives in biology* **6**, a022616, doi:10.1101/cshperspect.a022616 (2014).
184 Goody, R. S., Rak, A. & Alexandrov, K. The structural and mechanistic basis for recycling of Rab proteins between membrane compartments. *Cellular and molecular life sciences : CMLS* **62**, 1657-1670, doi:10.1007/s00018-005-4486-8 (2005).
185 de Renzis, S., Sonnichsen, B. & Zerial, M. Divalent Rab effectors regulate the sub-compartmental organization and sorting of early endosomes. *Nature cell biology* **4**, 124-133, doi:10.1038/ncb744 (2002).
186 Vetter, I. R. & Wittinghofer, A. The guanine nucleotide-binding switch in three dimensions. *Science (New York, N.Y.)* **294**, 1299-1304, doi:10.1126/science.1062023 (2001).
187 Mattera, R., Tsai, Y. C., Weissman, A. M. & Bonifacino, J. S. The Rab5 guanine nucleotide exchange factor Rabex-5 binds ubiquitin (Ub) and functions as a Ub ligase through an atypical Ub-interacting motif and a zinc finger domain. *J Biol Chem* **281**, 6874-6883, doi:10.1074/jbc.M509939200 (2006).
188 Lee, S. *et al.* Structural basis for ubiquitin recognition and autoubiquitination by Rabex-5. *Nature structural & molecular biology* **13**, 264-271, doi:10.1038/nsmb1064 (2006).
189 Linford, A. *et al.* Rab14 and its exchange factor FAM116 link endocytic recycling and adherens junction stability in migrating cells. *Developmental cell* **22**, 952-966, doi:10.1016/j.devcel.2012.04.010 (2012).
190 Poteryaev, D., Datta, S., Ackema, K., Zerial, M. & Spang, A. Identification of the switch in early-to-late endosome transition. *Cell* **141**, 497-508, doi:10.1016/j.cell.2010.03.011 (2010).
191 Yasuda, S. *et al.* Mon1-Ccz1 activates Rab7 only on late endosomes and dissociates from the lysosome in mammalian cells. *Journal of cell science* **129**, 329-340, doi:10.1242/jcs.178095 (2016).
192 Nakamura, S. & Yoshimori, T. New insights into autophagosome-lysosome fusion. *Journal of cell science* **130**, 1209-1216, doi:10.1242/jcs.196352 (2017).
193 Kuma, A. & Mizushima, N. Physiological role of autophagy as an intracellular recycling system: with an emphasis on nutrient metabolism. *Seminars in cell & developmental biology* **21**, 683-690, doi:10.1016/j.semcdb.2010.03.002 (2010).
194 Glick, D., Barth, S. & Macleod, K. F. Autophagy: cellular and molecular mechanisms. *The Journal of pathology* **221**, 3-12, doi:10.1002/path.2697 (2010).
195 Fletcher, D. A. & Mullins, R. D. Cell mechanics and the cytoskeleton. *Nature* **463**, 485-492, doi:10.1038/nature08908 (2010).
196 Hohmann, T. & Dehghani, F. The Cytoskeleton-A Complex Interacting Meshwork. *Cells* **8**, doi:10.3390/cells8040362 (2019).
197 Cross, J. A. & Dodding, M. P. Motor-cargo adaptors at the organelle-cytoskeleton interface. *Current opinion in cell biology* **59**, 16-23, doi:10.1016/j.ceb.2019.02.010 (2019).
198 Kikkawa, M., Ishikawa, T., Wakabayashi, T. & Hirokawa, N. Three-dimensional structure of the kinesin head-microtubule complex. *Nature* **376**, 274-277, doi:10.1038/376274a0 (1995).
199 Jordens, I. *et al.* The Rab7 effector protein RILP controls lysosomal transport by inducing the recruitment of dynein-dynactin motors. *Current biology : CB* **11**, 1680-1685 (2001).
200 Rezaul, K. *et al.* Engineered Tug-of-War Between Kinesin and Dynein Controls Direction of Microtubule Based Transport In Vivo. *Traffic (Copenhagen, Denmark)* **17**, 475-486, doi:10.1111/tra.12385 (2016).
201 Pauza, C. D. & Price, T. M. Human immunodeficiency virus infection of T cells and monocytes proceeds via receptor-mediated endocytosis. *The Journal of cell biology* **107**, 959-968, doi:10.1083/jcb.107.3.959 (1988).

202 Daecke, J., Fackler, O. T., Dittmar, M. T. & Krausslich, H. G. Involvement of clathrin-mediated endocytosis in human immunodeficiency virus type 1 entry. *J Virol* **79**, 1581-1594, doi:10.1128/jvi.79.3.1581-1594.2005 (2005).
203 Miyauchi, K., Kim, Y., Latinovic, O., Morozov, V. & Melikyan, G. B. HIV enters cells via endocytosis and dynamin-dependent fusion with endosomes. *Cell* **137**, 433-444, doi:10.1016/j.cell.2009.02.046 (2009).
204 Qi, M. *et al.* Rab11-FIP1C and Rab14 direct plasma membrane sorting and particle incorporation of the HIV-1 envelope glycoprotein complex. *PLoS pathogens* **9**, e1003278, doi:10.1371/journal.ppat.1003278 (2013).
205 Kirschman, J. *et al.* HIV-1 Envelope Glycoprotein Trafficking through the Endosomal Recycling Compartment Is Required for Particle Incorporation. *J Virol* **92**, doi:10.1128/jvi.01893-17 (2018).
206 Murray, J. L. *et al.* Rab9 GTPase is required for replication of human immunodeficiency virus type 1, filoviruses, and measles virus. *J Virol* **79**, 11742-11751, doi:10.1128/jvi.79.18.11742-11751.2005 (2005).
207 Gerber, P. P. *et al.* Rab27a controls HIV-1 assembly by regulating plasma membrane levels of phosphatidylinositol 4,5-bisphosphate. *The Journal of cell biology* **209**, 435-452, doi:10.1083/jcb.201409082 (2015).
208 Caillet, M. *et al.* Rab7A is required for efficient production of infectious HIV-1. *PLoS pathogens* **7**, e1002347, doi:10.1371/journal.ppat.1002347 (2011).
209 Spearman, P. Viral interactions with host cell Rab GTPases. *Small GTPases* **9**, 192-201, doi:10.1080/21541248.2017.1346552 (2018).
210 Cinti, A. *et al.* HIV-1 enhances mTORC1 activity and repositions lysosomes to the periphery by co-opting Rag GTPases. *Scientific reports* **7**, 5515, doi:10.1038/s41598-017-05410-0 (2017).
211 Dharan, A. *et al.* Bicaudal D2 facilitates the cytoplasmic trafficking and nuclear import of HIV-1 genomes during infection. *Proceedings of the National Academy of Sciences of the United States of America* **114**, E10707-e10716, doi:10.1073/pnas.1712033114 (2017).
212 Dharan, A. & Campbell, E. M. The Role of Microtubules and Microtubule Associated Proteins in HIV-1 Infection. *J Virol*, doi:10.1128/jvi.00085-18 (2018).
213 Lukic, Z., Dharan, A., Fricke, T., Diaz-Griffero, F. & Campbell, E. M. HIV-1 uncoating is facilitated by dynein and kinesin 1. *J Virol* **88**, 13613-13625, doi:10.1128/jvi.02219-14 (2014).
214 Ishino, Y., Shinagawa, H., Makino, K., Amemura, M. & Nakata, A. Nucleotide sequence of the iap gene, responsible for alkaline phosphatase isozyme conversion in Escherichia coli, and identification of the gene product. *J Bacteriol* **169**, 5429-5433 (1987).
215 Mojica, F. J., Diez-Villasenor, C., Soria, E. & Juez, G. Biological significance of a family of regularly spaced repeats in the genomes of Archaea, Bacteria and mitochondria. *Molecular microbiology* **36**, 244-246 (2000).
216 Jansen, R., Embden, J. D., Gaastra, W. & Schouls, L. M. Identification of genes that are associated with DNA repeats in prokaryotes. *Molecular microbiology* **43**, 1565-1575 (2002).
217 Bolotin, A., Quinquis, B., Sorokin, A. & Ehrlich, S. D. Clustered regularly interspaced short palindrome repeats (CRISPRs) have spacers of extrachromosomal origin. *Microbiology (Reading, England)* **151**, 2551-2561, doi:10.1099/mic.0.28048-0 (2005).
218 Mojica, F. J., Diez-Villasenor, C., Garcia-Martinez, J. & Soria, E. Intervening sequences of regularly spaced prokaryotic repeats derive from foreign genetic elements. *Journal of molecular evolution* **60**, 174-182, doi:10.1007/s00239-004-0046-3 (2005).
219 Pourcel, C., Salvignol, G. & Vergnaud, G. CRISPR elements in Yersinia pestis acquire new repeats by preferential uptake of bacteriophage DNA, and provide additional tools for

evolutionary studies. *Microbiology (Reading, England)* **151**, 653-663, doi:10.1099/mic.0.27437-0 (2005).

220 Makarova, K. S., Grishin, N. V., Shabalina, S. A., Wolf, Y. I. & Koonin, E. V. A putative RNA-interference-based immune system in prokaryotes: computational analysis of the predicted enzymatic machinery, functional analogies with eukaryotic RNAi, and hypothetical mechanisms of action. *Biol Direct* **1**, 7, doi:10.1186/1745-6150-1-7 (2006).

221 Barrangou, R. *et al.* CRISPR provides acquired resistance against viruses in prokaryotes. *Science (New York, N.Y.)* **315**, 1709-1712, doi:10.1126/science.1138140 (2007).

222 Brouns, S. J. *et al.* Small CRISPR RNAs guide antiviral defense in prokaryotes. *Science (New York, N.Y.)* **321**, 960-964, doi:10.1126/science.1159689 (2008).

223 Hale, C. R. *et al.* RNA-guided RNA cleavage by a CRISPR RNA-Cas protein complex. *Cell* **139**, 945-956, doi:10.1016/j.cell.2009.07.040 (2009).

224 Deltcheva, E. *et al.* CRISPR RNA maturation by trans-encoded small RNA and host factor RNase III. *Nature* **471**, 602-607, doi:10.1038/nature09886 (2011).

225 Deveau, H. *et al.* Phage response to CRISPR-encoded resistance in Streptococcus thermophilus. *J Bacteriol* **190**, 1390-1400, doi:10.1128/jb.01412-07 (2008).

226 Mojica, F. J., Diez-Villasenor, C., Garcia-Martinez, J. & Almendros, C. Short motif sequences determine the targets of the prokaryotic CRISPR defence system. *Microbiology (Reading, England)* **155**, 733-740, doi:10.1099/mic.0.023960-0 (2009).

227 Gasiunas, G., Barrangou, R., Horvath, P. & Siksnys, V. Cas9-crRNA ribonucleoprotein complex mediates specific DNA cleavage for adaptive immunity in bacteria. *Proceedings of the National Academy of Sciences of the United States of America* **109**, E2579-2586, doi:10.1073/pnas.1208507109 (2012).

228 Jinek, M. *et al.* A programmable dual-RNA-guided DNA endonuclease in adaptive bacterial immunity. *Science (New York, N.Y.)* **337**, 816-821, doi:10.1126/science.1225829 (2012).

229 Nishimasu, H. *et al.* Crystal structure of Cas9 in complex with guide RNA and target DNA. *Cell* **156**, 935-949, doi:10.1016/j.cell.2014.02.001 (2014).

230 Jinek, M. *et al.* Structures of Cas9 endonucleases reveal RNA-mediated conformational activation. *Science (New York, N.Y.)* **343**, 1247997, doi:10.1126/science.1247997 (2014).

231 Marraffini, L. A. & Sontheimer, E. J. CRISPR interference: RNA-directed adaptive immunity in bacteria and archaea. *Nature reviews. Genetics* **11**, 181-190, doi:10.1038/nrg2749 (2010).

232 Cong, L. *et al.* Multiplex genome engineering using CRISPR/Cas systems. *Science (New York, N.Y.)* **339**, 819-823, doi:10.1126/science.1231143 (2013).

233 Liu, Z. *et al.* Genome editing of the HIV co-receptors CCR5 and CXCR4 by CRISPR-Cas9 protects CD4+ T cells from HIV-1 infection. *Cell & Bioscience* **7**, 47, doi:10.1186/s13578-017-0174-2 (2017).

234 Wang, Z. *et al.* CRISPR/Cas9-Derived Mutations Both Inhibit HIV-1 Replication and Accelerate Viral Escape. *Cell Rep* **15**, 481-489, doi:10.1016/j.celrep.2016.03.042 (2016).

235 Wang, Z. *et al.* HIV-1 Employs Multiple Mechanisms To Resist Cas9/Single Guide RNA Targeting the Viral Primer Binding Site. *J Virol* **92**, doi:10.1128/jvi.01135-18 (2018).

236 Cyranoski, D. & Ledford, H. Genome-edited baby claim provokes international outcry. *Nature* **563**, 607-608, doi:10.1038/d41586-018-07545-0 (2018).

237 Ribeiro, L. F., Ribeiro, L. F. C., Barreto, M. Q. & Ward, R. J. Protein Engineering Strategies to Expand CRISPR-Cas9 Applications. *International journal of genomics* **2018**, 1652567, doi:10.1155/2018/1652567 (2018).

238 Smith, I. *et al.* Evaluation of RNAi and CRISPR technologies by large-scale gene expression profiling in the Connectivity Map. *PLoS biology* **15**, e2003213, doi:10.1371/journal.pbio.2003213 (2017).

239 Yau, E. H. & Rana, T. M. Next-Generation Sequencing of Genome-Wide CRISPR Screens. *Methods in molecular biology (Clifton, N.J.)* **1712**, 203-216, doi:10.1007/978-1-4939-7514-3_13 (2018).
240 Kim, H. S. *et al.* Arrayed CRISPR screen with image-based assay reliably uncovers host genes required for coxsackievirus infection. *Genome research* **28**, 859-868, doi:10.1101/gr.230250.117 (2018).
241 Henser-Brownhill, T., Monserrat, J. & Scaffidi, P. Generation of an arrayed CRISPR-Cas9 library targeting epigenetic regulators: from high-content screens to in vivo assays. *Epigenetics* **12**, 1065-1075, doi:10.1080/15592294.2017.1395121 (2017).
242 Park, R. J. *et al.* A genome-wide CRISPR screen identifies a restricted set of HIV host dependency factors. *Nature genetics* **49**, 193-203, doi:10.1038/ng.3741 (2017).
243 Marceau, C. D. *et al.* Genetic dissection of Flaviviridae host factors through genome-scale CRISPR screens. *Nature* **535**, 159-163, doi:10.1038/nature18631 (2016).
244 Zhang, R. *et al.* A CRISPR screen defines a signal peptide processing pathway required by flaviviruses. *Nature* **535**, 164-168, doi:10.1038/nature18625 (2016).
245 Richardson, R. B. *et al.* A CRISPR screen identifies IFI6 as an ER-resident interferon effector that blocks flavivirus replication. *Nature microbiology* **3**, 1214-1223, doi:10.1038/s41564-018-0244-1 (2018).
246 Hultquist, J. F. *et al.* A Cas9 Ribonucleoprotein Platform for Functional Genetic Studies of HIV-Host Interactions in Primary Human T Cells. *Cell Rep* **17**, 1438-1452, doi:10.1016/j.celrep.2016.09.080 (2016).
247 Jin, S. *et al.* TSC1 and DEPDC5 regulate HIV-1 latency through the mTOR signaling pathway. *Emerging microbes & infections* **7**, 138, doi:10.1038/s41426-018-0139-5 (2018).
248 Besnard, E. *et al.* The mTOR Complex Controls HIV Latency. *Cell host & microbe* **20**, 785-797, doi:10.1016/j.chom.2016.11.001 (2016).
249 Wei, X. *et al.* Emergence of resistant human immunodeficiency virus type 1 in patients receiving fusion inhibitor (T-20) monotherapy. *Antimicrobial agents and chemotherapy* **46**, 1896-1905 (2002).
250 Sarzotti-Kelsoe, M. *et al.* Optimization and validation of the TZM-bl assay for standardized assessments of neutralizing antibodies against HIV-1. *Journal of immunological methods* **409**, 131-146, doi:10.1016/j.jim.2013.11.022 (2014).
251 Xing, L., Wang, S., Hu, Q., Li, J. & Zeng, Y. Comparison of three quantification methods for the TZM-bl pseudovirus assay for screening of anti-HIV-1 agents. *Journal of virological methods* **233**, 56-61, doi:10.1016/j.jviromet.2016.03.008 (2016).
252 Marechal, V. *et al.* Human immunodeficiency virus type 1 entry into macrophages mediated by macropinocytosis. *J Virol* **75**, 11166-11177, doi:10.1128/jvi.75.22.11166-11177.2001 (2001).
253 Carter, G. C., Bernstone, L., Baskaran, D. & James, W. HIV-1 infects macrophages by exploiting an endocytic route dependent on dynamin, Rac1 and Pak1. *Virology* **409**, 234-250, doi:10.1016/j.virol.2010.10.018 (2011).
254 Gobeil, L. A., Lodge, R. & Tremblay, M. J. Macropinocytosis-like HIV-1 internalization in macrophages is CCR5 dependent and leads to efficient but delayed degradation in endosomal compartments. *J Virol* **87**, 735-745, doi:10.1128/jvi.01802-12 (2013).
255 van Wilgenburg, B., Moore, M. D., James, W. S. & Cowley, S. A. The productive entry pathway of HIV-1 in macrophages is dependent on endocytosis through lipid rafts containing CD4. *PLoS One* **9**, e86071, doi:10.1371/journal.pone.0086071 (2014).
256 Pritschet, K. *et al.* CD4- and dynamin-dependent endocytosis of HIV-1 into plasmacytoid dendritic cells. *Virology* **423**, 152-164, doi:10.1016/j.virol.2011.11.026 (2012).

257 Garcia-Exposito, L. *et al.* HIV-1 requires Arf6-mediated membrane dynamics to efficiently enter and infect T lymphocytes. *Molecular biology of the cell* **22**, 1148-1166, doi:10.1091/mbc.E10-08-0722 (2011).
258 de la Vega, M. *et al.* Inhibition of HIV-1 endocytosis allows lipid mixing at the plasma membrane, but not complete fusion. *Retrovirology* **8**, 99, doi:10.1186/1742-4690-8-99 (2011).
259 Kondo, N., Marin, M., Kim, J. H., Desai, T. M. & Melikyan, G. B. Distinct requirements for HIV-cell fusion and HIV-mediated cell-cell fusion. *J Biol Chem* **290**, 6558-6573, doi:10.1074/jbc.M114.623181 (2015).
260 Marin, M., Kushnareva, Y., Mason, C. S., Chanda, S. K. & Melikyan, G. B. HIV-1 Fusion with CD4+ T cells Is Promoted by Proteins Involved in Endocytosis and Intracellular Membrane Trafficking. *Viruses* **11**, doi:10.3390/v11020100 (2019).
261 Marechal, V., Clavel, F., Heard, J. M. & Schwartz, O. Cytosolic Gag p24 as an index of productive entry of human immunodeficiency virus type 1. *J Virol* **72**, 2208-2212 (1998).
262 Fredericksen, B. L., Wei, B. L., Yao, J., Luo, T. & Garcia, J. V. Inhibition of endosomal/lysosomal degradation increases the infectivity of human immunodeficiency virus. *J Virol* **76**, 11440-11446 (2002).
263 Fackler, O. T. & Peterlin, B. M. Endocytic entry of HIV-1. *Current biology : CB* **10**, 1005-1008 (2000).
264 Permanyer, M., Ballana, E. & Este, J. A. Endocytosis of HIV: anything goes. *Trends in microbiology* **18**, 543-551, doi:10.1016/j.tim.2010.09.003 (2010).
265 Melikyan, G. B. HIV entry: a game of hide-and-fuse? *Current opinion in virology* **4**, 1-7, doi:10.1016/j.coviro.2013.09.004 (2014).
266 Byland, R., Vance, P. J., Hoxie, J. A. & Marsh, M. A conserved dileucine motif mediates clathrin and AP-2-dependent endocytosis of the HIV-1 envelope protein. *Molecular biology of the cell* **18**, 414-425, doi:10.1091/mbc.e06-06-0535 (2007).
267 Boge, M., Wyss, S., Bonifacino, J. S. & Thali, M. A membrane-proximal tyrosine-based signal mediates internalization of the HIV-1 envelope glycoprotein via interaction with the AP-2 clathrin adaptor. *J Biol Chem* **273**, 15773-15778, doi:10.1074/jbc.273.25.15773 (1998).
268 Ohno, H. *et al.* Interaction of endocytic signals from the HIV-1 envelope glycoprotein complex with members of the adaptor medium chain family. *Virology* **238**, 305-315, doi:10.1006/viro.1997.8839 (1997).
269 Noble, B., Abada, P., Nunez-Iglesias, J. & Cannon, P. M. Recruitment of the adaptor protein 2 complex by the human immunodeficiency virus type 2 envelope protein is necessary for high levels of virus release. *J Virol* **80**, 2924-2932, doi:10.1128/jvi.80.6.2924-2932.2006 (2006).
270 Batonick, M. *et al.* Interaction of HIV-1 Gag with the clathrin-associated adaptor AP-2. *Virology* **342**, 190-200, doi:10.1016/j.virol.2005.08.001 (2005).
271 Ren, X., Park, S. Y., Bonifacino, J. S. & Hurley, J. H. How HIV-1 Nef hijacks the AP-2 clathrin adaptor to downregulate CD4. *eLife* **3**, e01754, doi:10.7554/eLife.01754 (2014).
272 Roeth, J. F., Williams, M., Kasper, M. R., Filzen, T. M. & Collins, K. L. HIV-1 Nef disrupts MHC-I trafficking by recruiting AP-1 to the MHC-I cytoplasmic tail. *The Journal of cell biology* **167**, 903-913, doi:10.1083/jcb.200407031 (2004).
273 Wolfe, B. L. & Trejo, J. Clathrin-dependent mechanisms of G protein-coupled receptor endocytosis. *Traffic (Copenhagen, Denmark)* **8**, 462-470, doi:10.1111/j.1600-0854.2007.00551.x (2007).
274 Unutmaz, D., KewalRamani, V. N. & Littman, D. R. G protein-coupled receptors in HIV and SIV entry: new perspectives on lentivirus-host interactions and on the utility of animal models. *Seminars in immunology* **10**, 225-236, doi:10.1006/smim.1998.0134 (1998).

275 Shimizu, N. *et al.* Broad usage spectrum of G protein-coupled receptors as coreceptors by primary isolates of HIV. *Aids* **23**, 761-769, doi:10.1097/QAD.0b013e328326cc0d (2009).
276 Bhattacharyya, S., Hope, T. J. & Young, J. A. Differential requirements for clathrin endocytic pathway components in cellular entry by Ebola and Marburg glycoprotein pseudovirions. *Virology* **419**, 1-9, doi:10.1016/j.virol.2011.07.018 (2011).
277 Vendeville, A. *et al.* HIV-1 Tat enters T cells using coated pits before translocating from acidified endosomes and eliciting biological responses. *Molecular biology of the cell* **15**, 2347-2360, doi:10.1091/mbc.e03-12-0921 (2004).
278 Xiao, H. *et al.* Selective CXCR4 antagonism by Tat: implications for in vivo expansion of coreceptor use by HIV-1. *Proceedings of the National Academy of Sciences of the United States of America* **97**, 11466-11471, doi:10.1073/pnas.97.21.11466 (2000).
279 Sagnier, S. *et al.* Autophagy restricts HIV-1 infection by selectively degrading Tat in CD4+ T lymphocytes. *J Virol* **89**, 615-625, doi:10.1128/jvi.02174-14 (2015).
280 Meyerholz, A. *et al.* Effect of clathrin assembly lymphoid myeloid leukemia protein depletion on clathrin coat formation. *Traffic (Copenhagen, Denmark)* **6**, 1225-1234, doi:10.1111/j.1600-0854.2005.00355.x (2005).
281 Wen, X., Ding, L., Hunter, E. & Spearman, P. An siRNA screen of membrane trafficking genes highlights pathways common to HIV-1 and M-PMV virus assembly and release. *PLoS One* **9**, e106151, doi:10.1371/journal.pone.0106151 (2014).
282 Komano, J., Miyauchi, K., Matsuda, Z. & Yamamoto, N. Inhibiting the Arp2/3 complex limits infection of both intracellular mature vaccinia virus and primate lentiviruses. *Molecular biology of the cell* **15**, 5197-5207, doi:10.1091/mbc.e04-04-0279 (2004).
283 Spear, M., Guo, J. & Wu, Y. The trinity of the cortical actin in the initiation of HIV-1 infection. *Retrovirology* **9**, 45, doi:10.1186/1742-4690-9-45 (2012).
284 Monier, S., Jollivet, F., Janoueix-Lerosey, I., Johannes, L. & Goud, B. Characterization of novel Rab6-interacting proteins involved in endosome-to-TGN transport. *Traffic (Copenhagen, Denmark)* **3**, 289-297 (2002).
285 Ducut Sigala, J. L. *et al.* Activation of transcription factor NF-kappaB requires ELKS, an IkappaB kinase regulatory subunit. *Science (New York, N.Y.)* **304**, 1963-1967, doi:10.1126/science.1098387 (2004).
286 Khadka, S. *et al.* A physical interaction network of dengue virus and human proteins. *Molecular & cellular proteomics : MCP* **10**, M111.012187, doi:10.1074/mcp.M111.012187 (2011).
287 Anyanwu, S. I. *et al.* Detection of HIV-1 and Human Proteins in Urinary Extracellular Vesicles from HIV+ Patients. *Advances in virology* **2018**, 7863412, doi:10.1155/2018/7863412 (2018).
288 McNeil, B. D. & Wu, L. G. Location matters: synaptotagmin helps place vesicles near calcium channels. *Neuron* **63**, 419-421, doi:10.1016/j.neuron.2009.08.001 (2009).
289 Yasuda, J., Whitmarsh, A. J., Cavanagh, J., Sharma, M. & Davis, R. J. The JIP group of mitogen-activated protein kinase scaffold proteins. *Molecular and cellular biology* **19**, 7245-7254, doi:10.1128/mcb.19.10.7245 (1999).
290 Suzuki, H. *et al.* ALS-linked P56S-VAPB, an aggregated loss-of-function mutant of VAPB, predisposes motor neurons to ER stress-related death by inducing aggregation of co-expressed wild-type VAPB. *Journal of neurochemistry* **108**, 973-985, doi:10.1111/j.0022-3042.2008.05857.x (2009).
291 Langelier, C. *et al.* Human ESCRT-II complex and its role in human immunodeficiency virus type 1 release. *J Virol* **80**, 9465-9480, doi:10.1128/jvi.01049-06 (2006).

292 Ghoujal, B., Milev, M. P., Ajamian, L., Abel, K. & Mouland, A. J. ESCRT-II's involvement in HIV-1 genomic RNA trafficking and assembly. *Biology of the cell* **104**, 706-721, doi:10.1111/boc.201200021 (2012).
293 Meng, B., Ip, N. C., Prestwood, L. J., Abbink, T. E. & Lever, A. M. Evidence that the endosomal sorting complex required for transport-II (ESCRT-II) is required for efficient human immunodeficiency virus-1 (HIV-1) production. *Retrovirology* **12**, 72, doi:10.1186/s12977-015-0197-x (2015).
294 Zhang, X. H., Tee, L. Y., Wang, X. G., Huang, Q. S. & Yang, S. H. Off-target Effects in CRISPR/Cas9-mediated Genome Engineering. *Molecular therapy. Nucleic acids* **4**, e264, doi:10.1038/mtna.2015.37 (2015).
295 Haapaniemi, E., Botla, S., Persson, J., Schmierer, B. & Taipale, J. CRISPR-Cas9 genome editing induces a p53-mediated DNA damage response. *Nature medicine* **24**, 927-930, doi:10.1038/s41591-018-0049-z (2018).
296 Sato, Y. & Tsurumi, T. Genome guardian p53 and viral infections. *Reviews in medical virology* **23**, 213-220, doi:10.1002/rmv.1738 (2013).
297 Lazo, P. A. & Santos, C. R. Interference with p53 functions in human viral infections, a target for novel antiviral strategies? *Reviews in medical virology* **21**, 285-300, doi:10.1002/rmv.696 (2011).
298 Herold, N. *et al.* HIV-1 entry in SupT1-R5, CEM-ss, and primary CD4+ T cells occurs at the plasma membrane and does not require endocytosis. *J Virol* **88**, 13956-13970, doi:10.1128/jvi.01543-14 (2014).
299 Kuchitsu, Y., Homma, Y., Fujita, N. & Fukuda, M. Rab7 knockout unveils regulated autolysosome maturation induced by glutamine starvation. *Journal of cell science* **131**, doi:10.1242/jcs.215442 (2018).
300 Mauvezin, C. & Neufeld, T. P. Bafilomycin A1 disrupts autophagic flux by inhibiting both V-ATPase-dependent acidification and Ca-P60A/SERCA-dependent autophagosome-lysosome fusion. *Autophagy* **11**, 1437-1438, doi:10.1080/15548627.2015.1066957 (2015).

APPENDIX

Supplementary Information

1.0 96-Well Plate Layout for CRISPR Screen

PLATE 1 (Pooled 4 crRNAs/gene)

Well	1	2	3	4	5	6	7	8	9	10	11	12
A		ARRB1	SNX2	SNAP91	TSG101	DNM2	SYNJ2	EEA1	CIB1	RAC1	MAPK8IP3	
B		ARF1	DIAPH1	PIK3CG	ARFIP2	RHOA	RAB2A	PACSIN1	BIN1	RAB3B	RAB3A	
C		RAB7B	VPS36	VPS4A	STAU1	EPN1	RAB11B	CBL	VCP	RAB4B	EFS	
D		AMPH	MAP4K2	HIP1R	PDCD6IP	CIB3	ARPC1B	RAB6A	ARPC4	EPN2	ROCK1	
E		IP6K3	PAK1	AP1M2	WASF2	SH3GLB1	CYTH3	WAS	SEC13	SNX1	NEDD4L	
F		VAV2	ARPC3	RAB5B	HIP1	ATG12	RAB6B	WASF1	LIMK1	CAV2	EPS15L1	
G		CDC42	PIP5K1A	NSF	PI4KA	AP4E1	RAB11A	COPA	ADAM10	GIT1	CAMK1	
H		CFL1	RAB29	FYN	SAR1A	EZR	CLTCL1	AP3D1	ITSN1	RAB4A	CAV1	

=Empty Well

PLATE 2 (Pooled 4 crRNAs/gene)

Well	1	2	3	4	5	6	7	8	9	10	11	12
A		AP2B1	EPN3	ACTR3	HGS	ACTR2	GRB2	PACSIN3	VAPB	AP2M1	SYNJ1	
B		SYT2	ATP6V0A1	ROCK2	GORASP1	CLTA	RAB1A	BECN1	DAB2	CLTB	AP2A2	
C		PICALM	EPS15	AP1M1	ITSN2	RAB5C	PIK3C2G	CIB2	RAB11FIP5	CLINT1	TNIK	
D		CBLB	AP2A1	DNM1	RAB3D	ARRB2	ATM	ARPC2	SYT1	RAB8A	AP1B1	
E		MAPK8IP2	NEDD4	WASF3	ARPC5	MAPK8IP1	RAB3C	VAMP1	RAB5A	MAP1LC3A	DNM3	
F		ERC1	VAMP2	ASAP2	SH3GLB2	CLTC	CBLC	RAB8B	CAV3	VAPA	ARF6	
G		TZM-bl Cas9	TZM-bl Cas9	TZM-bl Cas9 [non-infected]	TZM-bl Cas9 [non-infected]	TZM-bl-Cas9 + NTC	TZM-bl-Cas9 + NTC	TZM-bl-Cas9 + NTC [non-infected]	TZM-bl-Cas9 + NTC [non-infected]			
H		WT TZM-bl	WT TZM-bl	WT TZM-bl [non-infected]	WT TZM-bl [non-infected]							

=Empty Well
=Controls

2.0 crRNA Sequences in Membrane Trafficking CRISPR Screen Library

Dharmacon EDIT-R™ crRNA Library - Human Membrane Trafficking
GC-005500 Lot 17114

Plate Name	Well	Gene Symbol	Target Sequence	Genomic Location	PAM
Plate 1 crRNA 1	A02	*ARRB1*	TCCTACCTCCTTATCCAGAG	hg38l+chr11:75278603-75278625	AGG
Plate 1 crRNA 1	A03	*SNX2*	GTGCCGACCTAATCCTCAGA	hg38l+chr5:122775422-122775444	GGG
Plate 1 crRNA 1	A04	*SNAP91*	GTTGCAAATAAATCAACCGG	hg38l+chr6:83607723-83607745	TGG
Plate 1 crRNA 1	A05	*TSG101*	GGCGGATAGGATGCCGAAAT	hg38l+chr11:18509568-18509590	AGG
Plate 1 crRNA 1	A06	*DNM2*	GTTCAGGAATCGTCACCCGG	hg38l+chr19:10759755-10759777	CGG
Plate 1 crRNA 1	A07	*SYNJ2*	TTGATCTGCTTGACATTATA	hg38l-chr6:158089866-158089888	AGG
Plate 1 crRNA 1	A08	*EEA1*	AATCTTGCTTTGAAGCGGTA	hg38l-chr12:92864854-92864876	CGG
Plate 1 crRNA 1	A09	*CIB1*	CTTCAAGGAGCGAATCTGCA	hg38l-chr15:90231477-90231499	GGG
Plate 1 crRNA 1	A10	*RAC1*	AATCCTTACTGTTTGCGGAT	hg38l-chr7:6392028-6392050	AGG

Plate 1 crRNA 1	A11	*MAPK8IP3*	GCCTGGGCCATGGAGCAGTA	hg38l-chr16:1768300-1768322	GGG
Plate 1 crRNA 1	B02	*ARF1*	GTGTTCGCCAACAAGCAGGT	hg38l+chr1:228097698-228097720	AGG
Plate 1 crRNA 1	B03	*DIAPH1*	ATTGAGGCGAGGCCGCAGTC	hg38l+chr5:141528906-141528928	GGG
Plate 1 crRNA 1	B04	*PIK3CG*	GTGGGCAGCACGAACTCGAT	hg38l-chr7:106867676-106867698	GGG
Plate 1 crRNA 1	B05	*ARFIP2*	CCATGACGGACGGGATCCTA	hg38l-chr11:6480401-6480423	GGG
Plate 1 crRNA 1	B06	*RHOA*	GGCCACTCACCTAAACTATC	hg38l+chr3:49368418-49368440	AGG
Plate 1 crRNA 1	B07	*RAB2A*	TACATCATAATCGGCGACAC	hg38l+chr8:60517232-60517254	AGG
Plate 1 crRNA 1	B08	*PACSIN1*	GCCGTCATCGATGCGCTTCA	hg38l-chr6:34527351-34527373	CGG
Plate 1 crRNA 1	B09	*BIN1*	CCGCCCTTCTGTAGCCGCGT	hg38l-chr2:127063638-127063660	AGG
Plate 1 crRNA 1	B10	*RAB3B*	GACACAGACCCGTCGATGCT	hg38l-chr1:51919991-51920013	GGG
Plate 1 crRNA 1	B11	*RAB3A*	CCTCTTGTCGTTGCGATAGA	hg38l+chr19:18202531-18202553	TGG
Plate 1 crRNA 1	C02	*RAB7B*	ATGGTGTCCACGTTCTACAA	hg38l-chr1:205992637-205992659	GGG
Plate 1 crRNA 1	C03	*VPS36*	TTGGACCTTATGCAGTCGGA	hg38l-chr13:52449987-52450009	GGG
Plate 1 crRNA 1	C04	*VPS4A*	GAGTGCTCCCGAGATGCAAC	hg38l-chr16:69321108-69321130	CGG
Plate 1 crRNA 1	C05	*STAU1*	CTGCAGGATCCTCAACGCTT	hg38l+chr20:49151609-49151631	TGG
Plate 1 crRNA 1	C06	*EPN1*	TGCCGTCGCGGTCCACGTAC	hg38l-chr19:55685494-55685516	TGG
Plate 1 crRNA 1	C07	*RAB11B*	CACCCGCAACGAGTTCAACC	hg38l+chr19:8399915-8399937	TGG
Plate 1 crRNA 1	C08	*CBL*	GAAGGCGGCCGTTCCACCTA	hg38l-chr11:119284963-119284985	GGG
Plate 1 crRNA 1	C09	*VCP*	TACCAAATCGCCGTAGAGCT	hg38l+chr9:35062000-35062022	GGG
Plate 1 crRNA 1	C10	*RAB4B*	GTGACGCGGAGTTATTACCG	hg38l+chr19:40783782-40783804	AGG
Plate 1 crRNA 1	C11	*EFS*	GGCTGACGCTCGTTTCAGGT	hg38l+chr14:23359794-23359816	TGG
Plate 1 crRNA 1	D02	*AMPH*	ATTAGTGGCTTACCGTCCAT	hg38l+chr7:38432176-38432198	AGG
Plate 1 crRNA 1	D03	*MAP4K2*	TATCTTCACGGCGGCCAGTT	hg38l+chr11:64802901-64802923	CGG
Plate 1 crRNA 1	D04	*HIP1R*	GGACCCACTTACGGTCGGCA	hg38l-chr12:122858935-122858957	GGG
Plate 1 crRNA 1	D05	*PDCD6IP*	CTTAAGTCGAGAGCCGACCG	hg38l+chr3:33825234-33825256	TGG
Plate 1 crRNA 1	D06	*CIB3*	CGACGACTACATTTGTGCGT	hg38l-chr19:16164881-16164903	GGG
Plate 1 crRNA 1	D07	*ARPC1B*	GGTCATCCTGCGGATCAACC	hg38l+chr7:99388139-99388161	GGG
Plate 1 crRNA 1	D08	*RAB6A*	GAACAGCCTCCTTCACTGAC	hg38l+chr11:73677905-73677927	TGG
Plate 1 crRNA 1	D09	*ARPC4*	AGAACTTCTTTATCCTTCGA	hg38l+chr3:9801722-9801744	AGG
Plate 1 crRNA 1	D10	*EPN2*	AGGTTCACCAGGGCCGCGTT	hg38l-chr17:19331984-19332006	GGG
Plate 1 crRNA 1	D11	*ROCK1*	ATCTTGTAGAAAGCGTTCGA	hg38l+chr18:20953633-20953655	GGG
Plate 1 crRNA 1	E02	*IP6K3*	ACCACCGGGAGAGCTACCGT	hg38l+chr6:33722876-33722898	GGG
Plate 1 crRNA 1	E03	*PAK1*	GTGGGTTGTTATGGAATACT	hg38l-chr11:77340720-77340742	TGG
Plate 1 crRNA 1	E04	*AP1M2*	GTCCTTCTGAGCGAAATCGT	hg38l-chr19:10581352-10581374	CGG
Plate 1 crRNA 1	E05	*WASF2*	TCGGTCGACCCTCTCAGCAA	hg38l+chr1:27418997-27419019	GGG
Plate 1 crRNA 1	E06	*SH3GLB1*	CTGCACGGCGCGACTGAGGA	hg38l-chr1:86704949-86704971	AGG
Plate 1 crRNA 1	E07	*CYTH3*	GCGATGAACCGTTCTGCCGT	hg38l+chr7:6170882-6170904	GGG
Plate 1 crRNA 1	E08	*WAS*	TCACGAGTTCACGATACCGT	hg38l+chrX:48686841-48686863	GGG
Plate 1 crRNA 1	E09	*SEC13*	TCTTTGATGTGCGCAATGGA	hg38l-chr3:10315347-10315369	GGG
Plate 1 crRNA 1	E10	*SNX1*	ACAGAAGCTTACGCGGACTA	hg38l-chr15:64131882-64131904	TGG
Plate 1 crRNA 1	E11	*NEDD4L*	ACCCGGCGTGGTATGTACAT	hg38l-chr18:58341048-58341070	AGG
Plate 1 crRNA 1	F02	*VAV2*	TCGGGCGGCAAAGTTATACC	hg38l+chr9:133768541-133768563	TGG
Plate 1 crRNA 1	F03	*ARPC3*	GATCCTGATACCAAACTCAT	hg38l-chr12:110445508-110445530	CGG

Plate 1 crRNA 1	F04	*RAB5B*	CGTAAACCACGATTGCAGCT	hg38l-chr12:55990062-55990084	TGG
Plate 1 crRNA 1	F05	*HIP1*	AATGGTTGAGGCCACAACGC	hg38l+chr7:75542879-75542901	CGG
Plate 1 crRNA 1	F06	*ATG12*	CCTCCAGCAGCAATTGAAGT	hg38l+chr5:115841497-115841519	AGG
Plate 1 crRNA 1	F07	*RAB6B*	GACGTCGTCGATCCACTTAG	hg38l+chr3:133839574-133839596	AGG
Plate 1 crRNA 1	F08	*WASF1*	ACATCGTACGTCTCCTGTAA	hg38l+chr6:110108570-110108592	TGG
Plate 1 crRNA 1	F09	*LIMK1*	TGGCCGGCAGACTACGCGGA	hg38l-chr7:74107096-74107118	GGG
Plate 1 crRNA 1	F10	*CAV2*	GCTCCATTGTGTACGAGCGT	hg38l+chr7:116506056-116506078	AGG
Plate 1 crRNA 1	F11	*EPS15L1*	TTGGAGGGTGGGATGAGGGA	hg38l+chr19:16425237-16425259	CGG
Plate 1 crRNA 1	G02	*CDC42*	GGAGTGTTCTGCACTTACAC	hg38l+chr1:22086845-22086867	AGG
Plate 1 crRNA 1	G03	*PIP5K1A*	TATCCGGCCCGATGATTACT	hg38l+chr1:151232344-151232366	TGG
Plate 1 crRNA 1	G04	*NSF*	AACGAAGTACCTTACCTGTA	hg38l-chr17:46751609-46751631	GGG
Plate 1 crRNA 1	G05	*PI4KA*	CGGGTCCAACCGAACGAGAC	hg38l+chr22:20727807-20727829	GGG
Plate 1 crRNA 1	G06	*AP4E1*	GTGCGCCTGAGATGTCAATT	hg38l-chr15:50958619-50958641	TGG
Plate 1 crRNA 1	G07	*RAB11A*	CATTTCGAGTAAATCGAGAC	hg38l-chr15:65877372-65877394	AGG
Plate 1 crRNA 1	G08	*COPA*	GCTTGGGCCCGAGTTCTAGT	hg38l+chr1:160291352-160291374	AGG
Plate 1 crRNA 1	G09	*ADAM10*	GGATTCATCCAGACTCGTGG	hg38l-chr15:58679210-58679232	TGG
Plate 1 crRNA 1	G10	*GIT1*	GCTGAGTATTCCGGGTTAAC	hg38l+chr17:29577658-29577680	AGG
Plate 1 crRNA 1	G11	*CAMK1*	TGTGGAACTCCGGGATACGT	hg38l-chr3:9761630-9761652	GGG
Plate 1 crRNA 1	H02	*CFL1*	GCATAGCGGCAGTCCTTATC	hg38l+chr11:65855998-65856020	TGG
Plate 1 crRNA 1	H03	*RAB29*	TGAGCCGGGACCAGATTGAC	hg38l-chr1:205770810-205770832	CGG
Plate 1 crRNA 1	H04	*FYN*	GATTGTGAACCTCCCGTACA	hg38l+chr6:111674569-111674591	GGG
Plate 1 crRNA 1	H05	*SAR1A*	TTCCAACACTACATCCGAGT	hg38l-chr10:70161614-70161636	AGG
Plate 1 crRNA 1	H06	*EZR*	GTAGCTCACCGGCTCGTACA	hg38l+chr6:158767408-158767430	CGG
Plate 1 crRNA 1	H07	*CLTCL1*	TCTGTAACAGAGCTCGACGT	hg38l+chr22:19191409-19191431	TGG
Plate 1 crRNA 1	H08	*AP3D1*	TTGCCCAGCCGCGGTTCCAA	hg38l+chr19:2129126-2129148	AGG
Plate 1 crRNA 1	H09	*ITSN1*	TTCCAAGTGCCGGCCAGTTA	hg38l+chr21:33813987-33814009	AGG
Plate 1 crRNA 1	H10	*RAB4A*	GTGACGAGAAGTTATTACCG	hg38l+chr1:229295852-229295874	AGG
Plate 1 crRNA 1	H11	*CAV1*	ACTAACCGCTCCGACAGCTA	hg38l-chr7:116526372-116526394	CGG
Plate 1 crRNA 2	A02	*ARRB1*	AGAAGCCTCTCTGGATAAGG	hg38l-chr11:75278608-75278630	AGG
Plate 1 crRNA 2	A03	*SNX2*	TCTGCCAGCACTTCATTCGA	hg38l-chr5:122826061-122826083	TGG
Plate 1 crRNA 2	A04	*SNAP91*	GATGTCGGGCCAAACGCTCA	hg38l-chr6:83707906-83707928	CGG
Plate 1 crRNA 2	A05	*TSG101*	GATTGGGAGGGTATCCGGAT	hg38l+chr11:18506861-18506883	GGG
Plate 1 crRNA 2	A06	*DNM2*	TGATGACACCGATGGTCCGT	hg38l-chr19:10777119-10777141	AGG
Plate 1 crRNA 2	A07	*SYNJ2*	ACCCGTGGCGTGAACGACGA	hg38l+chr6:158033627-158033649	CGG
Plate 1 crRNA 2	A08	*EEA1*	TTGACGTCCACTGTGTTTAT	hg38l+chr12:92891648-92891670	AGG
Plate 1 crRNA 2	A09	*CIB1*	ATGGGACTTGATGTCTGGCG	hg38l+chr15:90231376-90231398	TGG
Plate 1 crRNA 2	A10	*RAC1*	TACTGTTTGCGGATAGGATA	hg38l-chr7:6392022-6392044	GGG
Plate 1 crRNA 2	A11	*MAPK8IP3*	GAGCACGTGCGTAACGACGA	hg38l+chr16:1763715-1763737	CGG
Plate 1 crRNA 2	B02	*ARF1*	GAAATGCGCATCCTCATGGT	hg38l+chr1:228097163-228097185	GGG
Plate 1 crRNA 2	B03	*DIAPH1*	ACATGGTCTTGATTCCAAAC	hg38l+chr5:141580865-141580887	TGG
Plate 1 crRNA 2	B04	*PIK3CG*	ACTGTGAGGTCGGTGTTCCG	hg38l-chr7:106868681-106868703	AGG
Plate 1 crRNA 2	B05	*ARFIP2*	GGCATCAACACCTATAAGGT	hg38l-chr11:6479135-6479157	AGG
Plate 1 crRNA 2	B06	*RHOA*	CTGCTCTGCAAGCTAGACGT	hg38l-chr3:49360239-49360261	GGG

Plate 1 crRNA 2	B07	*RAB2A*	TCTGTAATACGACCTTGTGA	hg38l-chr8:60584230-60584252	TGG
Plate 1 crRNA 2	B08	*PACSIN1*	TCAGGTCGTTGCATAGACGG	hg38l-chr6:34527373-34527395	TGG
Plate 1 crRNA 2	B09	*BIN1*	ACCTGGCCTCCGTCAAAGGT	hg38l-chr2:127070757-127070779	AGG
Plate 1 crRNA 2	B10	*RAB3B*	GATGCCCACGGTGCTAACGA	hg38l+chr1:51976947-51976969	AGG
Plate 1 crRNA 2	B11	*RAB3A*	TGCATTGAAGGATTCCTCGT	hg38l+chr19:18200338-18200360	TGG
Plate 1 crRNA 2	C02	*RAB7B*	ACGTTCTACAAGGGCTCCGA	hg38l-chr1:205992628-205992650	TGG
Plate 1 crRNA 2	C03	*VPS36*	GGGAATAATGTCACTCACGG	hg38l-chr13:52423609-52423631	AGG
Plate 1 crRNA 2	C04	*VPS4A*	GGCCGCACGAAGTACCTGGA	hg38l-chr16:69311525-69311547	GGG
Plate 1 crRNA 2	C05	*STAU1*	GATCAATCCGATTAGCCGAC	hg38l-chr20:49123184-49123206	TGG
Plate 1 crRNA 2	C06	*EPN1*	CAGCGAGTCCAGGTCGACGA	hg38l-chr19:55694900-55694922	GGG
Plate 1 crRNA 2	C07	*RAB11B*	GGTGGCGAACTCCACGCCGA	hg38l-chr19:8399950-8399972	TGG
Plate 1 crRNA 2	C08	*CBL*	TAAAGGTACTGAACCCATCG	hg38l+chr11:119278551-119278573	TGG
Plate 1 crRNA 2	C09	*VCP*	CGATACGCTTCCAGGAAGTA	hg38l+chr9:35066689-35066711	CGG
Plate 1 crRNA 2	C10	*RAB4B*	CCCGGGTGGTCAACGTGGGT	hg38l+chr19:40780427-40780449	GGG
Plate 1 crRNA 2	C11	*EFS*	GAATGCCCTCGTACTCATTG	hg38l+chr14:23359352-23359374	TGG
Plate 1 crRNA 2	D02	*AMPH*	ACTGATTTGGTACAGCCGGT	hg38l-chr7:38429837-38429859	AGG
Plate 1 crRNA 2	D03	*MAP4K2*	TAGCTTGACTATCTTCACGG	hg38l+chr11:64802892-64802914	CGG
Plate 1 crRNA 2	D04	*HIP1R*	CGTGCTGGCTGCGATCTCGT	hg38l-chr12:122860738-122860760	GGG
Plate 1 crRNA 2	D05	*PDCD6IP*	CGTCCGCTGGACAAGCACGA	hg38l+chr3:33798894-33798916	GGG
Plate 1 crRNA 2	D06	*CIB3*	GATTGCCCAGGTATTCTCTG	hg38l-chr19:16168242-16168264	AGG
Plate 1 crRNA 2	D07	*ARPC1B*	GCCCTTCAGCGTCCACACGT	hg38l-chr7:99388096-99388118	AGG
Plate 1 crRNA 2	D08	*RAB6A*	TCACTGACTGGTTGCTCCTG	hg38l+chr11:73677917-73677939	AGG
Plate 1 crRNA 2	D09	*ARPC4*	GCCCGGCTCTCTCACCATCG	hg38l-chr3:9793117-9793139	CGG
Plate 1 crRNA 2	D10	*EPN2*	CTTGCTTGAGGCGACAGTCA	hg38l-chr17:19331922-19331944	GGG
Plate 1 crRNA 2	D11	*ROCK1*	ATGGCATCTTCGACACTCTA	hg38l+chr18:20954841-20954863	GGG
Plate 1 crRNA 2	E02	*IP6K3*	AATGAGCACACCACCTACGA	hg38l-chr6:33722793-33722815	TGG
Plate 1 crRNA 2	E03	*PAK1*	GATGTAGCCACGTCCCGAGT	hg38l+chr11:77355781-77355803	TGG
Plate 1 crRNA 2	E04	*AP1M2*	ATTGATCAGCCGCAACTACA	hg38l-chr19:10584046-10584068	AGG
Plate 1 crRNA 2	E05	*WASF2*	TTGAATGGTGGAACTTCTGA	hg38l+chr1:27418370-27418392	AGG
Plate 1 crRNA 2	E06	*SH3GLB1*	TCTGGAGGTCCAACATATAC	hg38l-chr1:86735144-86735166	TGG
Plate 1 crRNA 2	E07	*CYTH3*	AATAGAGGCAGTTATCGGTC	hg38l+chr7:6165751-6165773	AGG
Plate 1 crRNA 2	E08	*WAS*	GCCGTAAAGGCGGATGAAGT	hg38l-chrX:48684395-48684417	AGG
Plate 1 crRNA 2	E09	*SEC13*	ATGACCGGAAAGTCATTATC	hg38l-chr3:10312637-10312659	TGG
Plate 1 crRNA 2	E10	*SNX1*	GTGCAAACTCACGACCACCG	hg38l-chr15:64096162-64096184	CGG
Plate 1 crRNA 2	E11	*NEDD4L*	AAATTAGCATGGGTTACCGG	hg38l-chr18:58333887-58333909	TGG
Plate 1 crRNA 2	F02	*VAV2*	CGAACGTTCCCGGGACTTGT	hg38l+chr9:133770406-133770428	AGG
Plate 1 crRNA 2	F03	*ARPC3*	ATTGGCCTTGAAGTAATAGA	hg38l+chr12:110440339-110440361	TGG
Plate 1 crRNA 2	F04	*RAB5B*	TTGAGATCTGGGACACAGCT	hg38l+chr12:55989995-55990017	GGG
Plate 1 crRNA 2	F05	*HIP1*	CGCTCAATTAAGTGGTCCCT	hg38l+chr7:75561384-75561406	GGG
Plate 1 crRNA 2	F06	*ATG12*	TCGAGTGTCTCCAAGCAAGA	hg38l-chr5:115841549-115841571	TGG
Plate 1 crRNA 2	F07	*RAB6B*	GTTGTAGCCAGTCTTCGCAC	hg38l+chr3:133838175-133838197	TGG
Plate 1 crRNA 2	F08	*WASF1*	CTCATGACAGGCGGCGAGAA	hg38l-chr6:110105508-110105530	TGG
Plate 1 crRNA 2	F09	*LIMK1*	GATCCGGTCTCCGACGTGGA	hg38l-chr7:74105913-74105935	TGG

Plate 1 crRNA 2	F10	*CAV2*	CGTCCTACGCTCGTACACAA	hg38l-chr7:116506059-116506081	TGG
Plate 1 crRNA 2	F11	*EPS15L1*	CCTGGTGTGAACGCGCAAAG	hg38l+chr19:16402162-16402184	TGG
Plate 1 crRNA 2	G02	*CDC42*	GAAGCCTTTATACTTACAGT	hg38l-chr1:22078578-22078600	CGG
Plate 1 crRNA 2	G03	*PIP5K1A*	CTGGGAAGCCCGCCGTTTGT	hg38l-chr1:151234348-151234370	AGG
Plate 1 crRNA 2	G04	*NSF*	TATGCAGGCCCTCCTCACAG	hg38l+chr17:46713846-46713868	TGG
Plate 1 crRNA 2	G05	*PI4KA*	GAGACGACCGCGTCCATGTA	hg38l+chr22:20709974-20709996	GGG
Plate 1 crRNA 2	G06	*AP4E1*	GGTCACAGCAGCAATTAACC	hg38l-chr15:50958598-50958620	AGG
Plate 1 crRNA 2	G07	*RAB11A*	GAGTACGACTACCTCTTTAA	hg38l+chr15:65869604-65869626	AGG
Plate 1 crRNA 2	G08	*COPA*	CATGTCATAATTGAGCTGGT	hg38l+chr1:160290621-160290643	AGG
Plate 1 crRNA 2	G09	*ADAM10*	GGCAACTTTGGATTACTACT	hg38l+chr15:58599618-58599640	TGG
Plate 1 crRNA 2	G10	*GIT1*	TGTGTGTTCCGCCCGTTCAC	hg38l+chr17:29576358-29576380	TGG
Plate 1 crRNA 2	G11	*CAMK1*	GGCATCATTCTCGTCATAGA	hg38l+chr3:9760729-9760751	AGG
Plate 1 crRNA 2	H02	*CFL1*	ATTGCAAGCAAACTGCTACG	hg38l-chr11:65855413-65855435	AGG
Plate 1 crRNA 2	H03	*RAB29*	GACCGGTTCAGTAAAGAGAA	hg38l-chr1:205770793-205770815	CGG
Plate 1 crRNA 2	H04	*FYN*	GTGAACTCTTCGTCTCATAC	hg38l-chr6:111719831-111719853	GGG
Plate 1 crRNA 2	H05	*SAR1A*	GATCTTGGTGGGCACGAGCA	hg38l-chr10:70161003-70161025	AGG
Plate 1 crRNA 2	H06	*EZR*	TAGCTCACCGGCTCGTACAC	hg38l+chr6:158767409-158767431	GGG
Plate 1 crRNA 2	H07	*CLTCL1*	GTCCGGCTAGGGTTGACCTA	hg38l+chr22:19222077-19222099	GGG
Plate 1 crRNA 2	H08	*AP3D1*	ATGTCCTCGTCGCTCTCCGT	hg38l+chr19:2115265-2115287	GGG
Plate 1 crRNA 2	H09	*ITSN1*	GATGTCGATTGACCACCCAA	hg38l+chr21:33775011-33775033	AGG
Plate 1 crRNA 2	H10	*RAB4A*	TTGGAAACAAGTGCGCTCAC	hg38l+chr1:229298988-229299010	AGG
Plate 1 crRNA 2	H11	*CAV1*	AGTGTACGACGCGCACACCA	hg38l+chr7:116526614-116526636	AGG
Plate 1 crRNA 3	A02	*ARRB1*	ACGTGGACGTTGACGCTGAT	hg38l+chr11:75277408-75277430	GGG
Plate 1 crRNA 3	A03	*SNX2*	CGTGATCTTTGATAGATCCA	hg38l+chr5:122799828-122799850	GGG
Plate 1 crRNA 3	A04	*SNAP91*	TTGCAAATAAATCAACCGGT	hg38l+chr6:83607724-83607746	GGG
Plate 1 crRNA 3	A05	*TSG101*	TAGGGATGGCACAATCAGCG	hg38l-chr11:18484043-18484065	AGG
Plate 1 crRNA 3	A06	*DNM2*	CGTGTGGCGAGTAGACTCGA	hg38l-chr19:10772606-10772628	AGG
Plate 1 crRNA 3	A07	*SYNJ2*	GCATTTGTCGCTTGTATCGT	hg38l-chr6:158076696-158076718	AGG
Plate 1 crRNA 3	A08	*EEA1*	GTGGTGGTTAAACCATGTTA	hg38l-chr12:92929058-92929080	AGG
Plate 1 crRNA 3	A09	*CIB1*	CTGCAGATTCGCTCCTTGAA	hg38l+chr15:90231479-90231501	GGG
Plate 1 crRNA 3	A10	*RAC1*	TATCCTATCCGCAAACAGTA	hg38l+chr7:6392025-6392047	AGG
Plate 1 crRNA 3	A11	*MAPK8IP3*	GAAGCGCGACAGCCGCAACA	hg38l+chr16:1747214-1747236	TGG
Plate 1 crRNA 3	B02	*ARF1*	ATCCTCTACAAGCTTAAGCT	hg38l+chr1:228097211-228097233	GGG
Plate 1 crRNA 3	B03	*DIAPH1*	CTTGGTCCGAAATGACTATG	hg38l-chr5:141577479-141577501	AGG
Plate 1 crRNA 3	B04	*PIK3CG*	ACAACTGCCGAAGGCGCCGG	hg38l+chr7:106867605-106867627	AGG
Plate 1 crRNA 3	B05	*ARFIP2*	TATGAGAGTGTCCTGCAGCT	hg38l-chr11:6478835-6478857	GGG
Plate 1 crRNA 3	B06	*RHOA*	TATAACATCGGTATCTGGGT	hg38l+chr3:49368465-49368487	AGG
Plate 1 crRNA 3	B07	*RAB2A*	CTGGCGGGCATCTTCTAACC	hg38l-chr8:60584749-60584771	AGG
Plate 1 crRNA 3	B08	*PACSIN1*	AGTGGTCAGACGACGAGAGT	hg38l+chr6:34531638-34531660	GGG
Plate 1 crRNA 3	B09	*BIN1*	TCATCCCTGCCGGGCCAATC	hg38l+chr2:127070572-127070594	GGG
Plate 1 crRNA 3	B10	*RAB3B*	ACATACCAAGCTGCTCTGCA	hg38l+chr1:51933312-51933334	AGG
Plate 1 crRNA 3	B11	*RAB3A*	GACATCCACCAGGCGCTCAA	hg38l+chr19:18197587-18197609	AGG
Plate 1 crRNA 3	C02	*RAB7B*	ACAAGATCGATCTGGCAGAC	hg38l-chr1:205992483-205992505	CGG

Plate 1 crRNA 3	C03	*VPS36*	TATTCCCATGCTCAGCAAGT	hg38l+chr13:52426028-52426050	AGG
Plate 1 crRNA 3	C04	*VPS4A*	TGCCACGGCTTTGGCCAGGT	hg38l-chr16:69319444-69319466	AGG
Plate 1 crRNA 3	C05	*STAU1*	CAAACTCCCTGCGGCGCGGG	hg38l+chr20:49123100-49123122	AGG
Plate 1 crRNA 3	C06	*EPN1*	TTCAGGGTGAGCGTCGCGGG	hg38l-chr19:55695195-55695217	AGG
Plate 1 crRNA 3	C07	*RAB11B*	TGATGGCGCGGTAGCGCTCC	hg38l-chr19:8400029-8400051	TGG
Plate 1 crRNA 3	C08	*CBL*	ATCAAACGGATCTACCACGA	hg38l-chr11:119278565-119278587	TGG
Plate 1 crRNA 3	C09	*VCP*	GCTGCCCATTGATGACACAG	hg38l-chr9:35066750-35066772	TGG
Plate 1 crRNA 3	C10	*RAB4B*	GGTGTACGACATCACCAGGT	hg38l+chr19:40783823-40783845	GGG
Plate 1 crRNA 3	C11	*EFS*	GGACACCACAATGAGTACGA	hg38l-chr14:23359357-23359379	GGG
Plate 1 crRNA 3	D02	*AMPH*	CCTCGGTCACCTTCACAGGT	hg38l-chr7:38462970-38462992	AGG
Plate 1 crRNA 3	D03	*MAP4K2*	CAGTGCCTCTCGGCAGACGT	hg38l+chr11:64802069-64802091	AGG
Plate 1 crRNA 3	D04	*HIP1R*	GATGGTATCCGCAGCCAGGT	hg38l-chr12:122858874-122858896	GGG
Plate 1 crRNA 3	D05	*PDCD6IP*	AATCGCTGCTAAACATTACC	hg38l+chr3:33822061-33822083	AGG
Plate 1 crRNA 3	D06	*CIB3*	CCCATCCTCAGAGAATACCT	hg38l+chr19:16168237-16168259	GGG
Plate 1 crRNA 3	D07	*ARPC1B*	CTGTGCCGCAGGTCACAATA	hg38l-chr7:99388064-99388086	CGG
Plate 1 crRNA 3	D08	*RAB6A*	GCTACACGTCGAAAGAGCTG	hg38l+chr11:73679704-73679726	TGG
Plate 1 crRNA 3	D09	*ARPC4*	CCTCCACAGGCTTCCTTCGA	hg38l-chr3:9801735-9801757	AGG
Plate 1 crRNA 3	D10	*EPN2*	GATTGTACGGTGGCTCCAGT	hg38l-chr17:19328749-19328771	GGG
Plate 1 crRNA 3	D11	*ROCK1*	CCTGCTGCGGGATCCCAAAT	hg38l-chr18:21110841-21110863	CGG
Plate 1 crRNA 3	E02	*IP6K3*	CGCATCTGCGGCATGCAGGT	hg38l-chr6:33725436-33725458	AGG
Plate 1 crRNA 3	E03	*PAK1*	TATTCCTGCAGTTACCTCGT	hg38l-chr11:77340752-77340774	GGG
Plate 1 crRNA 3	E04	*AP1M2*	ATCCCAGAGACGGTGAAGTA	hg38l+chr19:10574908-10574930	GGG
Plate 1 crRNA 3	E05	*WASF2*	CTAGCCAGCCATTACCTGTA	hg38l+chr1:27418254-27418276	AGG
Plate 1 crRNA 3	E06	*SH3GLB1*	TTTGGCCCAGGAACAGCTTA	hg38l+chr1:86719614-86719636	TGG
Plate 1 crRNA 3	E07	*CYTH3*	CGACAATCTAACTTCCGTAG	hg38l-chr7:6187661-6187683	AGG
Plate 1 crRNA 3	E08	*WAS*	ATCGTGAACTCGTGATGTCA	hg38l-chrX:48686833-48686855	GGG
Plate 1 crRNA 3	E09	*SEC13*	CCTGGAGGCAACCATAGCTA	hg38l+chr3:10311683-10311705	AGG
Plate 1 crRNA 3	E10	*SNX1*	TCAGGGTCCTGTAACATGGT	hg38l-chr15:64127756-64127778	AGG
Plate 1 crRNA 3	E11	*NEDD4L*	GTATAGGGTCGCTCCATGGT	hg38l-chr18:58322434-58322456	TGG
Plate 1 crRNA 3	F02	*VAV2*	GGCCATCGACGTGTCCGTGA	hg38l-chr9:133806127-133806149	TGG
Plate 1 crRNA 3	F03	*ARPC3*	AACCCTCACCGGCATCTTGG	hg38l+chr12:110450246-110450268	CGG
Plate 1 crRNA 3	F04	*RAB5B*	TACCAGGAGAGCACCATTGG	hg38l+chr12:55987102-55987124	AGG
Plate 1 crRNA 3	F05	*HIP1*	AATGGCGTCGCTGGTCAAGT	hg38l+chr7:75554162-75554184	GGG
Plate 1 crRNA 3	F06	*ATG12*	GTCTCCAAGCAAGATGGCGG	hg38l-chr5:115841543-115841565	AGG
Plate 1 crRNA 3	F07	*RAB6B*	CGTGTGGCGTCGGCTCTACC	hg38l-chr3:133834610-133834632	CGG
Plate 1 crRNA 3	F08	*WASF1*	TATACTCACTCCTTATAGGT	hg38l-chr6:110108523-110108545	AGG
Plate 1 crRNA 3	F09	*LIMK1*	ATTCCATCCACGTCGGAGAC	hg38l+chr7:74105910-74105932	CGG
Plate 1 crRNA 3	F10	*CAV2*	AATTCCCGCAATGAAGGCCA	hg38l-chr7:116500393-116500415	GGG
Plate 1 crRNA 3	F11	*EPS15L1*	CGATCCGGCATACACAGGGA	hg38l-chr19:16441957-16441979	GGG
Plate 1 crRNA 3	G02	*CDC42*	AGAAAGGAGTCTTTGGACAG	hg38l-chr1:22086689-22086711	TGG
Plate 1 crRNA 3	G03	*PIP5K1A*	GCTGCTTCCAGGATACTACA	hg38l+chr1:151232682-151232704	TGG
Plate 1 crRNA 3	G04	*NSF*	GAGAACAGATCTTGATGAAC	hg38l-chr17:46713911-46713933	GGG
Plate 1 crRNA 3	G05	*PI4KA*	CACCCTCTCACGGCGCAGTA	hg38l-chr22:20727258-20727280	CGG

Plate 1 crRNA 3	G06	*AP4E1*	GCCCTCACCTCCAAGCACGT	hg38l+chr15:50908911-50908933	AGG
Plate 1 crRNA 3	G07	*RAB11A*	GTTTGCAACAAGAAGCATCC	hg38l+chr15:65877432-65877454	AGG
Plate 1 crRNA 3	G08	*COPA*	GATTCTTCTCACAGGCAGAC	hg38l+chr1:160290653-160290675	AGG
Plate 1 crRNA 3	G09	*ADAM10*	ATCTCGGTCTGTGAAGACAT	hg38l+chr15:58640823-58640845	AGG
Plate 1 crRNA 3	G10	*GIT1*	GTTGGTCGTCGAGGTCACTC	hg38l+chr17:29576949-29576971	TGG
Plate 1 crRNA 3	G11	*CAMK1*	CTGTGGAACTCCGGGATACG	hg38l-chr3:9761631-9761653	TGG
Plate 1 crRNA 3	H02	*CFL1*	CTCATAGGTTGCATCATAGA	hg38l+chr11:65855976-65855998	GGG
Plate 1 crRNA 3	H03	*RAB29*	AACCGTTCTCTTTACTGAAC	hg38l+chr1:205770791-205770813	CGG
Plate 1 crRNA 3	H04	*FYN*	TGGATACTACATTACCACCC	hg38l-chr6:111702927-111702949	GGG
Plate 1 crRNA 3	H05	*SAR1A*	AGACAATCCCATTAATTGCT	hg38l+chr10:70157820-70157842	GGG
Plate 1 crRNA 3	H06	*EZR*	GTCCTGGCCTGGCTGTTACA	hg38l+chr6:158766899-158766921	GGG
Plate 1 crRNA 3	H07	*CLTCL1*	CACCACGCTGCTGTCATAGT	hg38l+chr22:19221458-19221480	AGG
Plate 1 crRNA 3	H08	*AP3D1*	CTGGATGGTGAACACATACT	hg38l+chr19:2110187-2110209	GGG
Plate 1 crRNA 3	H09	*ITSN1*	TTTGGCTCTCCAAGGATATA	hg38l-chr21:33818298-33818320	GGG
Plate 1 crRNA 3	H10	*RAB4A*	ATGGGCTCAGGTATTCAGTA	hg38l+chr1:229302882-229302904	CGG
Plate 1 crRNA 3	H11	*CAV1*	ATGTTGCCCTGTTCCCGGAT	hg38l-chr7:116526543-116526565	GGG
Plate 1 crRNA 4	A02	*ARRB1*	ATCTCAAAGAGCGGAGAGGT	hg38l-chr11:75284230-75284252	AGG
Plate 1 crRNA 4	A03	*SNX2*	TGATGGCATGAATGCCTATA	hg38l+chr5:122802082-122802104	TGG
Plate 1 crRNA 4	A04	*SNAP91*	TCATCTCTTGCCAGCTTAGT	hg38l-chr6:83580452-83580474	AGG
Plate 1 crRNA 4	A05	*TSG101*	CTGATTGTGCCATCCCTACT	hg38l+chr11:18484048-18484070	GGG
Plate 1 crRNA 4	A06	*DNM2*	TCTGGTCTGCCGAGGAGTAT	hg38l-chr19:10829071-10829093	AGG
Plate 1 crRNA 4	A07	*SYNJ2*	GTGCTTCTGAAGGAGCAGTA	hg38l+chr6:158059264-158059286	CGG
Plate 1 crRNA 4	A08	*EEA1*	CTGTAGATCCAATCTTGTAC	hg38l+chr12:92802707-92802729	TGG
Plate 1 crRNA 4	A09	*CIB1*	AAAGATGCGGAAGGCATAAT	hg38l+chr15:90231358-90231380	GGG
Plate 1 crRNA 4	A10	*RAC1*	CATGGCTAAGGAGATTGGTA	hg38l+chr7:6402011-6402033	TGG
Plate 1 crRNA 4	A11	*MAPK8IP3*	GTTCCGCTCCATGAGCACAC	hg38l-chr16:1762400-1762422	GGG
Plate 1 crRNA 4	B02	*ARF1*	CACCCAGCTTAAGCTTGTAG	hg38l-chr1:228097213-228097235	AGG
Plate 1 crRNA 4	B03	*DIAPH1*	ATTGAGATTGAGGGATTAAT	hg38l-chr5:141576755-141576777	TGG
Plate 1 crRNA 4	B04	*PIK3CG*	TCTGCTGTGAGAGGGTTAAG	hg38l-chr7:106869248-106869270	TGG
Plate 1 crRNA 4	B05	*ARFIP2*	GTGCTTAAATCCTACCTTAT	hg38l+chr11:6479125-6479147	AGG
Plate 1 crRNA 4	B06	*RHOA*	AACCAGGATGATGGGCACGT	hg38l+chr3:49362559-49362581	TGG
Plate 1 crRNA 4	B07	*RAB2A*	TACTAGTTTACGATATTACA	hg38l+chr8:60584269-60584291	CGG
Plate 1 crRNA 4	B08	*PACSIN1*	CCAAGATCGAGAAGGCGTAC	hg38l+chr6:34527417-34527439	GGG
Plate 1 crRNA 4	B09	*BIN1*	GTGTATGAGCCCGATTGGCC	hg38l-chr2:127070581-127070603	CGG
Plate 1 crRNA 4	B10	*RAB3B*	TATGGGTCTCATACCAGTCT	hg38l+chr1:51937280-51937302	TGG
Plate 1 crRNA 4	B11	*RAB3A*	GATGCCCACGGTGCTGACGA	hg38l+chr19:18202570-18202592	AGG
Plate 1 crRNA 4	C02	*RAB7B*	CATGGTGTCCACGTTCTACA	hg38l-chr1:205992638-205992660	AGG
Plate 1 crRNA 4	C03	*VPS36*	TCATATTTGAACAGGAACGA	hg38l-chr13:52423631-52423653	GGG
Plate 1 crRNA 4	C04	*VPS4A*	GTTGGGCTTCTCCATCACGA	hg38l-chr16:69318826-69318848	CGG
Plate 1 crRNA 4	C05	*STAU1*	TTGACTAACTCCTACAGCCT	hg38l+chr20:49117990-49118012	GGG
Plate 1 crRNA 4	C06	*EPN1*	CTTCCGCCCTGGATTATAGG	hg38l-chr19:55695347-55695369	AGG
Plate 1 crRNA 4	C07	*RAB11B*	CCAGCGCTCCACGTTCTCAT	hg38l-chr19:8402142-8402164	AGG
Plate 1 crRNA 4	C08	*CBL*	GTGCTGCTCTCGGTGATAGA	hg38l-chr11:119297454-119297476	TGG

Plate 1 crRNA 4	C09	*VCP*	TGGGTGCTCCACAGGATACT	hg38l+chr9:35060508-35060530	AGG
Plate 1 crRNA 4	C10	*RAB4B*	GGTGATGTCGTACACCAGCA	hg38l-chr19:40783816-40783838	GGG
Plate 1 crRNA 4	C11	*EFS*	AGCCATGGCCATTGCCACGT	hg38l-chr14:23365007-23365029	CGG
Plate 1 crRNA 4	D02	*AMPH*	CATCCAAGGAGCGCCCAGGT	hg38l-chr7:38465462-38465484	AGG
Plate 1 crRNA 4	D03	*MAP4K2*	GAGGAAGAGTGGACACTACT	hg38l-chr11:64798812-64798834	GGG
Plate 1 crRNA 4	D04	*HIP1R*	GAGCTGCTCATTATCCACCA	hg38l-chr12:122856065-122856087	GGG
Plate 1 crRNA 4	D05	*PDCD6IP*	GCTCGAGACGCTCCTGAGGT	hg38l+chr3:33798920-33798942	GGG
Plate 1 crRNA 4	D06	*CIB3*	ATACCTGGGCAATCCTCTGG	hg38l+chr19:16168251-16168273	CGG
Plate 1 crRNA 4	D07	*ARPC1B*	ATGTGCTTGCAAACCCACCT	hg38l-chr7:99389900-99389922	GGG
Plate 1 crRNA 4	D08	*RAB6A*	GAGCAACCAGTCAGTGAAGG	hg38l-chr11:73677911-73677933	AGG
Plate 1 crRNA 4	D09	*ARPC4*	TATCCTTCGAAGGAAGCCTG	hg38l+chr3:9801732-9801754	TGG
Plate 1 crRNA 4	D10	*EPN2*	CAGTGAGTCCAGGTTCACCA	hg38l-chr17:19331994-19332016	GGG
Plate 1 crRNA 4	D11	*ROCK1*	TATTCAGGGAAGTGAGGTTA	hg38l-chr18:21039548-21039570	GGG
Plate 1 crRNA 4	E02	*IP6K3*	CTTGGGTGAGCGTGCCAGCT	hg38l+chr6:33728092-33728114	GGG
Plate 1 crRNA 4	E03	*PAK1*	GCAGAGCAAACGGAGCACCA	hg38l-chr11:77336226-77336248	TGG
Plate 1 crRNA 4	E04	*AP1M2*	TTGATCAGCCGCAACTACAA	hg38l-chr19:10584045-10584067	GGG
Plate 1 crRNA 4	E05	*WASF2*	GTCGGTCGACCCTCTCAGCA	hg38l+chr1:27418996-27419018	AGG
Plate 1 crRNA 4	E06	*SH3GLB1*	TTGGACCTCCAGAAACAACT	hg38l+chr1:86735154-86735176	GGG
Plate 1 crRNA 4	E07	*CYTH3*	ATGAACCGCGGCATCAACGA	hg38l-chr7:6170858-6170880	GGG
Plate 1 crRNA 4	E08	*WAS*	TTGTATCTTCTCCTGCACGA	hg38l-chrX:48685789-48685811	GGG
Plate 1 crRNA 4	E09	*SEC13*	CTGCTTGGGAGCACACAACA	hg38l+chr3:10311742-10311764	AGG
Plate 1 crRNA 4	E10	*SNX1*	CACCTGTGTTGTAACTTTGT	hg38l-chr15:64123527-64123549	AGG
Plate 1 crRNA 4	E11	*NEDD4L*	ACATGAGGTCCAGCTCAGTA	hg38l-chr18:58373218-58373240	GGG
Plate 1 crRNA 4	F02	*VAV2*	TACTCACTGAACTTGCAGGG	hg38l+chr9:133783496-133783518	AGG
Plate 1 crRNA 4	F03	*ARPC3*	TGCCATGTTTCCGATGAGTT	hg38l+chr12:110445498-110445520	TGG
Plate 1 crRNA 4	F04	*RAB5B*	GTTGTCATCTGCATATGCCT	hg38l-chr12:55991364-55991386	GGG
Plate 1 crRNA 4	F05	*HIP1*	TGTCCAGGGAGTTGAATACT	hg38l+chr7:75573884-75573906	AGG
Plate 1 crRNA 4	F06	*ATG12*	AGAAGTTGGAACTCTCTATG	hg38l-chr5:115832601-115832623	AGG
Plate 1 crRNA 4	F07	*RAB6B*	AGACGGACCTGGCTGATAAG	hg38l-chr3:133839505-133839527	AGG
Plate 1 crRNA 4	F08	*WASF1*	TCAATATACTCACTCCTTAT	hg38l-chr6:110108527-110108549	AGG
Plate 1 crRNA 4	F09	*LIMK1*	GTGAAGAATTCCATCCACGT	hg38l+chr7:74105903-74105925	CGG
Plate 1 crRNA 4	F10	*CAV2*	TGCCTTCAGTGCAGACAATA	hg38l+chr7:116506009-116506031	TGG
Plate 1 crRNA 4	F11	*EPS15L1*	GATGTTCTGCTGTCACACCA	hg38l+chr19:16402257-16402279	GGG
Plate 1 crRNA 4	G02	*CDC42*	TGAGTCCCAACAAGCAAGAA	hg38l-chr1:22086705-22086727	AGG
Plate 1 crRNA 4	G03	*PIP5K1A*	CGCTACTTCCGGGAGCTATT	hg38l+chr1:151232321-151232343	TGG
Plate 1 crRNA 4	G04	*NSF*	TATGAACGGTATCATCAAAT	hg38l+chr17:46711001-46711023	GGG
Plate 1 crRNA 4	G05	*PI4KA*	ACAATGGCCTCAGGGTTGCT	hg38l+chr22:20714667-20714689	GGG
Plate 1 crRNA 4	G06	*AP4E1*	GTGCCATACACACTTCTACT	hg38l-chr15:50925115-50925137	AGG
Plate 1 crRNA 4	G07	*RAB11A*	GAGTGATCTACGTCATCTCA	hg38l+chr15:65877900-65877922	GGG
Plate 1 crRNA 4	G08	*COPA*	TAGTAGGCGCCGAGCAAAGG	hg38l+chr1:160291368-160291390	TGG
Plate 1 crRNA 4	G09	*ADAM10*	AAGTGTCCCTCTTCATTCGT	hg38l+chr15:58682283-58682305	AGG
Plate 1 crRNA 4	G10	*GIT1*	GTGTGCGGCCATTAACATCA	hg38l+chr17:29581943-29581965	GGG
Plate 1 crRNA 4	G11	*CAMK1*	GATGTAGGCGATGACACCTA	hg38l+chr3:9761463-9761485	TGG

Plate 1 crRNA 4	H02	*CFL1*	TTGCATCATAGAGGGCATAG	hg38l+chr11:65855984-65856006	CGG
Plate 1 crRNA 4	H03	*RAB29*	AGATTGGCCACATACCTTGT	hg38l+chr1:205771457-205771479	TGG
Plate 1 crRNA 4	H04	*FYN*	TTGCTGATCGCAGATCTCTA	hg38l+chr6:111694465-111694487	TGG
Plate 1 crRNA 4	H05	*SAR1A*	CAAGATAAGGATTGGCACAT	hg38l+chr10:70153922-70153944	TGG
Plate 1 crRNA 4	H06	*EZR*	CAATGTCCGAGTTACCACCA	hg38l-chr6:158789347-158789369	TGG
Plate 1 crRNA 4	H07	*CLTCL1*	AGTGCTCCTGAAAGCGAACA	hg38l+chr22:19291605-19291627	GGG
Plate 1 crRNA 4	H08	*AP3D1*	TTCACATACTGATCTGACAT	hg38l+chr19:2115391-2115413	AGG
Plate 1 crRNA 4	H09	*ITSN1*	CTGTGGGAACAGAAGATACT	hg38l-chr21:33750231-33750253	AGG
Plate 1 crRNA 4	H10	*RAB4A*	TAACTTCACGATCTGCATCC	hg38l-chr1:229297578-229297600	AGG
Plate 1 crRNA 4	H11	*CAV1*	TGCCATCGGGATGCCAAAGA	hg38l-chr7:116559064-116559086	GGG
Plate 2 crRNA 1	A02	*AP2B1*	GAGCCTCCCGATCATCTTTA	hg38l-chr17:35624561-35624583	GGG
Plate 2 crRNA 1	A03	*EPN3*	TTCCAGTACATCGACCGCGA	hg38l+chr17:50536881-50536903	CGG
Plate 2 crRNA 1	A04	*ACTR3*	AGAACGGACGTTGACCGGTA	hg38l+chr2:113934323-113934345	CGG
Plate 2 crRNA 1	A05	*HGS*	GTTACCTAGGAGACGCTCGA	hg38l-chr17:81684086-81684108	AGG
Plate 2 crRNA 1	A06	*ACTR2*	GCTCTTCCCTGGGCGGACGA	hg38l+chr2:65227891-65227913	TGG
Plate 2 crRNA 1	A07	*GRB2*	GGTCTGAGTTATCCATGACA	hg38l+chr17:75320451-75320473	TGG
Plate 2 crRNA 1	A08	*PACSIN3*	AGGTGCGGGAGAAGCTGCAA	hg38l-chr11:47180590-47180612	GGG
Plate 2 crRNA 1	A09	*VAPB*	GCATCGATGATTCCGCTGTT	hg38l-chr20:58418318-58418340	GGG
Plate 2 crRNA 1	A10	*AP2M1*	AAATGTTGGACCGCTTAACG	hg38l-chr3:184178950-184178972	TGG
Plate 2 crRNA 1	A11	*SYNJ1*	GTTGCTGGCTGCGCGTCAAT	hg38l+chr21:32645762-32645784	AGG
Plate 2 crRNA 1	B02	*SYT2*	TCAGGTGGATCTTCACGTAC	hg38l+chr1:202599328-202599350	GGG
Plate 2 crRNA 1	B03	*ATP6V0A1*	CTTGTGCACGTAGTCGCCCT	hg38l-chr17:42480662-42480684	AGG
Plate 2 crRNA 1	B04	*ROCK2*	TGTTTAGGGAGGTACGACTT	hg38l-chr2:11222159-11222181	GGG
Plate 2 crRNA 1	B05	*GORASP1*	GAGAAATTCCCGACACGTCC	hg38l+chr3:39098867-39098889	AGG
Plate 2 crRNA 1	B06	*CLTA*	CTGAGTGGGAACGGGTGGCC	hg38l+chr9:36211653-36211675	CGG
Plate 2 crRNA 1	B07	*RAB1A*	GCTCTCCTGAACTCACTATT	hg38l+chr2:65129877-65129899	CGG
Plate 2 crRNA 1	B08	*BECN1*	TTGCGCTATACTGACCTGTA	hg38l+chr17:42811640-42811662	GGG
Plate 2 crRNA 1	B09	*DAB2*	CGTCTACTCCGCTGAGTAAT	hg38l-chr5:39382957-39382979	GGG
Plate 2 crRNA 1	B10	*CLTB*	GTAGCCATCAGCAGGACCGT	hg38l+chr5:176398021-176398043	TGG
Plate 2 crRNA 1	B11	*AP2A2*	ACCCGGCTACGAGGACCTTA	hg38l-chr11:972235-972257	GGG
Plate 2 crRNA 1	C02	*PICALM*	GATGTAAATTGGAGTCAACC	hg38l-chr11:85981205-85981227	AGG
Plate 2 crRNA 1	C03	*EPS15*	GTTGGAGTTCCGATCTTTGG	hg38l+chr1:51363889-51363911	TGG
Plate 2 crRNA 1	C04	*AP1M1*	CCACGTCGCCACGGTAGTTC	hg38l-chr19:16203470-16203492	CGG
Plate 2 crRNA 1	C05	*ITSN2*	GGGCCGGCAGACCTGATTGT	hg38l+chr2:24313479-24313501	AGG
Plate 2 crRNA 1	C06	*RAB5C*	CATTGCACTCGCGGGTAACA	hg38l-chr17:42128296-42128318	AGG
Plate 2 crRNA 1	C07	*PIK3C2G*	AGGAAGCCCGGGATTTAGAT	hg38l-chr12:18346755-18346777	AGG
Plate 2 crRNA 1	C08	*CIB2*	CGCCACGATCCTTTCTTTGA	hg38l+chr15:78109353-78109375	AGG
Plate 2 crRNA 1	C09	*RAB11FIP5*	ATCGGCGTCGACAAGTTCCT	hg38l-chr2:73112404-73112426	GGG
Plate 2 crRNA 1	C10	*CLINT1*	GGATCAGCTGATTTATTCGG	hg38l-chr5:157794948-157794970	AGG
Plate 2 crRNA 1	C11	*TNIK*	AGCAGCTGGAGCAGCAGCAG	hg38l-chr3:171157547-171157569	CGG
Plate 2 crRNA 1	D02	*CBLB*	TTGTGGGATGTCGACTCCTA	hg38l-chr3:105702220-105702242	GGG
Plate 2 crRNA 1	D03	*AP2A1*	TCACGTAGTCGCCCGCAATG	hg38l-chr19:49800045-49800067	CGG
Plate 2 crRNA 1	D04	*DNM1*	ATCTGGAACTCGATGTCGGG	hg38l-chr9:128219108-128219130	AGG

Plate 2 crRNA 1	D05	*RAB3D*	AGTCGTCCGCGTATCGGAAC	hg38l+chr19:11337264-11337286	AGG
Plate 2 crRNA 1	D06	*ARRB2*	GACTACCTGAAGGACCGCAA	hg38l+chr17:4716170-4716192	AGG
Plate 2 crRNA 1	D07	*ATM*	GACACAATGCAACTTCCGTA	hg38l-chr11:108250839-108250861	AGG
Plate 2 crRNA 1	D08	*ARPC2*	GATGGTGTTGTCTCGAGCAC	hg38l-chr2:218249388-218249410	TGG
Plate 2 crRNA 1	D09	*SYT1*	TTGCCACCCAATTCCGAGTA	hg38l-chr12:79299387-79299409	TGG
Plate 2 crRNA 1	D10	*RAB8A*	CGTCCGAAACCGTTCCTGAC	hg38l-chr19:16121758-16121780	CGG
Plate 2 crRNA 1	D11	*AP1B1*	TTGTGGGCGAGTACGCGGAA	hg38l-chr22:29349281-29349303	CGG
Plate 2 crRNA 1	E02	*MAPK8IP2*	CTGAGAAGCCGCTCGAGCGG	hg38l+chr22:50603993-50604015	CGG
Plate 2 crRNA 1	E03	*NEDD4*	CCACTTTATCCATTACCGGT	hg38l-chr15:55873953-55873975	TGG
Plate 2 crRNA 1	E04	*WASF3*	CGTTACGGATTACTCTTACC	hg38l+chr13:26681069-26681091	CGG
Plate 2 crRNA 1	E05	*ARPC5*	CAGTGTCGTCGGCCCGCTTC	hg38l-chr1:183635624-183635646	CGG
Plate 2 crRNA 1	E06	*MAPK8IP1*	TCTCCGATGGCCGACTCATA	hg38l-chr11:45903031-45903053	GGG
Plate 2 crRNA 1	E07	*RAB3C*	ATCATCGGCAATAGCAGTGT	hg38l+chr5:58617721-58617743	GGG
Plate 2 crRNA 1	E08	*VAMP1*	TCTTCCTGTTCGTGGACCGA	hg38l+chr12:6462965-6462987	GGG
Plate 2 crRNA 1	E09	*RAB5A*	TTGGTTGTGTGGGTTCGGTA	hg38l-chr3:19983775-19983797	AGG
Plate 2 crRNA 1	E10	*MAP1LC3A*	GGTGATCATCGAGCGCTACA	hg38l+chr20:34559346-34559368	AGG
Plate 2 crRNA 1	E11	*DNM3*	TTACAATGCCCGACCCTCGA	hg38l-chr1:171921757-171921779	GGG
Plate 2 crRNA 1	F02	*ERC1*	GCTAATGGCCGACAACTACG	hg38l+chr12:1408166-1408188	AGG
Plate 2 crRNA 1	F03	*VAMP2*	GGCTGCGCTTGTTTCAAACT	hg38l+chr17:8161644-8161666	GGG
Plate 2 crRNA 1	F04	*ASAP2*	GAACATGGGACCGAGCGGAA	hg38l+chr2:9344589-9344611	CGG
Plate 2 crRNA 1	F05	*SH3GLB2*	GCGGTAGCACTGTGCGTAGT	hg38l+chr9:129009803-129009825	AGG
Plate 2 crRNA 1	F06	*CLTC*	CTGGATCCTTTCGACGTACC	hg38l-chr17:59679438-59679460	AGG
Plate 2 crRNA 1	F07	*CBLC*	GAAGACGTCGAACTCGAAGA	hg38l-chr19:44781326-44781348	TGG
Plate 2 crRNA 1	F08	*RAB8B*	ATCACGACAGCGTACTACAG	hg38l+chr15:63249676-63249698	AGG
Plate 2 crRNA 1	F09	*CAV3*	GTGGATATCCTTGACGATCT	hg38l-chr3:8733908-8733930	GGG
Plate 2 crRNA 1	F10	*VAPA*	CAGACCTCAAATTCAAAGGT	hg38l+chr18:9914318-9914340	AGG
Plate 2 crRNA 1	F11	*ARF6*	CTCATCGATGCGGTCGCGGT	hg38l-chr14:49894008-49894030	CGG
Plate 2 crRNA 2	A02	*AP2B1*	GGTGGTGGCTAATGCCGTAG	hg38l+chr17:35624396-35624418	CGG
Plate 2 crRNA 2	A03	*EPN3*	TCTCGGACATGAGCGAACTA	hg38l-chr17:50536661-50536683	GGG
Plate 2 crRNA 2	A04	*ACTR3*	TAATAGTGGCCAATCCGCCA	hg38l+chr2:113927339-113927361	TGG
Plate 2 crRNA 2	A05	*HGS*	ACTCTTCATGCGGTTCACGA	hg38l-chr17:81695859-81695881	AGG
Plate 2 crRNA 2	A06	*ACTR2*	GTGGTGTGCGACAACGGCAC	hg38l+chr2:65227934-65227956	CGG
Plate 2 crRNA 2	A07	*GRB2*	AGTACTTCCCGGCTCCATCT	hg38l+chr17:75321772-75321794	CGG
Plate 2 crRNA 2	A08	*PACSIN3*	CTCCACCGTGACTTGCACCA	hg38l-chr11:47179247-47179269	GGG
Plate 2 crRNA 2	A09	*VAPB*	CGGGTTGCCAAGCTTTAGGT	hg38l-chr20:58418235-58418257	TGG
Plate 2 crRNA 2	A10	*AP2M1*	GAGAGGGTATCAAGTATCGT	hg38l+chr3:184180907-184180929	CGG
Plate 2 crRNA 2	A11	*SYNJ1*	CGCCATTCTCCTTTCTTCGG	hg38l+chr21:32726890-32726912	AGG
Plate 2 crRNA 2	B02	*SYT2*	GCCATAGGCAAGATCTTCGT	hg38l-chr1:202596887-202596909	GGG
Plate 2 crRNA 2	B03	*ATP6V0A1*	ATGTTTGGAGACTTCGGTCA	hg38l+chr17:42494375-42494397	TGG
Plate 2 crRNA 2	B04	*ROCK2*	CTGATACTGCAGCCCGGTTA	hg38l-chr2:11215030-11215052	AGG
Plate 2 crRNA 2	B05	*GORASP1*	TTCCAGGCAGAGTGACTACA	hg38l-chr3:39100307-39100329	TGG
Plate 2 crRNA 2	B06	*CLTA*	GCGCCAAGAAGGCCGCAGCC	hg38l-chr9:36191146-36191168	GGG
Plate 2 crRNA 2	B07	*RAB1A*	AGTAGACTACACAACAGCGA	hg38l-chr2:65088938-65088960	AGG

Plate 2 crRNA 2	B08	*BECN1*	ATTGCGCTATACTGACCTGT	hg38l+chr17:42811639-42811661	AGG
Plate 2 crRNA 2	B09	*DAB2*	GCACCTACCTAGACCCACCA	hg38l+chr5:39381446-39381468	GGG
Plate 2 crRNA 2	B10	*CLTB*	ATCCGAGGAGGCTTTCGTGA	hg38l-chr5:176392920-176392942	AGG
Plate 2 crRNA 2	B11	*AP2A2*	TACCCGGCTACGAGGACCTT	hg38l-chr11:972236-972258	AGG
Plate 2 crRNA 2	C02	*PICALM*	TAGCAGGATAGGCCATTACA	hg38l+chr11:85976655-85976677	GGG
Plate 2 crRNA 2	C03	*EPS15*	TGCCAATTCTTCTTCGTAAG	hg38l+chr1:51408264-51408286	TGG
Plate 2 crRNA 2	C04	*AP1M1*	GTCCTGCGCAGCGAGATCGT	hg38l+chr19:16226439-16226461	GGG
Plate 2 crRNA 2	C05	*ITSN2*	GGAAAGCCAACTATGAGCGA	hg38l-chr2:24300131-24300153	GGG
Plate 2 crRNA 2	C06	*RAB5C*	GGTGATGTCATAGACCACGA	hg38l+chr17:42128655-42128677	TGG
Plate 2 crRNA 2	C07	*PIK3C2G*	GACCTAGGTCACTTACAGTA	hg38l-chr12:18391246-18391268	GGG
Plate 2 crRNA 2	C08	*CIB2*	CTTCAAAGAAAGGATCGTGG	hg38l-chr15:78109352-78109374	CGG
Plate 2 crRNA 2	C09	*RAB11FIP5*	GACCCAACTCGCTCCGACTT	hg38l+chr2:73088183-73088205	AGG
Plate 2 crRNA 2	C10	*CLINT1*	GGTTTGGAAGGCTGCATACC	hg38l+chr5:157789401-157789423	AGG
Plate 2 crRNA 2	C11	*TNIK*	GCGTGGCATCTCCACGCGGT	hg38l+chr3:171126014-171126036	GGG
Plate 2 crRNA 2	D02	*CBLB*	CCAATCGAGTGCAACTTAAC	hg38l+chr3:105740600-105740622	CGG
Plate 2 crRNA 2	D03	*AP2A1*	CTGCACTGCATCGCCAACGT	hg38l+chr19:49782645-49782667	GGG
Plate 2 crRNA 2	D04	*DNM1*	CGCCACTTGGCTGACCGTAT	hg38l+chr9:128220288-128220310	GGG
Plate 2 crRNA 2	D05	*RAB3D*	TGAAGGAGTCGTCCGCGTAT	hg38l+chr19:11337258-11337280	CGG
Plate 2 crRNA 2	D06	*ARRB2*	GTCCCGCTTGCCCAAGTACA	hg38l-chr17:4715977-4715999	CGG
Plate 2 crRNA 2	D07	*ATM*	GTTAGTGATGCAAACGAACC	hg38l+chr11:108267300-108267322	TGG
Plate 2 crRNA 2	D08	*ARPC2*	AGTTATTAAAGAGGGTGTAC	hg38l+chr2:218234350-218234372	GGG
Plate 2 crRNA 2	D09	*SYT1*	GTACCATACTCGGAATTGGG	hg38l+chr12:79299384-79299406	TGG
Plate 2 crRNA 2	D10	*RAB8A*	ACGGTTTCGGACGATCACAA	hg38l+chr19:16121768-16121790	CGG
Plate 2 crRNA 2	D11	*AP1B1*	GTTGTTCTTCACGGCCACCT	hg38l+chr22:29331516-29331538	AGG
Plate 2 crRNA 2	E02	*MAPK8IP2*	GTGAGCCGCATGATCTCCGA	hg38l+chr22:50604362-50604384	GGG
Plate 2 crRNA 2	E03	*NEDD4*	AAGTCCGGCATGCACCAAAT	hg38l-chr15:55850584-55850606	GGG
Plate 2 crRNA 2	E04	*WASF3*	GTCACATGCATCGGACGTTA	hg38l+chr13:26681054-26681076	CGG
Plate 2 crRNA 2	E05	*ARPC5*	TAGCACTGCTATTGTCAGAC	hg38l+chr1:183630484-183630506	GGG
Plate 2 crRNA 2	E06	*MAPK8IP1*	TCGAGACCGAATCCACTACC	hg38l+chr11:45902556-45902578	AGG
Plate 2 crRNA 2	E07	*RAB3C*	GCCCATGGCTCCACGATAAT	hg38l-chr5:58726042-58726064	AGG
Plate 2 crRNA 2	E08	*VAMP1*	TACAATAACTACCACGATGA	hg38l+chr12:6464891-6464913	TGG
Plate 2 crRNA 2	E09	*RAB5A*	CTACAACACTGATTCCTGGT	hg38l-chr3:19983794-19983816	TGG
Plate 2 crRNA 2	E10	*MAP1LC3A*	CTGCTCGTAGATGTCCGCGA	hg38l-chr20:34559813-34559835	TGG
Plate 2 crRNA 2	E11	*DNM3*	TTGGTAGGGTATCCCGAATG	hg38l-chr1:172038330-172038352	TGG
Plate 2 crRNA 2	F02	*ERC1*	GCAGTCATCCGAACACCGTA	hg38l-chr12:1028198-1028220	AGG
Plate 2 crRNA 2	F03	*VAMP2*	TGGCTGCGCTTGTTTCAAAC	hg38l+chr17:8161643-8161665	TGG
Plate 2 crRNA 2	F04	*ASAP2*	GGGAAGGCCTCCATCGAGAT	hg38l+chr2:9379038-9379060	AGG
Plate 2 crRNA 2	F05	*SH3GLB2*	GAGACTTGACGAACTCGTGG	hg38l+chr9:129009832-129009854	AGG
Plate 2 crRNA 2	F06	*CLTC*	TCAAGTAACCGCGTCTGTAA	hg38l-chr17:59666193-59666215	AGG
Plate 2 crRNA 2	F07	*CBLC*	TTCTGCCGCTGCGAGATCAA	hg38l+chr19:44793498-44793520	GGG
Plate 2 crRNA 2	F08	*RAB8B*	AGTACGCTGTCGTGATTGTT	hg38l-chr15:63249669-63249691	CGG
Plate 2 crRNA 2	F09	*CAV3*	TGATGCACTGGATCTCGATC	hg38l-chr3:8745741-8745763	AGG
Plate 2 crRNA 2	F10	*VAPA*	TACCGAAACAAGGAAACTAA	hg38l+chr18:9950484-9950506	TGG

Plate 2 crRNA 2	F11	*ARF6*	ACCAGTTCCTGTCCCGAATC	hg38l-chr14:49894162-49894184	CGG
Plate 2 crRNA 3	A02	*AP2B1*	TAATCCTTTGATTCGAGCCT	hg38l+chr17:35608156-35608178	TGG
Plate 2 crRNA 3	A03	*EPN3*	GATGTCAGCCAAGTCCAGGA	hg38l-chr17:50540251-50540273	TGG
Plate 2 crRNA 3	A04	*ACTR3*	TCCACTGTCTATTACCGTAC	hg38l-chr2:113934337-113934359	CGG
Plate 2 crRNA 3	A05	*HGS*	TCTGCGACCTGATCCGCCAA	hg38l+chr17:81685659-81685681	GGG
Plate 2 crRNA 3	A06	*ACTR2*	GGCTGTCCATCGTCCGCCCA	hg38l-chr2:65227897-65227919	GGG
Plate 2 crRNA 3	A07	*GRB2*	GCACTGAGCAGCGCTCAGAA	hg38l-chr17:75393625-75393647	TGG
Plate 2 crRNA 3	A08	*PACSIN3*	CTCCAGAAGAGGACGCTGGA	hg38l-chr11:47182701-47182723	GGG
Plate 2 crRNA 3	A09	*VAPB*	TGAAGACTACAGCACCACGT	hg38l+chr20:58418283-58418305	AGG
Plate 2 crRNA 3	A10	*AP2M1*	GCATGCCTGAATGCAAGTTT	hg38l+chr3:184181142-184181164	GGG
Plate 2 crRNA 3	A11	*SYNJ1*	GATTAAGCTGTGAACGAGCT	hg38l-chr21:32695123-32695145	GGG
Plate 2 crRNA 3	B02	*SYT2*	GGCCGTGGGCACATAGCGCA	hg38l+chr1:202600424-202600446	GGG
Plate 2 crRNA 3	B03	*ATP6V0A1*	GGTGGGCAACGGACCGACAG	hg38l+chr17:42507546-42507568	AGG
Plate 2 crRNA 3	B04	*ROCK2*	TAGTAGGTAAATCCGATGAA	hg38l+chr2:11221210-11221232	AGG
Plate 2 crRNA 3	B05	*GORASP1*	TTGGCTATGGGTATCTACAC	hg38l-chr3:39100467-39100489	CGG
Plate 2 crRNA 3	B06	*CLTA*	GAACGGATCCAGCTCAGCCA	hg38l-chr9:36191055-36191077	TGG
Plate 2 crRNA 3	B07	*RAB1A*	AGAACAGTCTTTCATGACGA	hg38l-chr2:65088606-65088628	TGG
Plate 2 crRNA 3	B08	*BECN1*	GGTTTCCGTAAGGAACAAGT	hg38l+chr17:42813983-42814005	CGG
Plate 2 crRNA 3	B09	*DAB2*	AATTTGACCAGATCTCTAAC	hg38l-chr5:39382900-39382922	CGG
Plate 2 crRNA 3	B10	*CLTB*	GCAGGCATAGAGAACGACGA	hg38l-chr5:176416236-176416258	GGG
Plate 2 crRNA 3	B11	*AP2A2*	CCTGGCTGAGAAGTACGCGG	hg38l+chr11:992520-992542	TGG
Plate 2 crRNA 3	C02	*PICALM*	GTGGGAGTTTGGCAACAGGA	hg38l+chr11:85981926-85981948	AGG
Plate 2 crRNA 3	C03	*EPS15*	TATGATCGAATGGGCCAAGA	hg38l-chr1:51356807-51356829	GGG
Plate 2 crRNA 3	C04	*AP1M1*	TTGTCTTCGGCCTCCACACT	hg38l-chr19:16233532-16233554	AGG
Plate 2 crRNA 3	C05	*ITSN2*	TGTGCTAACAGAAGGCACTA	hg38l+chr2:24310553-24310575	GGG
Plate 2 crRNA 3	C06	*RAB5C*	AGAGCCGTGGAATTCCAGGT	hg38l-chr17:42128256-42128278	GGG
Plate 2 crRNA 3	C07	*PIK3C2G*	AGTAAAGACGATGGGCAACC	hg38l-chr12:18424016-18424038	TGG
Plate 2 crRNA 3	C08	*CIB2*	CTGGTTACCATAGATCTTGA	hg38l+chr15:78109227-78109249	AGG
Plate 2 crRNA 3	C09	*RAB11FIP5*	TCAGGTTGTTGCGCGTGAAC	hg38l+chr2:73089227-73089249	TGG
Plate 2 crRNA 3	C10	*CLINT1*	ACTGCCAAAGAACTCGCCAC	hg38l+chr5:157791898-157791920	TGG
Plate 2 crRNA 3	C11	*TNIK*	GTTAACCTACCCACAGACGT	hg38l+chr3:171066566-171066588	GGG
Plate 2 crRNA 3	D02	*CBLB*	TGTGACACATCCAGGTTACA	hg38l-chr3:105745978-105746000	TGG
Plate 2 crRNA 3	D03	*AP2A1*	GTTCGGGCCTGCAACCAGCT	hg38l+chr19:49799343-49799365	GGG
Plate 2 crRNA 3	D04	*DNM1*	GATCGAGGCCGAGACCGACA	hg38l+chr9:128218646-128218668	GGG
Plate 2 crRNA 3	D05	*RAB3D*	TTCCTTCCTGTTCCGATACG	hg38l-chr19:11337270-11337292	CGG
Plate 2 crRNA 3	D06	*ARRB2*	CCAGGTCTTCACGGCCATAG	hg38l-chr17:4716437-4716459	CGG
Plate 2 crRNA 3	D07	*ATM*	GACCAATACTGTGTCCTTTA	hg38l+chr11:108268507-108268529	GGG
Plate 2 crRNA 3	D08	*ARPC2*	CACTGGCATTGGTGTGACGA	hg38l-chr2:218249371-218249393	GGG
Plate 2 crRNA 3	D09	*SYT1*	ATTGCAATTAAGGCCCACGG	hg38l-chr12:79285789-79285811	TGG
Plate 2 crRNA 3	D10	*RAB8A*	GTTGTCGAAGGACTTCTCGT	hg38l-chr19:16125495-16125517	TGG
Plate 2 crRNA 3	D11	*AP1B1*	GTTCTTGAGGATGGTCTCGT	hg38l+chr22:29328824-29328846	AGG
Plate 2 crRNA 3	E02	*MAPK8IP2*	GGCCGTACCTGAACACAGCC	hg38l-chr22:50605429-50605451	CGG
Plate 2 crRNA 3	E03	*NEDD4*	ACATCCAAGTTACTTGACGG	hg38l+chr15:55860489-55860511	TGG

Plate 2 crRNA 3	E04	*WASF3*	TACCCATTCGAATAGCAGCG	hg38l-chr13:26682955-26682977	AGG
Plate 2 crRNA 3	E05	*ARPC5*	CCTGACTCTTGGTGTTGATA	hg38l+chr1:183633090-183633112	GGG
Plate 2 crRNA 3	E06	*MAPK8IP1*	AGTGGCCTCTAGTCGCACAT	hg38l-chr11:45902579-45902601	CGG
Plate 2 crRNA 3	E07	*RAB3C*	CACGAAGCGCCCATGCAGGT	hg38l+chr5:58583215-58583237	GGG
Plate 2 crRNA 3	E08	*VAMP1*	TATTAATGTGGGATAAGCCC	hg38l-chr12:6463052-6463074	AGG
Plate 2 crRNA 3	E09	*RAB5A*	AGACCCAACGGGCCAAATAC	hg38l+chr3:19950920-19950942	GGG
Plate 2 crRNA 3	E10	*MAP1LC3A*	GTAGCGCTCGATGATCACCT	hg38l-chr20:34559342-34559364	GGG
Plate 2 crRNA 3	E11	*DNM3*	CGATATGTCTGTAAGCCGGG	hg38l-chr1:172033199-172033221	TGG
Plate 2 crRNA 3	F02	*ERC1*	GTCGAACCAACAGTACGGGA	hg38l+chr12:1028001-1028023	GGG
Plate 2 crRNA 3	F03	*VAMP2*	CTCCAAACCTCACCAGTAAC	hg38l-chr17:8162282-8162304	AGG
Plate 2 crRNA 3	F04	*ASAP2*	GGCCCACTCACCTATCTCGA	hg38l-chr2:9379048-9379070	TGG
Plate 2 crRNA 3	F05	*SH3GLB2*	AGATTTCCCGGCACCTTCGT	hg38l-chr9:129009326-129009348	GGG
Plate 2 crRNA 3	F06	*CLTC*	CATGGCTCTGAGACATTCTA	hg38l-chr17:59666837-59666859	GGG
Plate 2 crRNA 3	F07	*CBLC*	GGTCGACGCATTGCTCTTCT	hg38l-chr19:44778012-44778034	AGG
Plate 2 crRNA 3	F08	*RAB8B*	CAGGATCATTCTTTCGACAT	hg38l-chr15:63256515-63256537	CGG
Plate 2 crRNA 3	F09	*CAV3*	CCACACGCCGTCAAAGCTGT	hg38l-chr3:8745563-8745585	AGG
Plate 2 crRNA 3	F10	*VAPA*	CCCACAGACCTCAAATTCAA	hg38l+chr18:9914314-9914336	AGG
Plate 2 crRNA 3	F11	*ARF6*	GAAATGCGGATCCTCATGTT	hg38l+chr14:49893773-49893795	GGG
Plate 2 crRNA 4	A02	*AP2B1*	TTGCAGTGGTAGTGCCAACA	hg38l-chr17:35657617-35657639	GGG
Plate 2 crRNA 4	A03	*EPN3*	ACCCATGGGACATCCCAGGT	hg38l+chr17:50540317-50540339	GGG
Plate 2 crRNA 4	A04	*ACTR3*	TCTTGGACCTCAAGACAAGT	hg38l+chr2:113934300-113934322	AGG
Plate 2 crRNA 4	A05	*HGS*	GTATCTCAACCGGAACTACT	hg38l+chr17:81694932-81694954	GGG
Plate 2 crRNA 4	A06	*ACTR2*	GGATGACATGAAACACCTGT	hg38l+chr2:65246610-65246632	GGG
Plate 2 crRNA 4	A07	*GRB2*	AATTGAACTTCACCACCCAG	hg38l+chr17:75321748-75321770	AGG
Plate 2 crRNA 4	A08	*PACSIN3*	TGAGAAGACCGCCCAGACGA	hg38l-chr11:47180278-47180300	GGG
Plate 2 crRNA 4	A09	*VAPB*	GGCCTCACACAGTACCTACG	hg38l-chr20:58418297-58418319	TGG
Plate 2 crRNA 4	A10	*AP2M1*	TACCCACAGAATTCCGAGAC	hg38l+chr3:184180186-184180208	AGG
Plate 2 crRNA 4	A11	*SYNJ1*	ACAGGACCCTCTGATATTGT	hg38l+chr21:32646458-32646480	AGG
Plate 2 crRNA 4	B02	*SYT2*	GATGCAGACAGTGAGCTTCC	hg38l+chr1:202600403-202600425	CGG
Plate 2 crRNA 4	B03	*ATP6V0A1*	CTGGGTTCAGCTGTAGAACA	hg38l-chr17:42495647-42495669	GGG
Plate 2 crRNA 4	B04	*ROCK2*	CTTAGCTTGAGGAAACTAAT	hg38l-chr2:11198757-11198779	AGG
Plate 2 crRNA 4	B05	*GORASP1*	CTGAGCTTCAAGCAGCTCGG	hg38l+chr3:39098329-39098351	CGG
Plate 2 crRNA 4	B06	*CLTA*	CCTTCAAAGATGCCAATTCT	hg38l+chr9:36204059-36204081	CGG
Plate 2 crRNA 4	B07	*RAB1A*	ATTCGTTGCATTCTTAGCAC	hg38l+chr2:65088631-65088653	TGG
Plate 2 crRNA 4	B08	*BECN1*	GAAGGTTGCATTAAAGACGT	hg38l+chr17:42815916-42815938	TGG
Plate 2 crRNA 4	B09	*DAB2*	CTGCTTTACGCCATTCTGTA	hg38l+chr5:39382717-39382739	TGG
Plate 2 crRNA 4	B10	*CLTB*	GGTCCTAGATGCTGCATCTA	hg38l-chr5:176397704-176397726	AGG
Plate 2 crRNA 4	B11	*AP2A2*	CTGCACTGCATCGCCAGCGT	hg38l+chr11:972176-972198	GGG
Plate 2 crRNA 4	C02	*PICALM*	ACCTGAGAAGCAGTTGACAT	hg38l+chr11:85996843-85996865	AGG
Plate 2 crRNA 4	C03	*EPS15*	ACTGGAGATTCCTGGTGTAT	hg38l+chr1:51405903-51405925	GGG
Plate 2 crRNA 4	C04	*AP1M1*	GAGTCTGTCAACCTCTTGGT	hg38l+chr19:16209160-16209182	AGG
Plate 2 crRNA 4	C05	*ITSN2*	ACTGAATAGGCTGCCGAGGT	hg38l+chr2:24254375-24254397	AGG
Plate 2 crRNA 4	C06	*RAB5C*	CTGGACCACTACAGCTGGAC	hg38l-chr17:42130505-42130527	GGG

Plate 2 crRNA 4	C07	*PIK3C2G*	TTGAAAGGCTCTCTTCAACC	hg38l+chr12:18282703-18282725	CGG
Plate 2 crRNA 4	C08	*CIB2*	AGAGCAGCTAGACAACTACC	hg38l-chr15:78131164-78131186	AGG
Plate 2 crRNA 4	C09	*RAB11FIP5*	GTGGCCCTGAAGGTCCAGAA	hg38l+chr2:73088637-73088659	GGG
Plate 2 crRNA 4	C10	*CLINT1*	ACTCGCCACTGGAAGCAACA	hg38l+chr5:157791909-157791931	GGG
Plate 2 crRNA 4	C11	*TNIK*	GCTCAGTTCTCCGGAGATCA	hg38l+chr3:171110852-171110874	GGG
Plate 2 crRNA 4	D02	*CBLB*	GCTGCTATAGATTTAGACGT	hg38l+chr3:105658966-105658988	GGG
Plate 2 crRNA 4	D03	*AP2A1*	GTGCGTCTTGACGGCTTCAT	hg38l-chr19:49799446-49799468	GGG
Plate 2 crRNA 4	D04	*DNM1*	CTTGTTCTCCAGCACATCAC	hg38l-chr9:128220045-128220067	GGG
Plate 2 crRNA 4	D05	*RAB3D*	CTGATAGGCAACAGCAGTGT	hg38l-chr19:11337299-11337321	GGG
Plate 2 crRNA 4	D06	*ARRB2*	GAGAAACCCGGGACCAGGTA	hg38l+chr17:4710728-4710750	AGG
Plate 2 crRNA 4	D07	*ATM*	AATGGAGACAGCTCACAGTT	hg38l-chr11:108250747-108250769	AGG
Plate 2 crRNA 4	D08	*ARPC2*	CATGCCAGCTTGATGCACAA	hg38l-chr2:218238718-218238740	TGG
Plate 2 crRNA 4	D09	*SYT1*	ATCATATACAGCCATCACTA	hg38l-chr12:79299412-79299434	GGG
Plate 2 crRNA 4	D10	*RAB8A*	GATCACAACGGCCTACTACA	hg38l+chr19:16121780-16121802	GGG
Plate 2 crRNA 4	D11	*AP1B1*	GATGTCCTTGATGACCACGA	hg38l+chr22:29350055-29350077	TGG
Plate 2 crRNA 4	E02	*MAPK8IP2*	GGGTTGCTGAGGAATAGGCA	hg38l-chr22:50604599-50604621	GGG
Plate 2 crRNA 4	E03	*NEDD4*	CTGTTCTTGAAGACTCTTAC	hg38l-chr15:55842098-55842120	CGG
Plate 2 crRNA 4	E04	*WASF3*	TATGGTGTCAGGATGTTCAG	hg38l-chr13:26667645-26667667	AGG
Plate 2 crRNA 4	E05	*ARPC5*	ACACCCTTAACTTCCATCAC	hg38l-chr1:183633152-183633174	AGG
Plate 2 crRNA 4	E06	*MAPK8IP1*	GGCACAGTTGTCATAGACGG	hg38l-chr11:45902996-45903018	TGG
Plate 2 crRNA 4	E07	*RAB3C*	CTGCATTCGTCAGCACAGTT	hg38l+chr5:58617788-58617810	GGG
Plate 2 crRNA 4	E08	*VAMP1*	TACCTCCTCCACTTGTGCCT	hg38l+chr12:6466222-6466244	GGG
Plate 2 crRNA 4	E09	*RAB5A*	GATAAAGCTATTACAATGTT	hg38l-chr3:19976101-19976123	AGG
Plate 2 crRNA 4	E10	*MAP1LC3A*	TCAGAAGCCGAAGGTTTCCT	hg38l-chr20:34559876-34559898	GGG
Plate 2 crRNA 4	E11	*DNM3*	TACCAGATCCACACTCTTCA	hg38l-chr1:172048686-172048708	AGG
Plate 2 crRNA 4	F02	*ERC1*	GTGATGCTCTCCAAATGCTA	hg38l-chr12:1028268-1028290	TGG
Plate 2 crRNA 4	F03	*VAMP2*	CACACTCACCTCATCCACCT	hg38l+chr17:8162240-8162262	GGG
Plate 2 crRNA 4	F04	*ASAP2*	ATGATTCGGACTGAAATAAG	hg38l+chr2:9323167-9323189	CGG
Plate 2 crRNA 4	F05	*SH3GLB2*	GGAGCTGCTGGCTCAGTACA	hg38l-chr9:129021130-129021152	TGG
Plate 2 crRNA 4	F06	*CLTC*	CGATCACACACAATGATAAG	hg38l-chr17:59673671-59673693	TGG
Plate 2 crRNA 4	F07	*CBLC*	GGTTGTGGGTCTTTCCATCT	hg38l-chr19:44790013-44790035	GGG
Plate 2 crRNA 4	F08	*RAB8B*	TACCTCTTCTACATTTGCAC	hg38l-chr15:63259673-63259695	TGG
Plate 2 crRNA 4	F09	*CAV3*	GTGGGCACCTACAGCTTTGA	hg38l+chr3:8745556-8745578	CGG
Plate 2 crRNA 4	F10	*VAPA*	TTCAGTGGAACAGCTTTGCT	hg38l-chr18:9950407-9950429	AGG
Plate 2 crRNA 4	F11	*ARF6*	CATTACTACACTGGGACCCA	hg38l+chr14:49893962-49893984	AGG